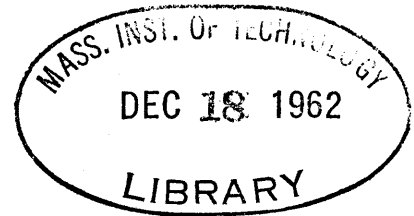


LIBRARY
COPY



FLAME SPREAD THROUGH A SOLID FUEL

by

Frank R. Steward

B.S., Massachusetts Institute of Technology
(1959)

M.S., Massachusetts Institute of Technology
(1960)

Submitted in Partial Fulfillment of
the Requirements for
the Degree of
Doctor of Science
at the
Massachusetts Institute of Technology
September, 1962

Signature of Author

Frank R. Steward
Department of Chemical Engineering

Certified by

Hoyt C. Hottel, Thesis Supervisor

Glenn C. Williams, Thesis Supervisor

Accepted by

Chairman, Departmental Committee
on Graduate Students

Department of Chemical Engineering
Massachusetts Institute of Technology
Cambridge 39, Massachusetts

September 9, 1962

Professor Philip Franklin
Secretary of the Faculty
Massachusetts Institute of Technology
Cambridge 39, Massachusetts

Dear Professor Franklin:

The attached thesis entitled "Flame Spread Through a Solid Fuel"
is hereby submitted in partial fulfillment of the requirements for the
degree of Doctor of Science in Chemical Engineering.

Respectfully submitted,

Frank R. Steward

ABSTRACT

Flame Spread Through a Solid Fuel

by

Frank R. Steward

Submitted to the Department of Chemical Engineering on September 9, 1962 in partial fulfillment of the requirements for the degree of Doctor of Science.

An investigation was made to increase the understanding of natural fire spread through solid fuel. The investigation included three not wholly connected parts, theoretical and experimental. I. The rate of fire spread over a horizontal surface covered with each of two types of fuel, shredded newspaper and computer punch outs, was measured for several humidities with various rates of artificially controlled irradiation from an external source. The results were interpreted by a mathematical model suggested in the Woods Hole Summer Study Fire Report. II. The flux density of radiation was measured around line fires of methane and propane on a perpendicular surface. The results compared favorably with intensity profiles based on the simplified model of a uniform temperature gray gas wedge of slope 0.25 calculated on the 709 and 7090 computers at the M. I. T. Computation Center. Additional calculations were made to obtain the intensity profiles on a perpendicular surface around an infinitely long uniform temperature gray gas rectangular parallelepiped over a wide range of heights and widths. III. Some flame heights of the propane and methane line fires were measured visually. They compared favorably with circular buoyant flame heights reported in the literature.

Some consideration was given as to how the various mechanisms of heat transfer can be estimated in a full scale fire so their relative importance can be evaluated by the suggested mathematical model.

Thesis Supervisors:

Hoyt C. Hottel
Professor of Chemical Engineering
Glenn C. Williams
Professor of Chemical Engineering

ACKNOWLEDGEMENTS

The author wishes to express his gratitude to his thesis supervisors, Professors Hoyt C. Hottel and Glenn C. Williams, for their advice and helpfulness throughout the duration of this project.

The research was supported by the National Science Foundation which supplied funds for my Research Assistantships and all the equipment that was required.

The author wishes to express his thanks to the other Doctoral candidates at the Fuels Research Laboratory, Chris Bonifaz, Keith Thompson, Henry Becker, Glen Miles, and Wayne Erickson, who supplied a congenial atmosphere and offered many suggestions.

A special thanks goes to Charles-Louis de Rochechouart who helped with the early experimental work.

Also, a thanks to Adel Sarofim, who was helpful with many suggestions concerning the parts on radiative heat transfer.

The author is very grateful to Miss Sally Drew and Miss Mina Harrington for the effort in typing this thesis at the very last minute.

The author is also very thankful to his wife Jacqueline who performed many tasks to make this thesis possible, and his son Richard whose important contribution was many smiles.

SUMMARY

An investigation was conducted to increase the understanding of natural fire spread through solid fuel. The work consisted of both experimental results and theoretical analysis.

The Woods Hole Summer Study Model (32) of an infinitely long line fire spreading through a uniform fuel bed discussed in Section 2-4 is considered to offer the best analysis for steady state fire spread at the present time. The form is general enough in order that any new observation can be included. It can also be used as a basis for determining future work to fill in missing information.

The three equations for the Woods Hole Summer Study Model are:

1. An energy balance on the unburned fuel,

$$Q_i V = Q/L)_B + Q/L)_R + Q/L)_C - Q/L)_L \quad 2-23$$

the right hand elements of which represent different modes of heat flux to bring the fuel to ignition, operating over the fuel bed and extending from infinity to the flame front.

$Q/L)_B$ is the radiation flux through the plane of ignition of the fuel from the embers below the gas flame.

$Q/L)_R$ is the integrated radiation rate from the overhead flame into the fuel.

$Q/L)_C$ is the integrated convective heat transfer rate from the burning gases to the unburned fuel.

$(Q/L)_L$ is the integrated rate of convection heat loss from the unburned fuel.

Q_i is the net energy required to produce piloted ignition.

V is the rate of fire spread.

2. A burning law,

$$\xi \eta Q_c V = \beta \left[(Q/L)_R' + (Q/L)_I' \right] \quad 2-28$$

which says that the heat liberation rate by burning (l.h.s.) is proportional to the heat input rate to the burning solid fuel bed.

$(Q/L)_R'$ is the integrated radiation rate to the burning fuel.

$(Q/L)_I'$ is the integrated internal heat generation rate in the burning fuel.

Q_c is the heat of combustion of the fuel.

ξ is the loading density of the fuel.

η is the fraction of fuel burned as the flame passes.

β is a constant of proportionality between the chemical energy in the gases liberated during decomposition of the fuel and the heat absorbed by the fuel.

3. A determination of the flame height,

$$\frac{H}{W} = f \left[\frac{(Q/L)^2}{W^3} \right] \quad 2-29$$

H is the flame height.

W is the width of the flame base.

Q/L is the integrated chemical energy liberation rate =

$$\beta \left((Q/L)_R' + (Q/L)_I' \right)$$

The results of this study have determined the form and importance of some of the terms in the above equations.

The experimental work of this thesis can be divided into three parts. The first part consisted of measuring the rate of spread of a line fire over several fuels (Figure 3-1a). The rate of fire spread over shredded newspaper was measured for different loading densities (Figure 3-2), different rates of external radiation supplied by electrically heated wires (Figure 3-3), and several humidities (Figure 3-6). The data indicate that after the surface is fully covered (about four equivalent layers when randomly distributed) the rate of spread is independent of the loading density. The importance of the effect of radiation can be shown from equation 2-23. On the assumption that the energy per unit area required for ignition, Q_i , is proportional to the time of heating to the $\frac{1}{4}$ power or is equal to $Q_o (V_o/V)^{\frac{1}{4}}$ (discussed in Section 3-4), and that radiation through the bed, $(Q/L)_B$, may be neglected, equation 2-23 becomes

$$V^{3/4} = \frac{1}{Q_o V_o^{\frac{1}{4}}} \left[(Q/L)_R - (Q/L)_L \right] + \frac{(Q/L)c_1}{Q_o V_o^{\frac{1}{4}}} \quad 3-4$$

A plot of fire spread velocity to the three-fourths power vs. the integrated external radiation rate minus the integrated heat loss from the fuel should give a straight line. Unfortunately the heat loss at the surface is not well known or easy to obtain. Using the solution of the conduction equation with external radiation on the surface of a solid as a function of time (6), it is shown in Section 3-4 that a good estimate of this rate of heat loss is

$$(Q/L)_L = K \left[\frac{(Q/L)_R}{V^{\frac{1}{2}}} \right]^{4/3} \quad 3-13$$

A plot of the rate of fire spread through shredded newspaper to the $3/4$ vs. the integrated radiation rate minus $K(Q/L)_R/V^{\frac{1}{2}})^{4/3}$ for different K's is shown in Figure 3-5. The proper K should give a straight line. Figure 3-5 indicates that a large amount of the impinging external radiation is lost (about $4/5$). The small change in curvature with the increase in K makes this only approximate. The slope and intercept of the line in Figure 3-5 give the ignition energy and the integrated convective heat transfer rate. The convective heat transfer rate was found to be 94.0 Btu/hr-ft (0.224 cal/cm-sec) which makes it an important mechanism. The ignition energy was found to be a function of humidity as shown in Table 3-1.

Table 3-1

Humidity %	Q_o Btu/ft ²	Q_o cal/cm ²	
27	1.94	0.53	Based on a velocity V_o
37-39	2.19	0.60	of 60 ft/hr
47-49	2.40	0.65	

Additional runs were made with computer cards as fuel. The results for two different fuel sizes are shown in Figure 3-8. The energy for ignition for this fuel was found to be 9.0 Btu/ft² (2.4 cal/cm²) for the more finely divided fuel and 7.5 Btu/ft² (2.0 cal/cm²) for the fuel of larger particles. Some exploratory runs were made to find the effect of wind on the rate of fire spread through the shredded newspaper with a

wind generator described in Section 3-7. The results shown in Figure 3-12 indicate that a 3.5 ft/sec wind velocity increases the rate of spread three fold underlining the importance of wind in fire spread.

The second part of the experimental work consisted of measuring the flux density of radiation around methane and propane flames (Figure 5-1). The original data are shown in Figures 5-2 and 5-3. The data were taken from flames only two feet long and a correction was necessary to estimate the radiation from infinitely long flames by using exchange factors from gray gas wedges. The corrected data for infinitely long flames are shown in Figures 5-5 and 5-6.

The distribution of radiation on a horizontal plane on either side of an inverted gray gas wedge is shown in Section 4-7 to be given by

$$\frac{d \overline{gs}}{L dx} = \frac{(1 - e^{-BZ})}{2} \left[1 - \frac{(x/Z-a)}{\sqrt{1 + (x/Z-a)^2}} \right] \quad 4-46$$

In the above expression \overline{gs} is the direct exchange area, which when multiplied by the difference in black emissive powers of the gas and surface gives the net flux. The bracketed term represents twice the exchange area for the case of a black flame. Z is the flame height, x is the horizontal distance from the flame base to the surface element, and "a" is the slope of the flame wedge. The burden of making the result fit the rigorous solution is put on the exponent B in the expression giving the "effective emissivity, $(1 - e^{-BZ'})$ ". Z' is the product of the flame height Z and the absorption coefficient k' and B is the ratio of the mean beam length to the flame height, given in Figure 4-12 for $a=0.25$.

If the flame is well approximated by a gray gas wedge a plot of the experimentally determined surface flux density due to flame radiation divided by the flame emissivity, $(1 - e^{-BZ'})$, vs. the distance from the flame over the flame height should give a single curve. This plot is shown in Figure 5-7, based on use of all the data of Figures 5-5 and 5-6, together with a mean absorption coefficient determined by total radiation measurements on a laminar luminous flame with and without a mirror behind; k' was 2 and 10 ft^{-1} for methane and propane respectively. The solid lines represent the distributions around gray gas wedges of 1260°F for propane. Near its base the flame is not wedge shaped.

The third part of the experimental work consisted of measuring the flame heights of the line methane and propane fires. Dimensional analysis or modelling principles indicate that the ratio of the flame height, H , to the base width, \mathcal{W} , should depend on a group containing, $(Q/L)^2/\mathcal{W}^3$, where Q/L is the heat liberation rate per unit horizontal flame length. The data are shown in Figure 6-2 along with some data of Thomas, Webster and Raftery (31) for fires of circular and cubical fuel beds. The data compare favorably when the radius and width are used for circular and line fires, respectively, as would be expected if they are to be compared at an equal mean hydraulic radius. The data indicate the flame height of line fires over a useful range where natural fires occur is given by

$$\frac{H}{\mathcal{W}} = \gamma \left[\frac{(Q/L)^2}{\mathcal{W}^3} \right]^c \quad 6-53$$

The exponent c is between 0.33 and 0.40 in the useful range.

The distribution of radiation around gray gas rectangular parallelepipeds and wedges of infinite length was calculated on 709 and 7090 computers. The results are shown in Figure 4-8(a-h) and 4-11 respectively. The methods of calculation are discussedⁱⁿ Chapter 4.

Returning to the Summer Study Model, it is now possible to discuss the knowledge available for each term in equation 2-23, 2-28 and 2-29.

The heating of unburned fuel by radiation from the embers in the fuel bed beneath the gas flame, $(Q/L)_B$, is readily amenable to theory. It was shown in Section 2-4 to be

$$(Q/L)_B = \int_0^{\infty} a'b \sigma T_f^4 e^{-a'x} dx = \sigma T_f^4 b \quad 2-17$$

where a' is the reciprocal mean path length for radiation through the randomly placed fuel and b is the height of the fuel bed.

Obtaining the radiation from the overhead flame $(Q/L)_R$, has been one of the major endeavors of this work. When no wind is present the radiation from the flame can be well approximated by

$$(Q/L)_R = \int_0^{\infty} \sigma T_f^4 \left(\frac{d \bar{g} \bar{s}}{L dx} \right) dx \quad 7-2$$

where $d \bar{g} \bar{s} / L dx$ is the exchange factor given by either the gray gas wedge or the rectangular parallelepiped exchange factors from Figures 4-11 and 4-8(a-h) respectively. T_f is the average gray gas temperature which according to measured flux densities around propane and methane flames (Figure 5-7) is about 1200⁰F.

The convective heat transfer at the flame front, $(Q/L)_C$, is undoubtedly the most elusive for quantitative treatment. In this work values of 94.0 Btu/hr-ft for shredded newspaper fuel and close to zero for the computer

punch out fuel were found in the absence of wind. In an exploratory experiment a wind velocity of 3.5 ft/sec caused nearly a three-fold increase in the rate of spread over calm conditions. This means a corresponding increase in the convective heat transfer.

The heat loss from the unburned fuel as it preheats, $Q/L)_L$, is also a strong function of fuel type. However, it is believed that the treatment of this term in Section 3-4 by relating it to the other heat transfer rates, is a promising start. Although fuel beds with significant air spaces would complicate matters a workable relation may still be found.

The energy required to produce ignition, Q_i , has been determined in this work for fuel beds of shredded newspaper and computer cut-outs. For the newspaper it was found to decrease with humidity by approximately 10% for a 10% decrease in humidity. This is about one third more than would be expected if the change is based on the increase in the heat necessary to reach a fixed ignition temperature. However, until other data over a wider range of humidities becomes available it is recommended that the following relation be used:

$$Q_i = K'' \left(\frac{V_o}{V} \right)^{\frac{1}{4}} Q_o (c_p (T_i - T_a) + M\Delta H) \quad 7-3$$

where Q_o is the ignition energy at V_o , T_i is the ignition temperature, M is the moisture content of the fuel, ΔH is the latent plus sensible heat of water, and K'' is a characteristic of fuel type to be determined by experiment.

The radiation heat transfer to the burning fuel, $Q/L)_R$, can be handled in the same manner as the flame radiation to the fresh fuel.

The heat generation in the bed itself, Q/L , has not been studied in this work.

The relation between the flame height and the burning base width and the heat liberation recommended in Section 6-4 is

$$\frac{H}{W} = \gamma \left[\frac{Q/L^2}{W^3} \right]^c \quad 6-53$$

where c is between 0.33 and 0.40 and γ is a slight function of fuel type. This relation seems well enough established to be used with confidence.

It is believed that the functions for equations 2-23, 2-28 and 2-29 are sufficiently well known to justify their numerical solution on a computer. There are still many problems to be studied, particularly the evaluation of the shift in relative importance of the different terms which appear in the equations of the model when full-scale fuel beds (forests or cities) are of interest.

TABLE OF CONTENTS

	<u>Page</u>
SUMMARY	i
I INTRODUCTION	1
II THE DEVELOPMENT OF A MATHEMATICAL MODEL	3
2.1 Introduction	3
2.2 Description of the Problem	3
2.3 Earlier Models	4
2.4 The Woods Hole Summer Study Model	9
III DEVELOPMENT OF A PHYSICAL MODEL	15
3.1 Introduction	15
3.2 The Apparatus	16
3.3 The Effect of Fuel Loading Density	16
3.4 The Effect of Radiation	17
3.5 The Effect of Humidity	23
3.6 The Effect of Fuel Type	25
3.7 The Effect of Wind	26
IV TWO DIMENSIONAL INTERCHANGE FACTORS WITH AN ABSORBING GAS	30
4.1 Introduction	30
4.2 Interchange Factors Between a Volume Element of Gray Gas Infinite in One Dimension and a Black Strip Separated by Gray and Clear Gas	30
4.3 Interchange Factors Between a Volume Element of Gray Gas and a Black Spot Centrally Located Between the Ends Separated by Gray and Clear Gas	33
4.4 Interchange Factor Between Two Infinite Parallel Strips with a Gray and Clear Gas Intervening	34
4.5 Interchange Factor Between a Finite Black Strip and a Black Spot Centrally Located with a Gray Gas Intervening	35
4.6 Interchange Factors Between a Gray Gas Rectangular Parallelepiped of Height Z , Width W , and Infinite Length and a Black Infinite Parallel Strip dx Wide on a Surrounding Horizontal Surface	36

	<u>Page</u>
4.7 Interchange Factors Between an Infinite Gray Gas Wedge and an Infinite Black Strip on the Horizontal Surface Surrounding its Base	40
4.8 Total Interchange Areas	42
V RADIATION FROM A LINE FIRE	44
5.1 Introduction	44
5.2 Apparatus	44
5.3 Data on Line Fire Radiation	45
5.4 Correction of Data to an Infinitely Long Flame	45
VI THE FLAME AND RESULTING CONVECTION COLUMN	49
6.1 Introduction	49
6.2 Buoyant Plumes	49
6.3 A Model of a Burning Jet	52
6.4 Flame Heights	59
VII DISCUSSION OF RESULTS	65
7.1 Introduction	65
7.2 Results of this Work Applied to Actual Fire Spread	65
7.3 Conclusions	69
7.4 Recommendations	69
VIII APPENDIX	71
A Solution of Differential Equations	72
A.1 The Solution of the Differential Equation of Atallah's Model	72
A.2 The Solution of the Differential Equation of Atallah's Model Neglecting Conduction and Assuming the Exponential View Factor	76

	<u>Page</u>
B Measurement of Radiation from the Wires	80
B.1 The Flux Density of Radiation Around a Single Wire	80
B.2 The Flux Density of Radiation Around Several Wires	81
B.3 The Solution for the Integrated Radiation Flux, $Q/L)_R$, Around Several Wires	81
C Derivation of Heat Losses From Fuel Surface Considering Convection Losses	83
D The View Factor Between a Black Surface Inclined at an Angle α and a Black Spot Midway Between the Ends	85
E Moisture Content of the Fuel	88
F Original Data	89
F.1 Data on Fire Spread Through Shredded Newspaper and Computer Cards	89
F.2 Data of Radiation Flux Densities Around Methane Flames by de Rochechouart	95
F.3 Data of Radiation Flux Densities Around Propane Flames	102
F.4 Data on Flame Heights of Methane and Propane	104
G Nomenclature	105
IX REFERENCES	112

FIGURES

	<u>Page</u>
2.1 Flame Spread Through Solid Fuel	4
3.1 (a-b) Apparatus	16
3.2 Effect of Fuel Loading Density on the Rate of Fire Spread (Heating Rate 290 Btu/hr-ft, Humidity 37-40%)	17
3.3 Effect of Radiation on the Rate of Fire Spread (Humidity 47-50%, Shredded Newspaper)	17
3.4 Normalized Temperature Distribution as a Function of Distance from the Flame Front	20
3.5 Determination of K for Shredded Newspaper	20
3.6 Effect of Humidity on the Rate of Fire Spread (Shredded Newspaper)	23
3.7 Determination of K for Three Humidities (Shredded Newspaper)	23
3.8 Effect of Radiation on the Rate of Fire Spread for Computer Card Fuel	25
3.9 Determination of K for Computer Card Fuel (1/16"x1/8"x0.007")	25
3.10 Determination of K for Computer Card Fuel (1/2"x1/2"x0.007")	25
3.11 Effect of Wind Velocity on the Rate of Fire Spread for Dry Ponderosa Pine Twigs (Data by Fons (7))	26
3.12 Effect of Wind Velocity on the Rate of Fire Spread for Shredded Newspaper (Humidity 73-77%)	27
4.1 Interchange Between a Gray Gas Volume and a Black Spot Separated by Gray and Clear Gas	30
4.2 Fraction of Path in Gray Gas Between Gray Gas Volume and Black Spot	30

	<u>Page</u>
4.3 Mean Beam Length to Shortest Absorbing Distance Ratio Between a Two Dimensional Gray Gas Volume of Length $2Y$ and a Black Spot Centrally Located as a Function of the Shortest Dimensionless Absorbing Distance	33
4.4 Interchange Between Two Black Spots Separated by a Gray and Clear Gas	34
4.5 Fraction of Path in Gray Gas Between Two Black Spots	34
4.6 Mean Beam Length to Shortest Absorbing Distance Ratio Between a Black Strip of Length $2Y$ and a Black Spot Centrally Located as a Function of the Shortest Dimensionless Absorbing Distance	36
4.7 Interchange Between a Rectangular Parallelepiped of Gray Gas and a Black Strip	37
4.8 (a-h) Interchange Factors for an Infinite Gray Gas Rectangular Parallelepiped of Height Z' and Width W' and the Surrounding Surface as a Function of the Distance from the Center Line to Height Ratio	39
4.9 (a-f) Mean Beam Length for Equation 4-40 as a Function of the Ratio of the Distance from the Front Face to the Height	39
4.10 Interchange Between a Gray Gas Wedge and a Black Strip	40
4.11 Interchange Factors for an Infinite Gray Gas Wedge of Height Z' and Slope 0.25 and the Surrounding Surface as a Function of the Distance from the Center Line to Height Ratio	41
4.12 Mean Beam Length for Equation 4-46 as a Function of the Ratio of the Distance from the Center Line to the Height	42
4.13 Total Gas-to-Surface Interchange Factors	43
5.1 Line Fires (Methane)	44
5.2 Flux Density of Radiation on a Horizontal Surface Surrounding a Line Methane Flame for Different Heat Liberation Rates (Data by de Rochechouart (24))	45

	<u>Page</u>
5.3 Flux Density of Radiation on a Horizontal Surface Surrounding a Line Propane Flame for Different Heat Liberation Rates	45
5.4 Ratios of Exchange Factors for Infinite and Finite Line Wedges	46
5.5 Flux Density of Radiation on a Horizontal Surface Surrounding an Infinite Line Methane Flame for Different Heat Liberation Rates (Corrected)	47
5.6 Flux Density of Radiation on a Horizontal Surface Surrounding an Infinite Line Propane Flame for Different Heat Liberation Rates (Corrected)	47
5.7 Radiation Flux Density to Flame Emissivity Ratio as a Function of the Ratio of the Distance from the Center of the Flame to the Flame Height	47
6.1 Line Jet	54
6.2 Effect of the Normalized Burning Rate on the Flame Height to Flame Base Ratio	63
B.1 Line Heat Source	80
B.2 Distribution of Radiation on the Surface 1.25" Below Four Wires (Center to Center Distance to Diameter Ratio Equal to 3.0)	81
B.3 Distribution of Radiation on a Surface 1.25" Below Eight Wires (Center to Center Distance to Diameter Ratio Equal to 6.0)	81
D.1 Interchange Between a Finite Black Plane and a Black Spot	85
E.1 Moisture Content as a Function of Humidity for Newspaper and Computer Cards	88

TABLES

	<u>Page</u>
3.1 Heat Impulse Required to Produce Ignition vs. Humidity	24
F.1 The Effect of Loading Density of the Rate of Fire Spread for Shredded Newspaper (0.0003" thick)	89
F.2 The Effect of Radiation on the Rate of Fire Spread for Shredded Newspaper	90
F.3 The Effect of Humidity on the Rate of Fire Spread for Shredded Newspaper	91
F.4 The Effect of Radiation on the Rate of Fire Spread for Computer Punch Outs (1/8"x1/16"x0.007")	92
F.5 The Effect of Radiation on the Rate of Fire Spread for Computer Cards (1/2"x1/2"x0.007")	93
F.6 The Effect of Wind Velocity on the Rate of Fire Spread for Shredded Newspaper Fuel	94
F.7 Reproducibility of Data (Methane)	95
F.8 Radiation Flux Densities for Different Heat Liberation Rates (Methane)	97
F.9 Radiation Flux Density for a Different Slot Width and Two Different Heat Liberation Rates (Methane)	101
F.10 Radiation Flux Densities for Different Heat Liberation Rates (Propane)	102
F.11 Methane and Propane Flame Heights	104

I. INTRODUCTION

Everyone has experienced fire in both its controlled and uncontrolled forms. Early man considered it one of the elements. Adopting fire for useful applications was one of the earliest discoveries of man, even before the beast of burden. Throughout early history fire with air supplied by natural convection (or natural fire) was the only type in existence. During this time man discovered such facts as: small fuel must be used to start a fire, wet fuel must be dried before it will burn, an isolated log will soon cease to burn while several logs will burn brightly, blowing on an ember will cause it to burn more rapidly and even burst into flame, etc. Today these concepts seem very elementary and qualitative, but sometimes they are forgotten, resulting in wasted effort. It should also be remembered that none of the above processes even today is treated in more than a semi-quantitative manner.

With the coming of the Industrial Revolution, fire was harnessed to industrial needs, and with this came the more quantitative study of combustion. However, since natural fire has been of very little industrial use it has been a field in which the analysis remained semi-quantitative. Today, natural fire is seldom useful in industrial countries but it remains a potential threat to properties and lives. The economic loss from fire in an industrial country is huge. Direct fire damage in the United States alone is \$1.5 billion annually and the total economic loss is several times this figure. Fire is responsible for 11,500 deaths a year. However, when one considers that more than a billion cigarettes a day are lighted in the United States, each a pilot for a potential fire, the above figures seem quite small. For over a quarter of a century there has been no leveling of a city by fire in the United States. This indeed indicates that the use of scientific methods to develop new fire fighting equipment is justified and necessary. With the possibility of a nuclear war in which many large fires would undoubtedly be started it is a necessity to develop methods to meet this eventuality for national survival.

Most previous research in the fire field has been of a developmental nature such as the invention and testing of a particular piece of equipment to do a particular job. The last few years, however, have seen the growth of an increasing interest in understanding unwanted fire phenomena. The work

in this thesis is in the latter category and aims only to increase the basic understanding of the spread of fire. Some of the phenomena have been studied in a quantitative manner to contribute to the development of a model which would be useful in understanding the overall problem of fire spread.

II. THE DEVELOPMENT OF A MATHEMATICAL MODEL

2.1 Introduction

The spread of a fire through a forest, a home, or a city is a very complex phenomenon. No two cities or forests are the same physically, and the weather conditions vary so greatly that even if it were feasible to conduct large scale experiments, their usefulness at this time would be of doubtful value. It becomes necessary therefore, to construct and study models to obtain meaningful results.

The word model, as used by engineers or scientists, usually refers to a physical or mathematical model. Physical models are small scale processes in which some important properties to be studied are identical with the same properties of the full scale prototype. These models are useful in studying certain specific details or fundamentals of a process.

The mathematical model, on the other hand, attempts to describe the system "as it actually is" only in mathematical terms, so that one can visualize how the changing of important variables affects the process without actual tests. In most instances it is impossible to describe the system mathematically "as it actually is" and simplifying assumptions must be made.

In this thesis both physical and mathematical models have been used to gain a better understanding of fire spread. Physical models have been used to obtain a better comprehension of some of the fundamentals in fire spread while a mathematical model developed by the Woods Hole Summer Study Group has been the basis for extending these fundamentals to the general problem of predicting the rate of fire spread.

2.2 Description of the Problem

The major object of this thesis has been to describe the propagation of a steady state line fire through a uniform fuel bed. Note that initially no attempt is made at describing the development of a fire in a single dwelling. Although this is indeed important it is believed that a basic understanding of the spread of a steady state fire is required before the unsteady state development of a conflagration can be investigated on a fundamental level.

As a line fire spreads through a uniform fuel bed (a forest, a wheat field, Levittown, Pennsylvania, etc.) as shown in Figure 2-1, it preheats the fuel it is approaching by radiation, convection at the flame front, and sometimes by fire brands. The fuel ignites and becomes part of the general conflagration until the combustible part of the fuel is depleted and finally is extinguished as the flame passes on. This description applies only to a fully developed fire in which the length of the fire line and the height of the flame are large compared to any irregularity in the fuel bed. A fundamental understanding of this type of fire is not only an end in itself since this is primarily the way a large forest fire spreads, but is also the first step in the comprehension of the development of a fire and its suppression and prevention.

2.3 Earlier Models

It is interesting to discuss some of the mathematical models suggested by previous experimentors and point out their advantages and disadvantages. The first mathematical model was probably that suggested by Fons (7) who studied fire spread through light forest fuel. He assumed the fire to proceed through a uniform fuel by a succession of ignitions (as from one twig to the next). With the distance between fuel particles \bar{L} and the ignition time θ_i , corresponding to a temperature rise T_1 to T_2 (that is, twig $n + 1$ in front of the fire is at a temperature T_1 when twig n ignites). The rate of spread V is given by

$$V = \bar{L} / \theta_i \quad 2-1$$

Fons then writes a heat balance on an individual twig as

$$q_c + q_r = \bar{\gamma} \bar{c}_p \bar{V} \frac{dT}{d\theta} \quad 2-2$$

where

q_c = heat transfer to the fuel particle by convection, Btu/hr

q_r = heat transfer to the fuel by radiation, Btu/hr

$\bar{\gamma}$ = density of moist fuel, lb/ft³

\bar{c}_p = heat capacity of moist fuel, Btu/lb-°F

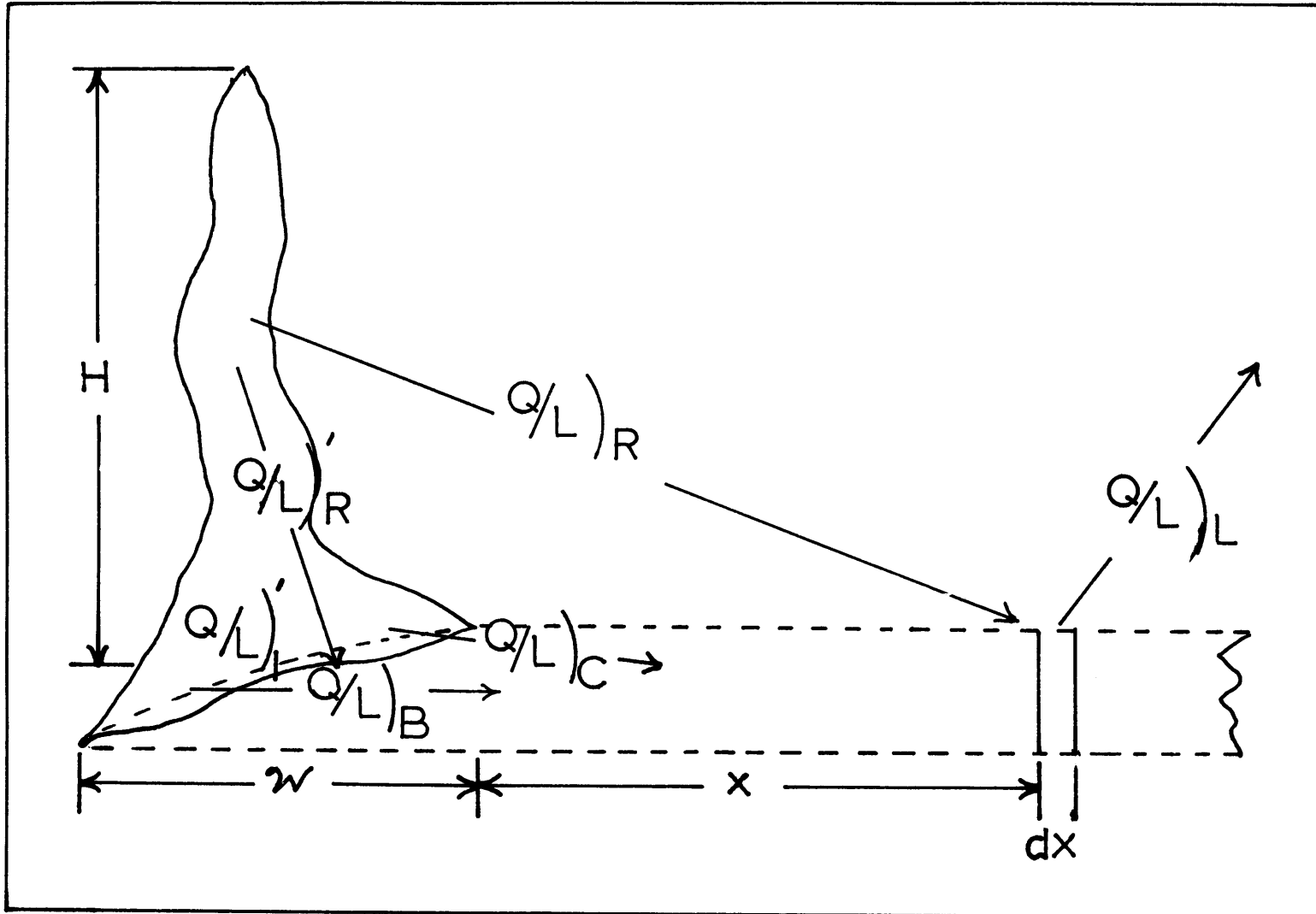


Figure 2-1 Flame Spread Through Solid Fuel

\bar{V} = volume of a fuel particle, ft³

T = temperature of the fuel particle, °F

Assuming the convection and radiation heat transfer to be given by

$$q_c = h_c A_s (T_f - T) \quad 2-3$$

$$q_r = h_r A_s (T_f - T) \quad 2-4$$

where A_s is the area of the fuel particle, h_c and h_r are the radiation and convection heat transfer coefficients respectively, and T_f is the flame temperature. Substituting and rearranging gives

$$\frac{dT}{T_f - T} = \frac{(h_c + h_r) A_s}{\gamma c_p \bar{V}} d\theta \quad 2-5$$

Integrating and applying the boundary conditions $T = T_1$ at $\theta = 0$ and $T = T_i$ at $\theta = \theta_i$ gives

$$\theta_i = \frac{\bar{\gamma} \bar{c}_p}{\bar{\sigma} (h_c + h_r)} \ln \frac{T_f - T_1}{T_f - T_i} \quad 2-6$$

where $\bar{\sigma} = A_s/\bar{V}$, the surface to volume ratio, and the rate of spread is given by

$$v = \frac{\bar{\sigma} (h_c + h_r) \bar{L}}{\bar{\gamma} \bar{c}_p \ln \frac{T_f - T_1}{T_f - T_i}} \quad 2-7$$

Fons points out that the rate of spread is influenced by

1. the convection heat transfer,
2. the radiation heat transfer,
3. the ignition temperature of the fuel,
4. fuel spacing,
5. surface to volume ratio,
6. specific heat of the fuel,
7. density of the fuel and
8. fuel temperature.

He says such things as wind velocity, moisture of fuel, fuel density, fuel size, fuel bed composition and slope are important in so far as they affect the fundamental variables.

Fons goes on to elaborate on some of the terms and how they are affected by the above indirect variables, but some of the deficiencies of this model are already apparent. The model is that of a fire which spreads by a series of ignitions as opposed to a continuous burning process. The use of the temperature of the twig next to the igniting twig T_1 is a clumsy choice. Finally, the size of the fire does not enter the analysis.¹ Therefore, it is futile to hope that constants obtained from the data on small fires could be extended to large fires. Consequently we must conclude that although this model is adequate to describe small fires it cannot be extended to large fires and therefore loses its usefulness as a mathematical model.

Another model is that suggested by Hottel (12) of a uniform flat fuel bed burning at a constant rate V . The flame front is infinite in length. The following assumptions have been made:

1. The density, the heat capacity, and the thermal conductivity of the fuel are independent of temperature.
2. The convection heat transfer coefficient at the surface U is independent of temperature.
3. The flame is approximated by a gray wall of constant emissivity ϵ_f and constant temperature T_f independent of height, and all back radiation not absorbed by the wall passes through it.
4. The temperature of the fuel is independent of depth, and no heat escapes through the bottom of the bed.

An energy balance around a small element of fuel which allows for heat transfer by radiation, convection and conduction, is given by

$$\begin{aligned}
 kl \frac{d^2T}{dx^2} + V \bar{c}_p \bar{y} l \frac{dT}{dx} - U(T - T_a) - \sigma \epsilon (T^4 - T_a^4)(1 - \epsilon_f F(x)) \\
 = - \sigma \epsilon \epsilon_f F(x) (T_f^4 - T^4)
 \end{aligned}
 \tag{2-8}$$

where

k is the thermal conductivity, Btu/hr-ft²/°F/ft

l is the thickness of the fuel, ft

T_1 is the ignition temperature of the fuel, °F

T is the temperature of the fuel, °F

T_f is the flame temperature, °F

T_a is the ambient temperature, °F

V velocity of the flame spread, ft/hr

\bar{c}_p heat capacity of the moist fuel, Btu/lb-°F

$\bar{\gamma}$ density of the moist fuel, lb/ft³

U convection heat transfer coefficient from the fuel, Btu/hr-ft²-°F

ϵ_f emissivity of the flame, dimensionless

ϵ emissivity of the fuel, dimensionless

σ Stefan-Boltzmann constant, Btu/hr-ft²-°R

F(x) view factor between dx and the flame, dimensionless

Use of the approximation,

$$T^4 - T_a^4 = \frac{(T_i^4 - T_a^4)}{(T_i - T_a)} (T - T_a) \quad 2-9$$

which is equivalent to making the radiation from the fuel dependent on the first power difference in temperature, with the coefficient correct only in the limit as T reaches T_i, gives with rearrangement

$$\begin{aligned} k \frac{dT}{dx} + U \bar{c}_p \bar{\gamma} \frac{dT}{dx} - \left[U + \frac{\sigma \epsilon (T_i^4 - T_a^4)}{(T_i - T_a)} \right] (T - T_a) \\ = - \sigma \epsilon \epsilon_f F(x) (T_f^4 - T_a^4) \end{aligned} \quad 2-10$$

the boundary conditions are

$$T = T_a \quad \text{at } x = \infty$$

$$T = T_i \quad \text{at } x = 0 \quad 2-11$$

$$\frac{dT}{dx} = 0 \quad \text{at } x = 0$$

Atallah (1) solved this equation but erred in the application of a boundary condition. The corrected solution is given in Appendix A-1 and is

$$C = - \frac{r_2}{\int_0^{\infty} e^{-r_1 z} F(z) dz} \quad 2-12$$

where

$$\begin{aligned}
 z &= x/H, \quad r_1 = \frac{-A + \sqrt{A^2 + 4B}}{2}, \quad r_2 = \frac{-A - \sqrt{A^2 + 4B}}{2}, \\
 A &= \frac{V \bar{c}_p \bar{\gamma} H}{k}, \quad B = \frac{UH^2}{kl} + \frac{\sigma \epsilon H^2 (T_i^4 - T_a^4)}{kl (T_i - T_a)}, \\
 C &= \frac{\sigma \epsilon_f H^2 (T_f^4 - T_a^4)}{kl (T_i - T_a)}
 \end{aligned} \tag{2-13}$$

It is impossible to obtain an explicit solution for the velocity of fire spread. If conduction is neglected and the true view factor $(1/2)(1 - \frac{z}{\sqrt{1+z^2}})$ is approximated by $e^{-z}/2$ (which is quite good, the area being the same under both curves) the solution (given in Appendix A-2) becomes

$$V = \left(\frac{B'}{2} - A' \right) \frac{H}{l} \tag{2-14}$$

where

$$\begin{aligned}
 A' &= \frac{\sigma \epsilon (T_i^4 - T_a^4)}{\bar{c}_p \bar{\gamma} (T_i - T_a)} - \frac{U}{\bar{c}_p \bar{\gamma}} \\
 B' &= \frac{\sigma \epsilon_f (T_f^4 - T_a^4)}{\bar{c}_p \bar{\gamma} (T_i - T_a)}
 \end{aligned} \tag{2-15}$$

The rate of spread is directly proportional to an effective radiation from the flame minus an effective radiation plus convection from the fuel, directly proportional to the height of the flame and inversely proportional to the depth of the fuel.

The disadvantages of this model are quite obvious. A great many assumptions are necessary to arrive at an answer which is then of doubtful value. A fuel bed which would possess a uniform temperature is so thin that some effective thickness must be used when a deep fuel bed is considered. B' and A' are given in defined variables but the simplifying assumption necessary to obtain an explicit solution can not be changed to provide for a more complex situation. No relation is given to obtain the flame height H which is a dependent variable. The undesirable characteristics of this model are the

usual ones encountered when writing a differential equation which one hopes to solve, because assumptions are necessary before the equation is written. In this case such things as an ignition temperature, a flame temperature, a distribution of heat in depth, a constant heat transfer coefficient were assumed to be known before the equation was written. The integral equations used in the Woods Hole Summer Study Model (2.4) do not suffer from this disadvantage.

Both of these models help to clarify one's thinking of fire spread but suffer from the questionable assumptions indicated.

2.4 The Woods Hole Summer Study Model (32)

This model has been presented in detail in the reference above with few changes, but it merits discussion here since the physical model developed in the present work was inspired by this mathematical model.

The model represents again mathematically the line fire in Figure 2-1 propagating across a fuel bed whose non-uniformities are small compared to the dimensions of the flame.

Consider first the preheating of the fuel. The fuel receives heat by various mechanisms, radiation, convection, and possibly even solar radiation. From whatever mechanism, the amount of energy reaching the fuel at a certain time per unit horizontal area per unit time is q . It is now necessary to define a quantity Q_1 which corresponds to the amount of heat per unit area that is necessary to produce combustion above the fuel when a pilot flame is present. It is apparent that this is the net amount of heat received by the fuel at the instant the flame reaches that part of the surface. Defining x as the distance from the leading edge of the flame, negative on the unignited side,

$$Q_1 = \int q \, dt = \frac{1}{V} \int_{-\infty}^0 q \, dx \quad 2-16$$

where V is the rate of spread. q , energy per unit horizontal area per unit time, is assumed to occur by four mechanisms of heat transfer, each independent of all the others.

$q_1(x)$ is the radiation through the fuel bed complex from the hot embers at

the base of the flame. Taking the embers as black radiators at a temperature T_f

$$q_1(x) = a' b \sigma T_f^4 e^{-a'x} \quad 2-17$$

where b is the height of the ember radiators, a' is the reciprocal mean free path or projected area per unit volume and σ is the Stefan-Boltzmann constant. The assumption of a black radiator requires the burning zone to be large compared to $1/a'$ and the height of the embers b must be large compared to $1/a'$ if losses through the top and bottom of the bed are to be neglected.

$q_2(x)$ represents the convection heat transfer due to bathing of the unburned fuel in a part of the flame. This mechanism depends on an eddy transfer at the flame front so that it will be a sensitive function of wind velocity, V_w , and wind turbulence, the flame height (if it is assumed that the wind produced by the fire is determined only by the flame height), the difference between the flame temperature and the local temperature, and the distance x from the flame. Therefore,

$$q_2(x) = [f_2(x, \text{flame height}, V_w, \text{wind structure})](T_f - T) \quad 2-18$$

$q_3(x)$ is the radiation from the flame itself to the unburned fuel. It will depend on the temperature and gas composition patterns in the flame, the distance x , and, since it will bend the flame, on the velocity of the wind. There is evidence that for a fixed flame without wind the radiation is determined uniquely by the flame height. Therefore,

$$q_3(x) = [f_3(H, V_w, x)] \sigma T_f^4 \quad 2-19$$

$q_4(x)$ is the heat lost by the fuel bed due to convective and radiative cooling of the unburned fuel. This heat loss will depend on the local velocity of the air, and therefore on the flame height, the wind velocity, and the local temperature difference. Thus,

$$q_4(x) = [f_4(V_w, H)](T - T_a) \quad 2-20$$

Since these four heating rates were assumed independent it is possible to write

$$vQ_i = \int_{-\infty}^0 (q_1(x) + q_2(x) + q_3(x) - q_4(x)) dx \quad 2-21$$

Define

$$\begin{aligned} Q/L)_B &= \int_{-\infty}^0 q_1(x) dx \\ Q/L)_C &= \int_{-\infty}^0 q_2(x) dx \\ Q/L)_R &= \int_{-\infty}^0 q_3(x) dx \\ Q/L)_L &= \int_{-\infty}^0 q_4(x) dx \end{aligned} \quad 2-22$$

The above quantities are the integrated heating rates to the unburned fuel. Equation (21) becomes

$$vQ_i = Q/L)_B + Q/L)_C + Q/L)_R - Q/L)_L \quad 2-23$$

This equation states that the velocity is directly proportional to the sum of the integrated heating rates and inversely proportional to the energy pulse required to produce ignition. There is no doubt of the validity of this equation where effects such as those of firebrands are absent, but the forms of the various quantities are not well known.

Consider now the burning zone where the combustible gases from the decomposing fuel feed the flame. It is assumed that the rate of chemical energy liberated in the evolving gases at a local point in the burning fuel is directly proportional to the amount of heat absorbed at that point. With q_g representing the heat of combustion or chemical energy of the gases liberated,

$$q_g = \beta q \quad 2-24$$

The heat input to the burning fuel q is assumed to consist of the radiation from the flame $q_3(x)$, described before, and the heat generation in the fuel bed itself $q_5(x)$. The latter is caused by combustion when air reaches into the

burning zone. This will be a function of the flame height, the wind velocity, and the distance from the flame front x . Thus,

$$q_g = \beta(q_3(x) + q_5(x)) \quad 2-25$$

It is now assumed that the evolution of combustible gas continues until a fraction η of the total fresh fuel is burned. Therefore,

$$\xi \eta Q_c v = \int_0^w \beta[q_3(x) + q_5(x)] dx \quad 2-26$$

where

ξ is the loading density of the fuel, lbs/ft²
 w is the width of the burning zone and
 Q_c is the heat of combustion of the fuel per unit mass.

Once again defining integrated energy transfer rates

$$\begin{aligned} Q/L)_R' &= \int_0^w q_3(x) dx \\ Q/L)_I' &= \int_0^w q_5(x) dx \end{aligned} \quad 2-27$$

gives

$$\frac{\xi \eta Q_c v}{\beta} = Q/L)_R' + Q/L)_I' \quad 2-28$$

Since there are three dependent variables, the velocity of spread, the width of the flame base and the height of the flame another relation is required which relates the flame height to the other variables. It was shown by Thomas (31) that the height-to-diameter ratio for a circular flame is a function of the square of the heat liberation rate in the flame divided by the radius of the flame source to the fifth power. Applying the same principles, the derivation for the line fire gives

$$\frac{H}{w} = f \left[\frac{(Q/L)^2}{w^3} \right] \quad 2-29$$

where

$$Q/L = \int_0^w q_g dx \quad 2-30$$

When the width of the flame becomes small compared to the flame height H the relation reduces to

$$H \propto (Q/L)^{2/3} \quad 2-31$$

This relation can be obtained by dimensional analysis or from the solution of the equations given in Section 6-3. However, the author's experience leads him to believe the simpler expression does not often occur in an actual forest fire.

There are now three equations and three unknowns (V , H , and W). Assuming the form of the Q/L functions and the function in equation 2-29 are known the equations 2-23, 2-28, and 2-29 would yield an explicit solution if the temperature distribution ahead of the flame did not appear in the heat loss term $(Q/L)_L$ of equation 2-23. However, by guessing a reasonable temperature distribution ahead of the flame, to be checked after the original result, a solution can be obtained.

Notice the advantages this model has over previous models. First, equation 2-23 depends only on the assumption that the various heating rates are independent. The equation is undoubtedly valid for any line fire no matter what the fuel arrangement. It is not necessary to make assumptions until the forms of the various Q/L 's are discussed. At some future time when better functions are available they can be inserted readily. This is the advantage the integral equation has over a differential equation. Secondly, this model advances on to determine the flame height and the thickness. These are dependent variables which the other models did not attempt to determine. Finally, although it is not presently possible to formulate some of the functions included in the analysis, the analysis shows where work should be done to fill in the missing information.

The disadvantage of this model compared with the other two is that no analytical solution is obtained.

On the basis of this model, the rate of spread is a function of the various mechanisms of heat transfer, the heat of combustion, the heat required for ignition, and the type and loading of fuel. The other variables such as wind velocity,

humidity, flame temperature, ignition temperature, etc. are important insofar as they affect these direct variables. This is a considerable reduction from those listed by Fons (7).

III. DEVELOPMENT OF A PHYSICAL MODEL

3.1 Introduction

The mathematical model of a line fire just developed showed that many important quantities are unknown. The development of physical models to obtain these quantities by experiment is necessary. Four earlier experimenters, Fons (7) and Fons, Bruce, Pong, and Richards (8) built line fires and measured the rate of fire propagation. Fons' (7) fires were built in a wind tunnel using as fuel ponderosa pine twigs mounted in saw dust. The distance between twigs and their diameters were varied in a series of experiments. Fons, Bruce, Pong, and Richards burned fuel cribs consisting of 1/2" to 1 1/4" square wood sticks on a moving conveyor belt. Some of Fons' data will be considered later.

Although the above experiments closely resemble actual forest fuel in many respects, they suffer from an inability to separate the various forms of heat transfer and do not offer much promise for extending an analysis to other fuel beds with larger fires.

The physical model developed in the present study came from a consideration of equation 2-23.

$$Q_i V = Q/L)_B + Q/L)_R + Q/L)_C - Q/L)_L \quad 2-23$$

Since the various mechanisms of heat transfer are assumed to be independent it was decided to eliminate all forms but one in order to study each individually. It is easy to eliminate $Q/L)_B$, the radiative transfer from the coals in the bed, by using a thin fuel bed which transmits a negligible amount of heat through itself. Choice of a fuel bed which burned with a small flame makes $Q/L)_R$, the radiative transfer from the overhead flame, of little importance. The fire now propagates only under the influence of the convection heat transfer at the flame front. If measured radiation from an external source is concentrated immediately in front of the fire it is possible to observe the effect of radiation on the rate of spread in a quantitative manner. This has been the objective of the following model.

3.2 The Apparatus

The apparatus, shown in Figure 3-1, consisted of a fuel bed 10 1/2-inches in width by 3 feet in length. The fuel rested on approximately 3 inches of non-flammable glass wool insulation on an asbestos sheet. It was possible to move the whole structure along the table when a fire was burning. Two fixed arrangements of No. 20 nichrome wires were stretched above the fuel bed and held in tension by weights over the side of the table. One set of wires consisted of four wires with center-to-center separating distances of three wire diameters. These wires were connected to an electric circuit capable of giving 15 amps and 110 volts. The other circuit consisted of eight No. 20 nichrome wires with center-to-center separating distances of 6 wire diameters and capable of conducting 15 amps and 220 volts. The radiation from the wires was measured at several points with a thermopile described by de Rochechouart (24). These measurements readily give the total radiation received by the fuel surface before ignition. The method is described in Appendix B. Several different kinds of fuels were distributed on the glass wool insulation. To prevent air from entering at the sides of the bed, glass wool strips were placed along the edges. The fuel beds were lighted evenly at one end. As the fire advanced over the fuel, the fuel bed structure was moved at such a rate as to keep the flame front directly below the closest wire. The top surface of the fuel was 1 1/4" below the wires. The fire was allowed to travel one foot to reach steady state. The rate of spread was measured over the last two feet by means of a stop watch. These fires were found to be quite reproducible. The original data are given in Appendix F-1.

3.3 The Effect of Fuel Loading Density

One of the fuels used in the experiments was small pieces of newspaper. The shapes of the individual pieces of newspaper were not uniform. The size was less than 1/2" in any dimension. The thickness was uniform, 0.003-inches. The particles of newspaper were scattered over the bed in a random fashion. Using this type of fuel, it was desired to find the effect of the fuel loading density (the amount of fuel per unit area). The data are shown in Figure 3-2 where the velocity of spread in ft/hr is plotted vs. the loading density at a single radiation rate of 290 Btu/hr-ft and a humidity of 37 - 40%. Also shown is the equivalent number of layers if the fuel had been evenly distributed.

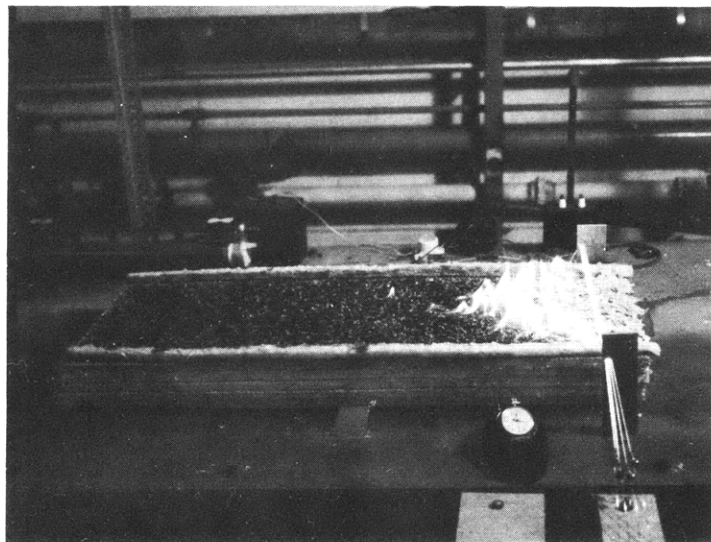
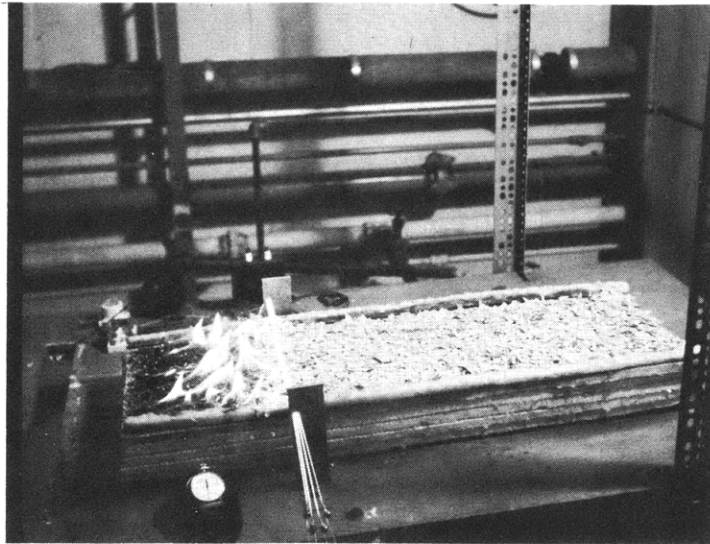


Figure 3-la Apparatus

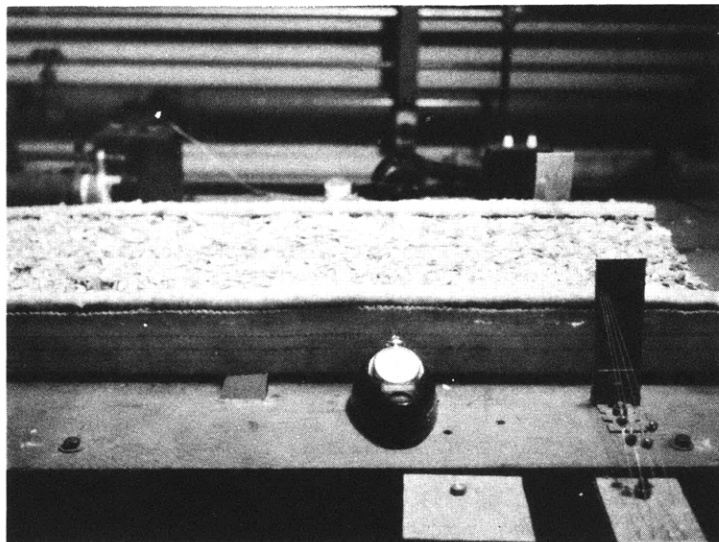
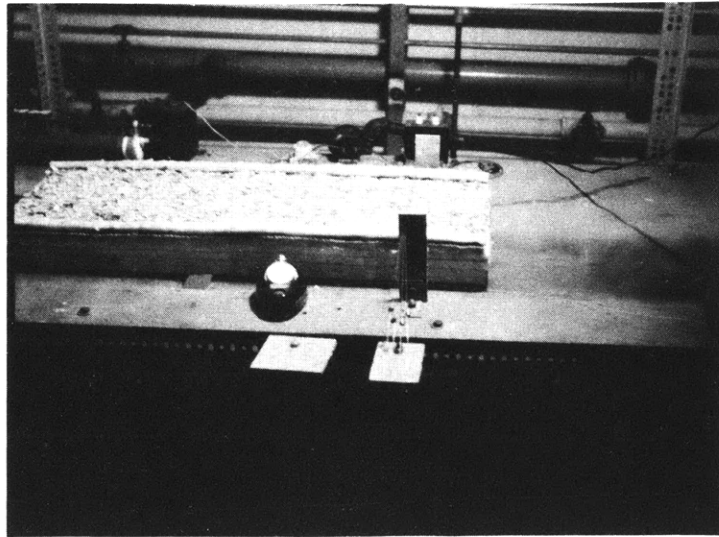


Figure 3-1b Apparatus

Inspection of Figure 3-2 shows that one equivalent layer will not burn, but that four equivalent layers burn with the same rate as ten equivalent layers and presumably as any greater number of equivalent layers. If it is assumed that the fuel is distributed on the surface at random the fraction of surface uncovered is given by

$$F = e^{-m} \quad 3-1$$

where m is the equivalent number of layers. If m is unity, the fraction uncovered is 0.368 and if m is 4 the fraction uncovered is 0.0183. Therefore, it can be concluded that if there is a continuous surface of fuel the amount of fuel present does not change the rate of fire spread. This would be expected if heat received by the fuel for preheat does not penetrate the fuel bed in depth to a significant extent and if the intensity of the fire is small so that the radiation from the flame itself is insignificant. Both of these qualifications are satisfied in the shredded newspaper fires. All newspaper fires studied subsequently contained six equivalent layers of fuel.

3.4 The Effect of Radiation

Fuel beds of shredded newspaper, identical with those described in the previous section and a loading density of approximately 0.0625 lbs/ft² (six equivalent layers of fuel), were burned with various amounts of radiation supplied by the wires. One set of data at constant relative humidity is shown in Figure 3-3 where the velocity of fire spread is plotted vs. the integrated radiation rate reaching the fuel surface in front of the fire. The above experiments show that irradiation at a rate of 600 Btu/hr-ft increases the rate of fire spread by a factor of approximately two over that with no irradiation.

For interpretation of these data refer to equation 2-23. Neglecting $Q/L)_B$, the radiation transfer through the bed itself,

$$Q_1 V = Q/L)_R - Q/L)_L + Q/L)_C \quad 3-2$$

The heat required to produce ignition Q_1 is undoubtedly a weak function of time. The heat impulse required to give a third degree skin burn, when exposed to radiation of different rates, varies with approximately the 1/3 power of

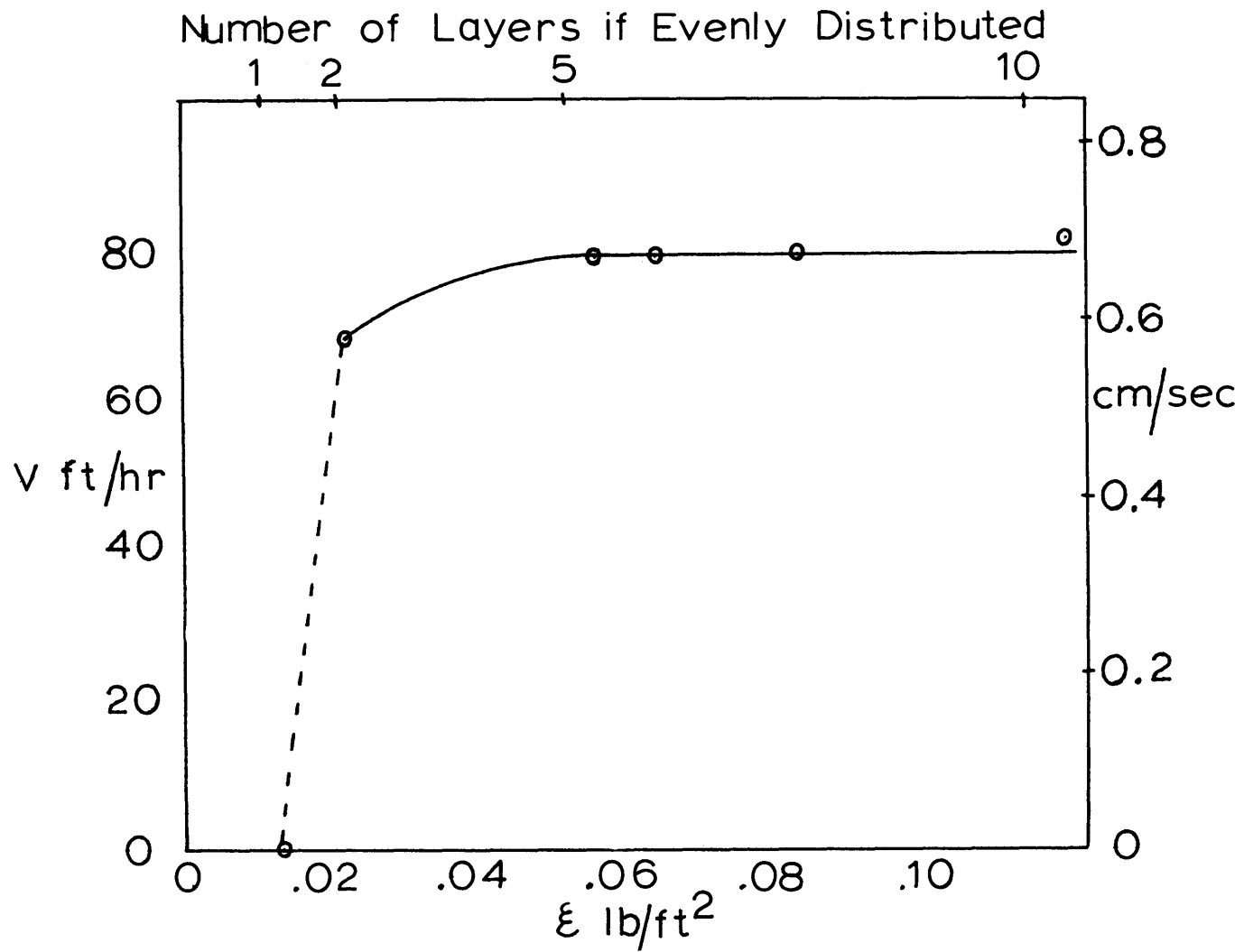


Figure 3-2 Effect of Fuel Loading Density on the Rate of Fire Spread
 (Heating Rate 290 Btu/hr-ft, Humidity 37-40%)

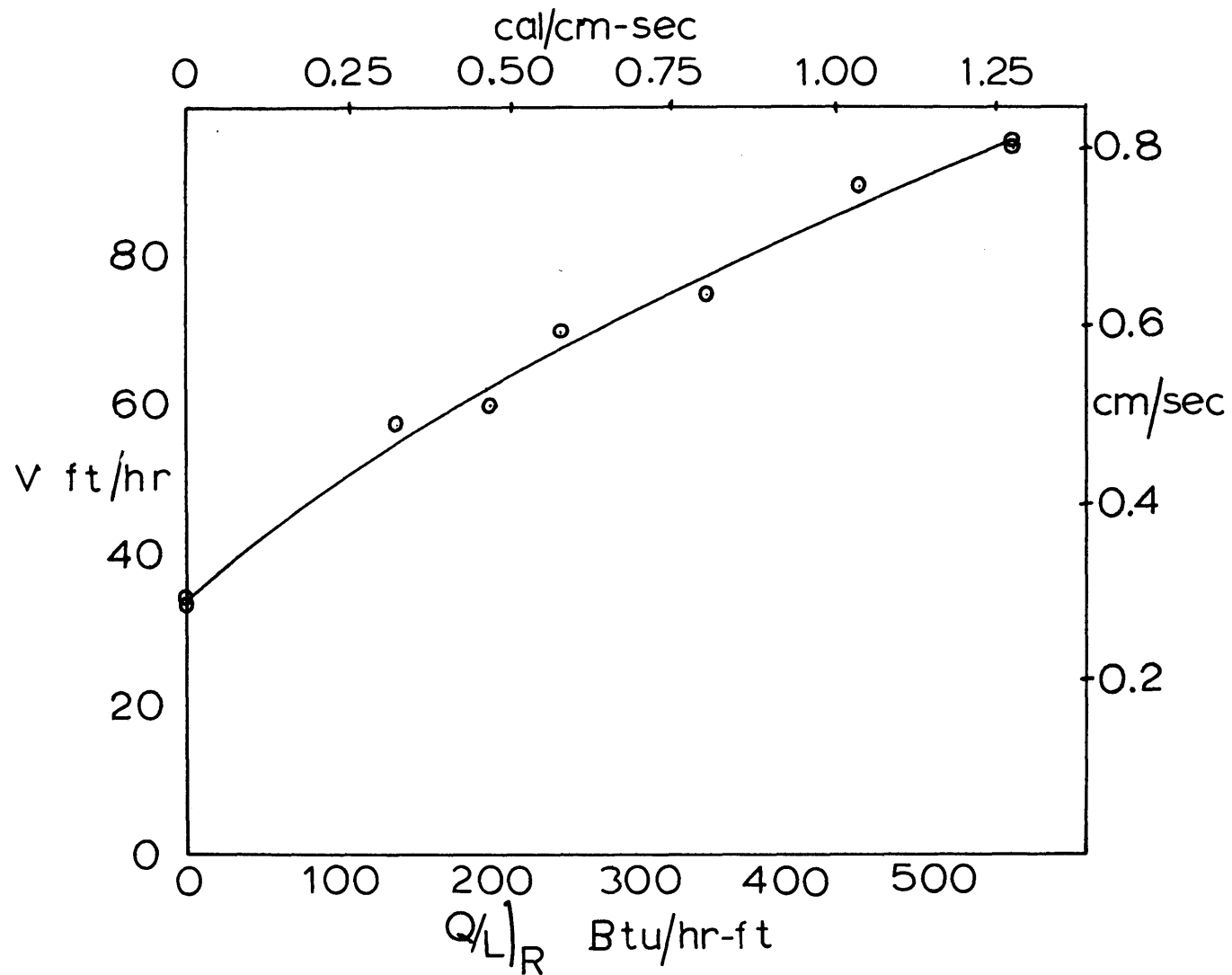


Figure 3-3 Effect of Radiation on the Rate of Flame Spread
(Humidity 47-49%, Shredded Newspaper)

time. Hottel and ^CWilliams (13) report the energy necessary to char wood to a prescribed depth depends on time raised to the 1/4 to 1/8 power. Bruce and Downs' (4) data show that the heat impulses required to produce spontaneous ignition of newspaper varies by the 1/4 to 1/5 power of time from 0.27 seconds to 3.18 seconds. Lawson and Simms (14) report piloted ignition of woods to depend on time to the 1/3 to 1/4 power over a range of 2 to 500 seconds. It is therefore reasonable to assume that in the range of heating rates provided by natural fire the energy required to produce ignition will vary with time raised to a low power; 1/4 is assumed. Therefore,

$$Q_i = \left(\frac{V}{V_o}\right)^{1/4} Q_o \quad 3-3$$

where Q_o is the pulse required at a reference velocity V_o . Equation 3-2 becomes

$$V^{3/4} = \frac{1}{Q_o V_o^{1/4}} [(Q/L)_R - (Q/L)_L] + \frac{(Q/L)_C}{Q_o V_o^{1/4}} \quad 3-4$$

If the heat transfer by convection at the flame front is assumed not to be a function of the heat added by radiation, a plot of the velocity of spread to the 3/4 power vs. the heat added by radiation minus the heat lost from the surface as it preheats, will give a straight line. It is unfortunate that the important quantity $(Q/L)_R - (Q/L)_L$, the net heat input to the fuel, can not be measured directly. However, it is now apparent that the distance between the wires and the fuel bed is not a variable of fundamental significance. The rate of spread will decrease as the distance from the wires increases with the same integrated radiation input, $(Q/L)_R$, because the heat is distributed over a wider area and a greater amount is lost by convection and back radiation. At any distance from the wires the same $(Q/L)_R - (Q/L)_L$ will give the same rate of fire spread over identical fuel. The problem remains to find the integrated heat loss, $(Q/L)_L$.

The solution for the temperature pattern of a semi-infinite solid of constant thermal properties, originally at a constant temperature T_a , ^{ir}radiated at the surface at a rate varying with time, is given by Carslaw and Jaeger (6) as

$$T - T_a = \frac{\sqrt{(\alpha/\pi)}}{k} \int_0^t \frac{Q(\lambda) e^{-(d^2/4\alpha(t-\lambda))} d\lambda}{(t-\lambda)^{1/2}} \quad 3-5$$

where

- α is the thermal diffusivity, ft^2/hr
- k is the thermal conductivity, $\text{Btu}/\text{hr}\cdot\text{ft}\cdot^\circ\text{F}/\text{ft}$
- $Q(\lambda)$ is the radiation flux density at the surface, $\text{Btu}/\text{hr}\cdot\text{ft}^2$
- d is the distance below the surface, ft
- t is the time of heating, hr
- λ is the dummy variable in time, hr

Notice that the above solution does not include a latent heat effect. However, let us assume that this equation gives the surface temperature of the fuel bed as it is moved under the radiating wires. Replacing the time variable by

$$t = y/V \quad \text{and} \quad \lambda = \bar{y}/V \quad 3-6$$

the surface temperature is given by

$$T - T_a = \frac{\sqrt{(\alpha/\pi)}}{kV^{1/2}} \int_0^y \frac{Q(\bar{y}/V) d\bar{y}}{(y - \bar{y})^{1/2}} \quad 3-7$$

Since it is more convenient to measure the distance of a point on the fuel bed surface from the flame instead of from infinity, let

$$x = -z + y \quad \text{and} \quad \bar{x} = -z + \bar{y} \quad 3-8$$

and let $z \rightarrow \infty$. Then the temperature of the surface is given as a function of the distance from the flame by

$$T - T_a = \frac{\sqrt{(\alpha/\pi)}}{kV^{1/2}} \int_{-\infty}^x \frac{Q\left(\frac{\bar{x} + z}{V}\right) d\bar{x}}{(x - \bar{x})^{1/2}} \quad 3-9$$

If the net heat flux at the surface is assumed to be only the radiation from the wires, the convection and back radiation being neglected, $Q(\bar{x})$ is given by

$$Q\left(\frac{\bar{x} + z}{V}\right) = Q_w \frac{\bar{x}(\bar{x})}{L} \quad 3-10$$

(see Appendix B) where Q_w is the heat per unit length radiated from a single wire and $\mathcal{F}(x)/L$ is the view factor between all the wires and a point on the flat fuel surface. Also shown in Appendix B, the radiation from a single wire is directly proportional to the rate at which radiation is received by the fuel $(Q/L)_R$. Therefore,

$$T - T_a = \frac{K' (Q/L)_R}{v^{1/2}} \int_{-\infty}^x \frac{\mathcal{F}(\bar{x})/L d\bar{x}}{(x - \bar{x})^{1/2}} \quad 3-11$$

If the above equation holds, $(T - T_a)v^{1/2}/(Q/L)_R$ should only be a function of x .

The temperature of the top layer of fuel was measured with a 0.003-inch copper-constantan thermal couple for five different heating rates at the same humidity. The normalized measured temperatures are shown in Figure 3-4 and show fair agreement with the above analysis. The curve on Figure 3-4 shows the shape of the integral on the right hand side of equation 3-11.

The heat loss, while the fuel preheats, is assumed to be given by

$$(Q/L)_L = \int_{-\infty}^0 h(T - T_a)^p dx \quad 3-12$$

where h is assumed constant. Therefore,

$$(Q/L)_L = K \left[\frac{(Q/L)_R}{v^{1/2}} \right]^p \quad 3-13$$

The heat loss is directly proportional to the rate of radiation divided by the velocity of spread to the $1/2$ power, all raised to the p power. Equation 3-4 becomes

$$v^{3/4} = \frac{1}{Q_o v_o^{1/4}} \left[(Q/L)_R - K \left[\frac{(Q/L)_R}{v^{1/2}} \right]^p \right] + \frac{(Q/L)_C}{Q_o v_o^{1/4}} \quad 3-14$$

Let p be $4/3$ as recommended for natural convection by McAdams (18). $v^{3/4}$ is plotted vs. $(Q/L)_R - K[(Q/L)_R/v^{1/2}]^{4/3}$ for various K 's in Figure 3-5. The proper K gives a straight line and appears to be approximately 2.0. This corresponds to a $Q_o v_o^{1/4}$ equal to 6.7. If the reference velocity v_o is taken as 60 ft/hr, Q_o equals 2.4 Btu/ft² (0.65 cal/cm²). This corresponds to a

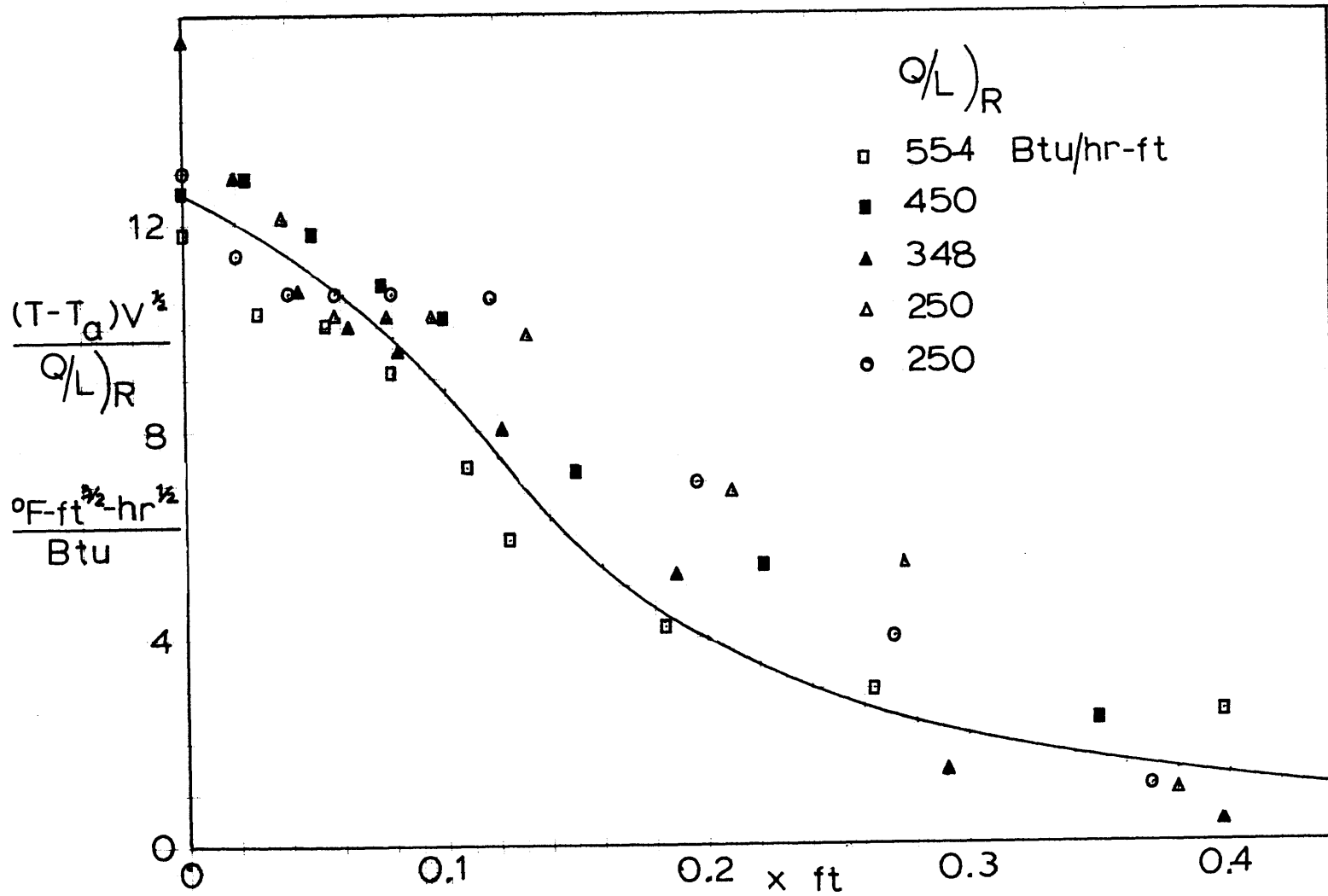


Figure 3-4 Normalized Temperature Distribution as a Function of Distance from the Flame Front

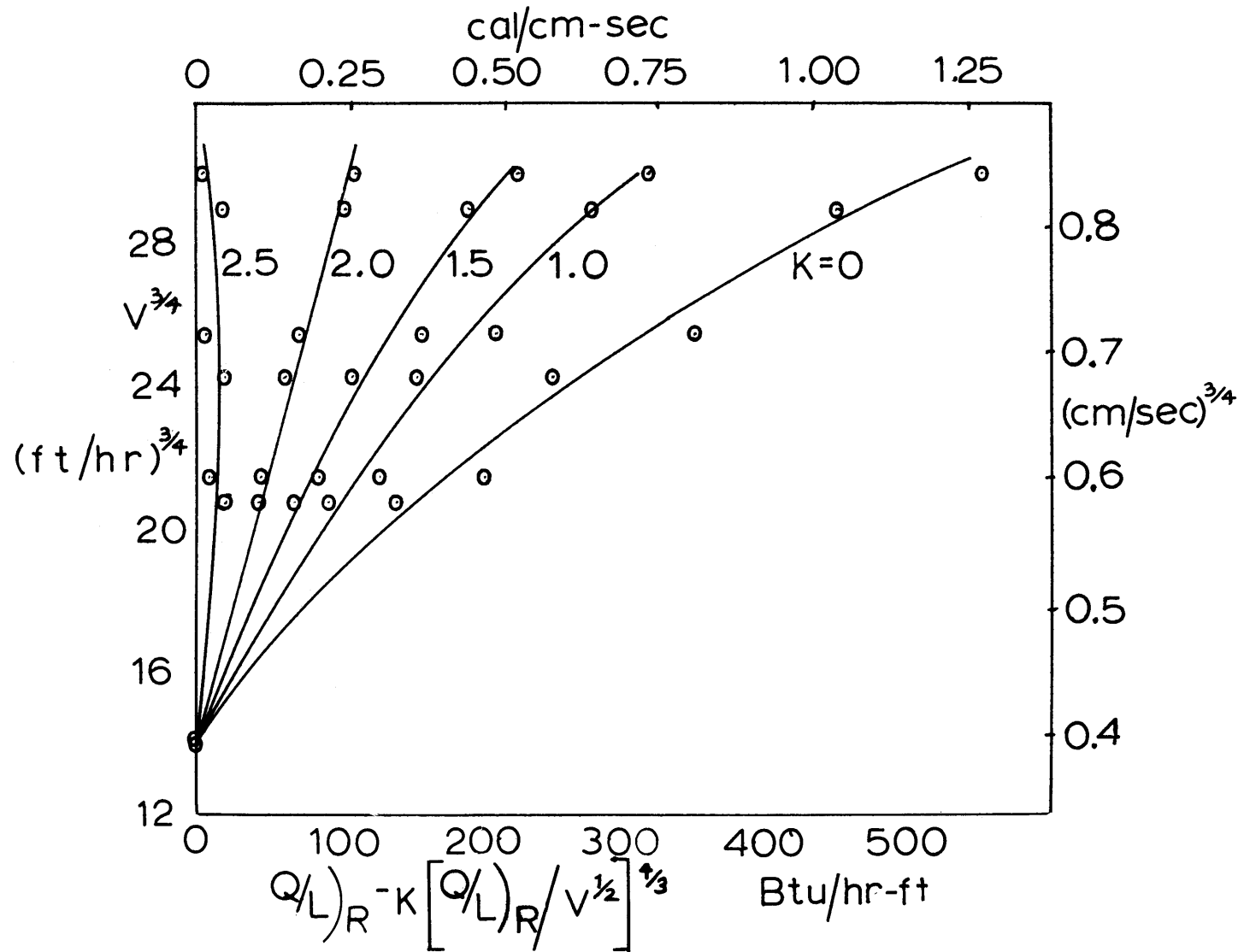


Figure 3-5 Determination of K for Shredded Newspaper Fuel

convection heat transfer rate of 94.0 Btu/hr-ft (0.224 cal/cm-sec.). Unfortunately the straightness of the line is not a very sensitive function of K.

A value of 0.65 cal/cm² may seem rather low to produce piloted ignition. However, Figure 3-5 indicates a considerable amount of the impinging radiation is back radiated or convected away from the surface (slightly more than 4/5). Broido and Martin (3) report values of from 5 to 14 cal/cm² to produce transient flaming and at least 11 cal/cm² to give sustained flaming at the surface of alphacellulose papers. The above values are for non piloted ignition. Bruce and Downs (4) report 5-8 cal/cm² to ignite newspaper in a similar experiment. Martin, Lincoln and Ramsted (16) report 4 to 20 cal/cm² to ignite various types of paper. Lawson and Simms (14) report values of 4 cal/cm² for fiber board and 7 cal/cm² for freijo to produce ignition in 5 seconds when a pilot flame is held 1/2" from the surface. They also report 6.5 and 12 cal/cm² for spontaneous ignition of the same materials, giving a ratio of about 1.7 for piloted ignition to spontaneous ignition. If the value of 5 cal/cm² reported by Bruce and Downs for newspaper is divided by the 1.7, a piloted ignition of 2.9 cal/cm² is obtained from the present data. Figure 3-5 indicates that a large amount of the total external radiation received at the fuel surface is lost by convection and back radiation. If a line were drawn through the data of Figure 3-5 with no consideration for heat loss at the surface, (K = 0) a value for the ignition energy of approximately 4.5 times that previously quoted would be obtained. With this consideration the 0.65 cal/cm² compares favorably with that reported by Bruce and Downs. The uncertainty of the amount of heat loss at the surface is indeed unfortunate.

It should be remembered, however, that in arriving at the relation $Q/L)_L = K [Q/L)_R / v^{1/2}]^{4/3}$ it was assumed that heat entering at the surface of the fuel $Q(\bar{x})$ came exclusively as radiation from the wires. Actually Figure 3-4 indicates a large amount of this heat leaves the surface by convection or back radiation. Consequently 3-10 could be replaced by

$$Q(\bar{x}) = Q_w \frac{\tilde{X}(\bar{x})}{L} - h_{r+c} (T - T_a)^p \quad 3-15$$

A derivation given in Appendix C indicates the form of the expression for the temperature distribution on the surface would be approximately

$$T - T_a = \left[K_1 \frac{(Q/L)_R}{\sqrt{1/2}} - \frac{K_2}{\sqrt{1/2}} \left[\frac{(Q/L)_R}{\sqrt{1/2}} \right]^p \right]^p \quad 3-16$$

Since the powers are not greatly different on the two terms it is unlikely that this change could affect the slope of the line in Figure 3-5 to a large extent.

Another possibility is that the heated wires change the convection across the unburned fuel by a significant amount. In this case the heat transfer coefficient h in equation 3-12 might be given by

$$h = h_o [(Q/L)_R]^s \quad 3-17$$

This would give a line on Figure 3-5 with a lower slope and consequently a higher value of Q_o . At the present time any attempt to determine the influence of the heated wires on the convection heat transfer at the surface would be only a guess. The given analysis is considered an adequate first approximation for present purposes.

The convective heat transfer at the flame front may be assumed to be

$$(Q/L)_C = h l' (T_f - T_i) \quad 3-18$$

where

- h is the convection coefficient, $\text{Btu/hr-ft}^2\text{-}^\circ\text{F}$
- l' is the distance over which the transfer occurs, ft
- T_f is the flame temperature, $^\circ\text{F}$
- T_i is the ignition temperature, $^\circ\text{F}$

Assuming the temperature difference to be 1000°F and l' as $1/4$ inch (a visual estimate), h would be $4.7 \text{ Btu/hr-ft}^2\text{-}^\circ\text{F}$, a reasonable number. Since this heat transfer occurs by an eddy process, $(Q/L)_C$ can be written as

$$(Q/L)_C = e c \mathcal{D}_e (T_f - T_i) \quad 3-19$$

and

$$D_e = u_e l'$$

3-20

The corresponding values for the eddy diffusivity and the eddy velocity are 2.0 ft²/hr and 1.59 ft/min (96 ft/hr). The eddy transfer occurs by the flame slipping under the fuel immediately ahead of it, presumably because air is drawn across the surface into the fire. Quantitative study of this process is indeed difficult.

3.5 The Effect of Humidity

Humidity greatly affects the spread of fire since natural fuels absorb and desorb moisture readily. Prolonged dry weather will cause vegetation to die and become very dry. Although absorption and desorption of moisture by living vegetation is a complex process, that of dead fuel is reversible. The fuel used in these experiments is so thin, 0.003 inches, that it is virtually in equilibrium with the humidity of the room at all times. The moisture content of a sample of the fuel vs. humidity is given in Appendix E. Figure 3-6 shows data for three humidity, 27%, 37-39% and 47-49%. A decrease in humidity of approximately 20%, at the same rate of radiation, gives about a 20% increase in flame spread. This corresponds to approximately 1.8% change in moisture content of the fuel.

If the line $K = 2.0$ in Figure 3-5 were extended to negative values it would intersect at the zero axis at $-Q/L)_C$. Since it is believed that this value is independent of humidity, the extended lines for the other two humidities must pass also through this point. Figure 3-7 shows these lines. The values for K which best fit the data are $K = 2.35$ for 27% humidity and $K = 2.14$ for 37-39% humidity. A different value for K is required since

$$\frac{Q/L)_L}{h_c + r} = \int_{-\infty}^0 \left[\sqrt{\frac{\pi}{k \bar{y} c_p v}} \int_{-\infty}^x \frac{Q(\bar{x}) d\bar{x}}{(x - \bar{x})^{1/2}} \right]^a dx \quad 3-21$$

The density is a slight function of humidity and the heat capacity is a strong one. If it is assumed that

$$\bar{c}_p = c_p + M \frac{\Delta H}{\Delta T} \quad 3-22$$

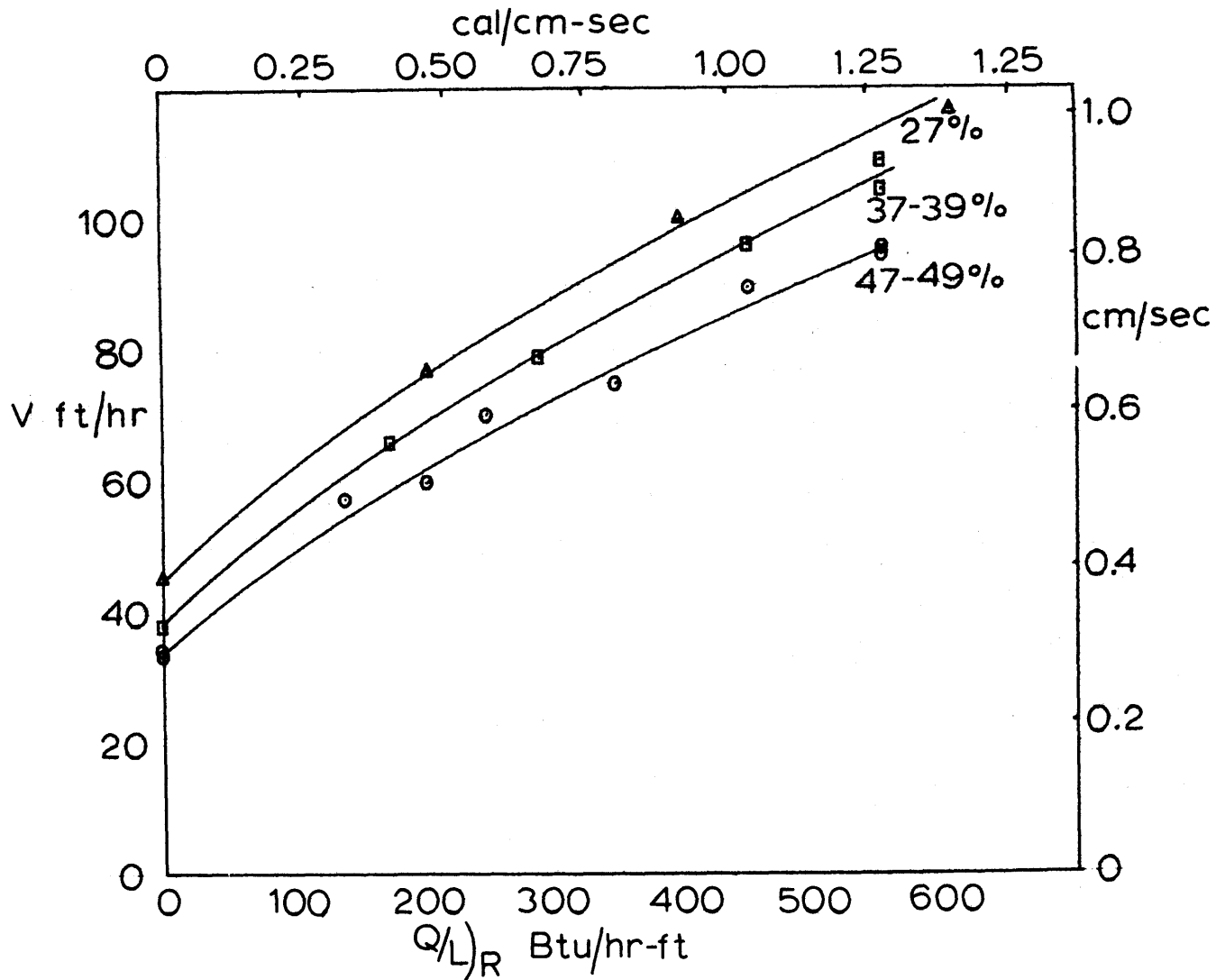


Figure 3-6 Effect of Humidity on the Rate of Fire Spread
(Shredded Newspaper)

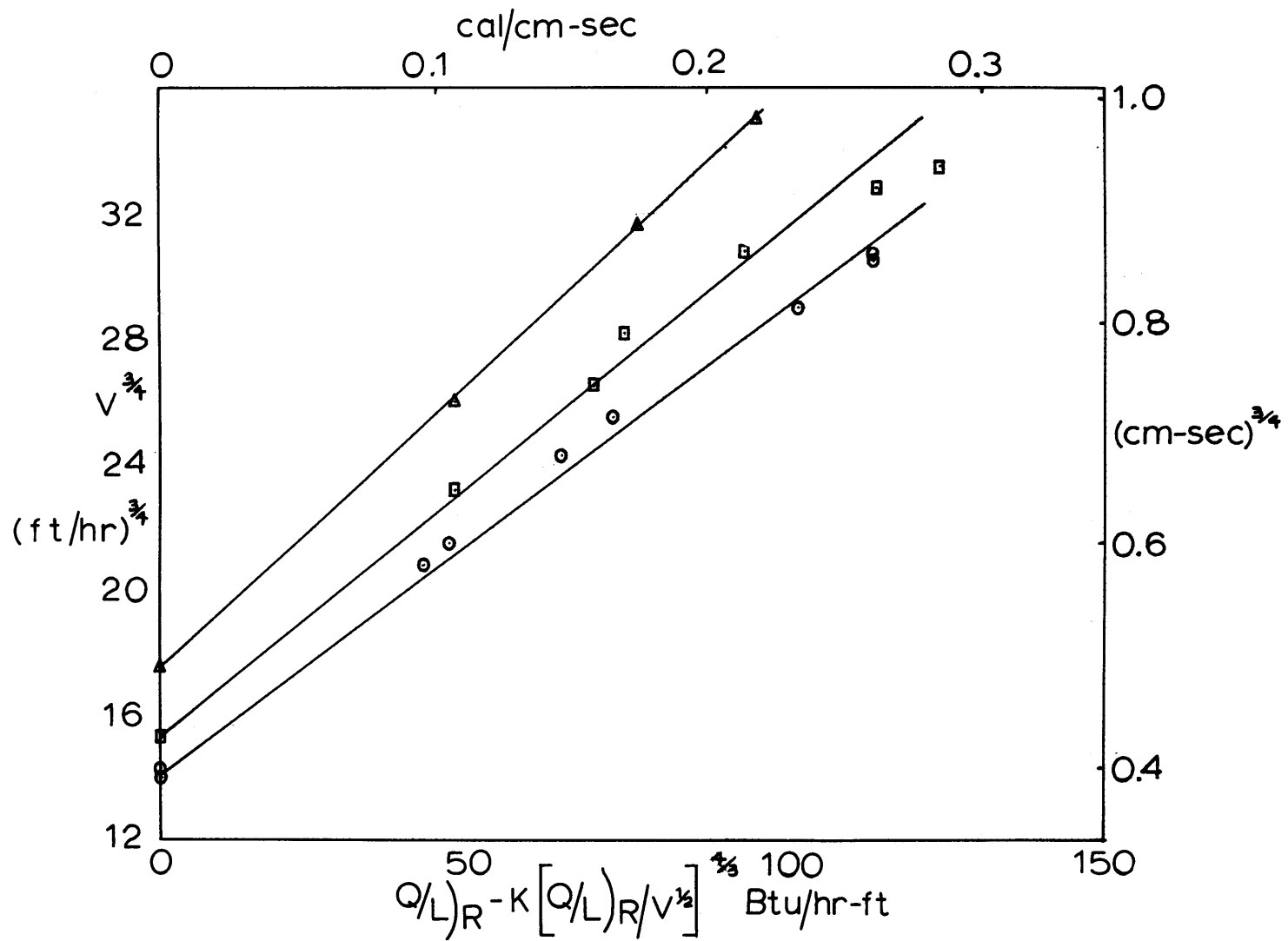


Figure 3-7 Determination of K for Three Humidities
(Shredded Newspaper)

where

- c_p is the heat capacity of the dry fuel, Btu/lb-°F
 M is the moisture content per lb of dry fuel, lb/lb
 ΔH is the enthalpy required to heat up and evaporate the moisture, Btu/lb
 ΔT is the overall temperature rise in the fuel, °F

Substituting reasonable values into equation 3-24 gives the following

$$\bar{c}_p = 0.24 + 1100 \frac{M}{\Delta T} \quad 2-23$$

The change in heat capacity due to the 1.8% decrease in moisture content would change K by approximately 9%, assuming an ignition temperature of 500°F. The change in K is about twice as great as would be expected from this consideration alone.

For a standard velocity of $V_o = 60$ ft/hr the ignition energy for pilot ignition for the three humidities is given below,

Table 3-1

Humidity	Q_o Btu/ft ²	cal/cm ²	
27	1.94	0.53	Based on a velocity of 60 ft/hr
37 - 39	2.19	0.60	
47 - 49	2.40	0.65	

Approximately a 20% change in relative humidity (1.8% change in moisture content) gives a 20% change in the heat required to produce ignition.

Bruce and Downs (4) report that a 10% increase in moisture content increases the heat required for spontaneous ignition by 10%. Since unpiloted ignition occurs at 500°C rather than the 300°C of piloted ignition, it would be expected that moisture would affect the latter to a greater extent. Also it is not improbable that water vapor leaving the surface increases turbulence which Simms (29) has shown, lowers the radiation required to produce spontaneous ignition. It also should be remembered that the values derived from the fire data are obtained by an indirect method and could be somewhat higher.

3.6 The Effect of Fuel Type

Any attempt to determine the influence of the type of fuel on the various integrated heat transfer rates and the energy pulse required to produce ignition in a quantitative manner is a problem of immense magnitude. When one considers the possible fuel beds, from pine needles on a forest floor to uniformly spaced houses in a city, there is much work to be done.

Two other fuels were used in this study, the punch outs of computer cards (1/16 x 1/8 x 0.007-inches) and computer cards cut in squares approximately 1/2 x 1/2 x 0.007-inches. The effect of added external radiation on the rate of fire spread for both fuels is shown in Figure 3-8. Neither of these fuels burned without external radiation. This has been confirmed by the extinguishment of developed fires when the external radiation was removed.

Figure 3-9 and 3-10 show the plot described in Section 3-6

$$v^{3/4} \text{ vs. } [(Q/L)_R - K(Q/L)_R/v^{1/2}]^{4/3}$$

It is demonstrated that a straight line through the origin can not be obtained with a positive slope. However, if the point at the origin is neglected, a K of 0.6 for the fine fuel and 0.7 for the 1/2" squares gives a straight line. This may be explained by the following: when a fire supported by radiation is burning, there is a small but finite amount of convection heat transfer at the flame front. When the radiation is removed, the heat loss is greater than this convection heat transfer and the fire is extinguished.

The energy required for ignition based on the lines in Figure 3-9 and 3-10 at the standard velocity of 60 ft/hr are 9.0 Btu/ft² (2.4 cal/cm²) for the fine fuel and 7.5 Btu/ft² (2.0 cal/cm²) for the 1/2 " squares. It is apparent that these values are quite crude. To determine a better value would require larger amounts of external radiation than was available. The larger energy rates required to produce ignition of the computer card fuel is undoubtedly due to the increase in the thermal conductivity of the fuel particles. The computer fuel elements are rigid and the fuel bed is considerably more compact than that of the newspaper fuel. Again looking at equation 3-23, the thermal conductivity and the fuel density are the variables changing in this instance. A three-fold change of K between the newspaper and the computer cards corresponds to

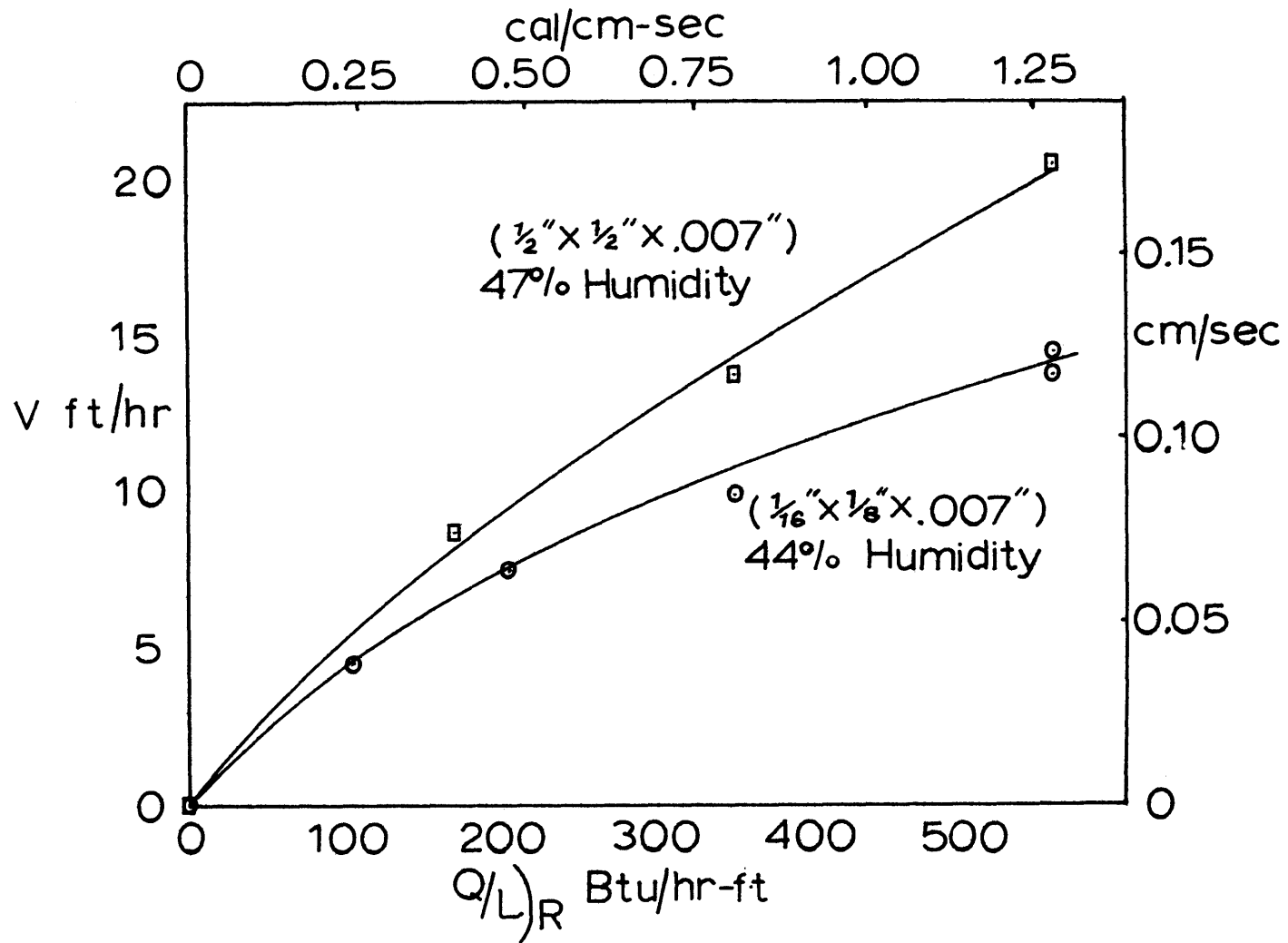


Figure 3-8 Effect of Radiation on the Rate of Fire Spread for Computer Card Fuel

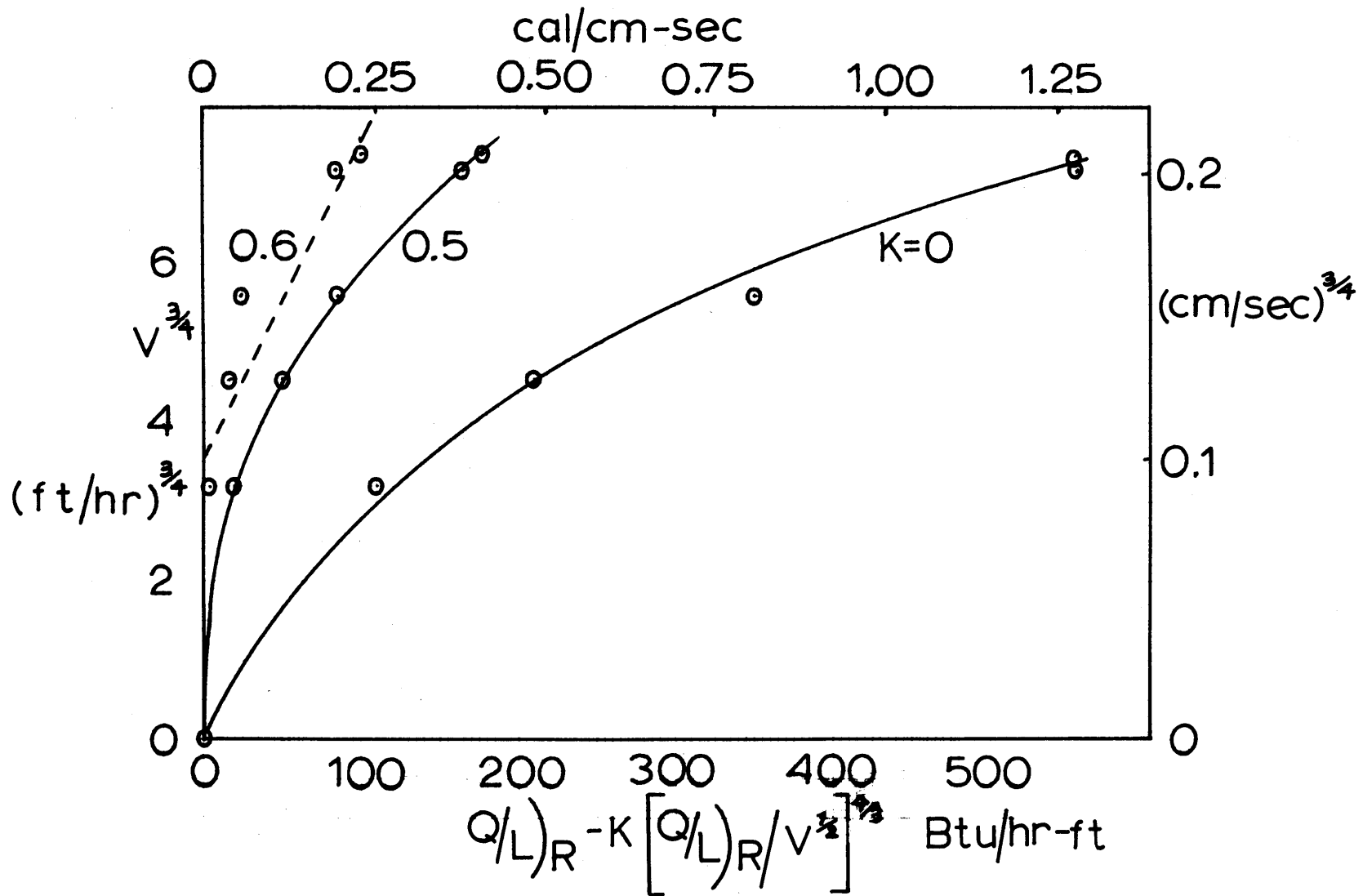


Figure 3-9 Determination of K for Computer Card Fuel (1/16"x1/8"x.007")

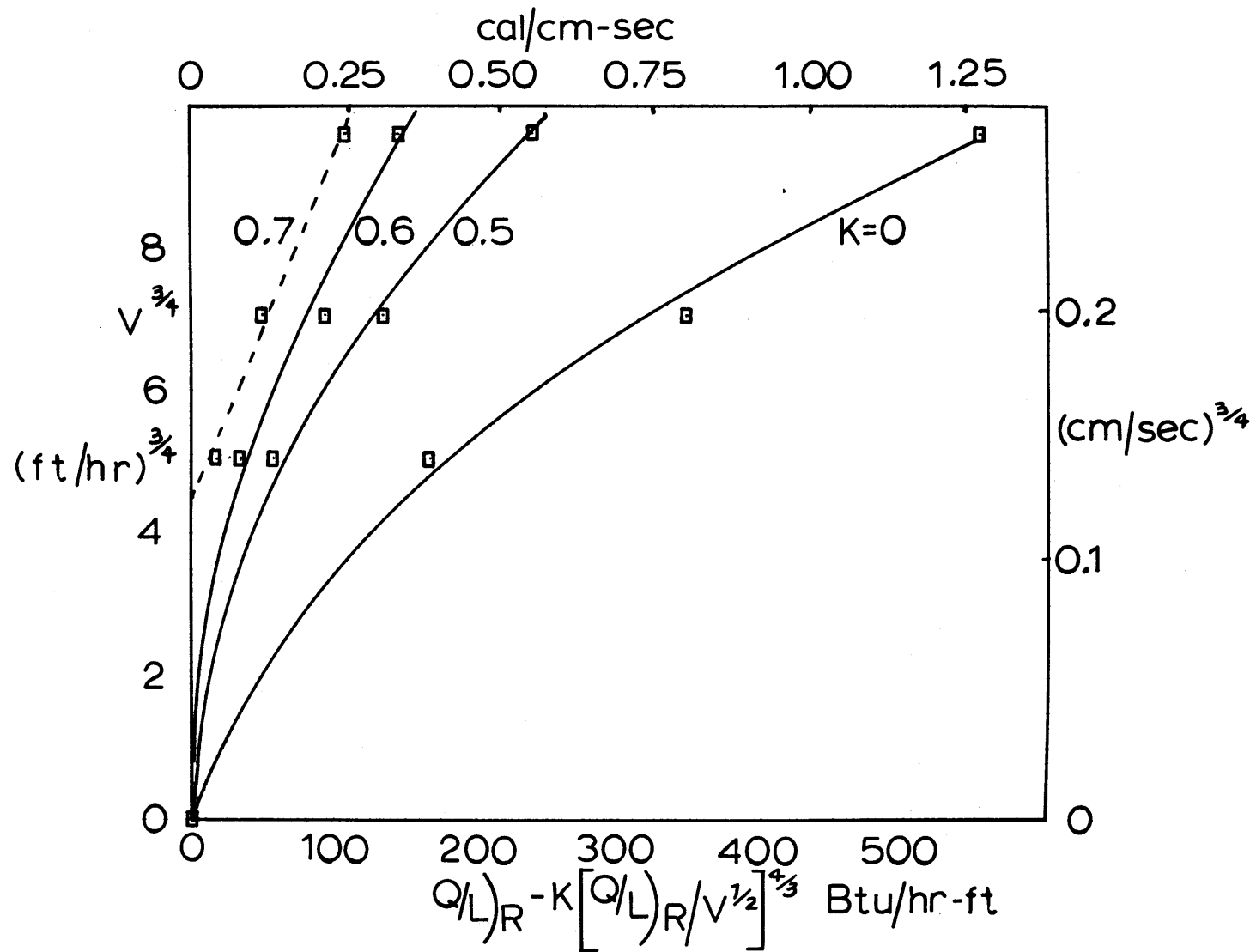


Figure 3-10 Determination of K for Computer Card Fuel ($\frac{1}{8} \times \frac{1}{8} \times .007$ ")

about a six-fold increase in the thermal conductivity. The data show that this gives a three-fold increase in Q_o . It should be emphasized that the values of Q_o for the computer fuel are rather uncertain.

3.7 The Effect of Wind

It takes only a casual observation to see that the wind velocity is of primary importance in the spread of a fire. With only a slightly less casual observation one also sees that it will be a very long time before a mathematical description of an external wind acting on a fire is obtained. However, any study which hopes eventually to predict the rate of spread of natural fire must sooner or later come to grips with this complex phenomenon.

Fons (7) has measured fire spread through ponderosa pine twigs at various imposed wind velocities. Several twig sizes and spacings were used. The wind velocity was varied between 4 and 8 miles per hour. According to the data the different spacings used, 1 to 1.75 inches, had no noticeable affect. The data were difficult to interpret because the moisture content of the fuel varied over such a wide range. However, if it is assumed that

$$\frac{Q_i \text{ moist}}{Q_i \text{ dry}} = \frac{c_p \Delta T + M \Delta H}{c_p \Delta T} \quad 3-34$$

the data can be roughly corrected for variation in moisture content. A plot for the three twigs sizes of $V \frac{Q_{\text{moist}}}{Q_{\text{dry}}}$ (presumably the spread over dry fuel) vs. wind velocity is given in Figure 3-11. An increase in wind velocity from 6 m.p.h. to 8 m.p.h. gives an increase of about 60% in the rate of spread, which is quite significant. However, the scatter of the data is very great.

In order to get a very rough idea of how wind influenced the newspaper fires, a few exploratory experiments were conducted. A wind across the burning fuel was produced by blowing air from a one-inch opening mounted behind the flame. The flow of air was measured by an upstream orifice. The wind velocity was calculated on the basis of a flat velocity profile through the one-inch opening. The air was fed through small holes throughout the length of a one-inch pipe at the back of a rectangular box. A fine mesh screen was placed between the pipe and the outlet.

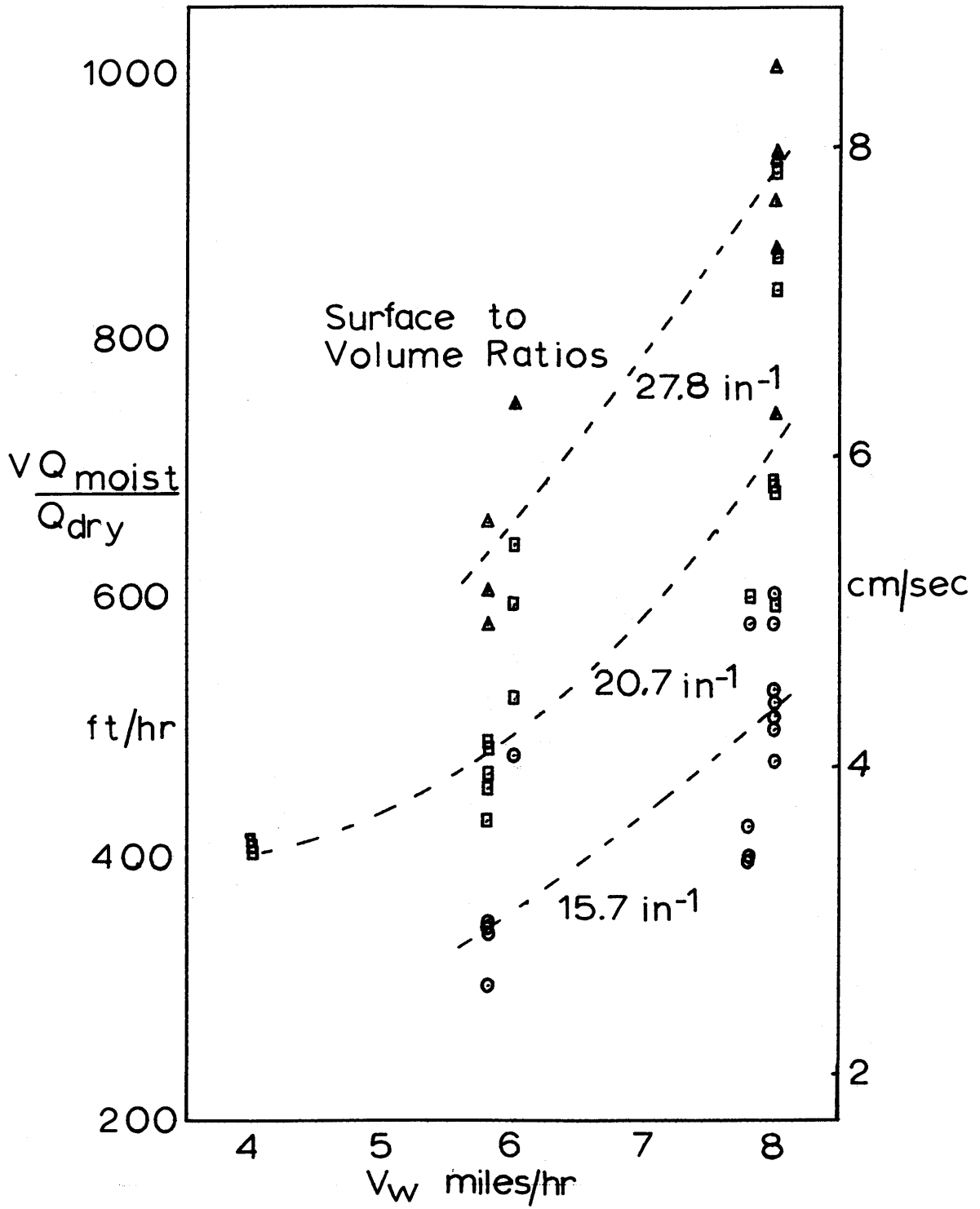


Figure 3-11 Effect of Wind Velocity on the Rate of Fire Spread for Dry Ponderosa Pine Twigs (data by Fons⁽⁷⁾)

The data are shown in Figure 3-12. A wind velocity of 1.3 ft/sec increases the rate of spread by only 5% over that of calm conditions. However, a velocity of 3.5 ft/sec increases the rate of fire spread by nearly three-fold.

There is a significant change in mechanism of the convection heat transfer as the wind velocity increases. As was discussed before, in the absence of wind, fire spread occurs by the flame slipping under new fuel as the fire draws air across the top of the surface. At a wind velocity of 1.3 ft/sec the above mechanism still seems to be the most important. At higher wind velocities the flame leans far over the unburned fuel. At 3.5 ft/sec the flame is nearly parallel to the surface. The fire now darts across the top of the surface from one piece of fuel to the next.

A 3.5 ft/sec wind velocity is considerable for such a small fire. The velocity in a turbulent convection column of a line heat source is shown by Hottel (11) from dimensional analysis to be

$$u = \left[\frac{Q/L \cdot g}{\rho \cdot c \cdot T_a} \right]^{1/3} f(R/z) \quad 3-25$$

where

- Q/L heat liberation at the source, Btu/hr-ft
- g the acceleration due to gravity, ft/hr²
- T_a surrounding temperature, °F
- ρ gas density, lbs/ft³
- c heat capacity of the gas, Btu/lb-°F

In order to model, the wind velocity V_w must be proportional to the velocity u in the convection column. Hottel also shows that

$$H^{3/2} \propto \frac{Q/L (T_a/g)^{1/2}}{\rho \cdot c (T_f - T_a)^{3/2}} \quad 3-26$$

Substitution of 3-26 into 3-25 gives

$$u \propto \left[\frac{(T_f - T_a) g H}{T_a} \right]^{1/2} \propto V_w \quad 3-27$$

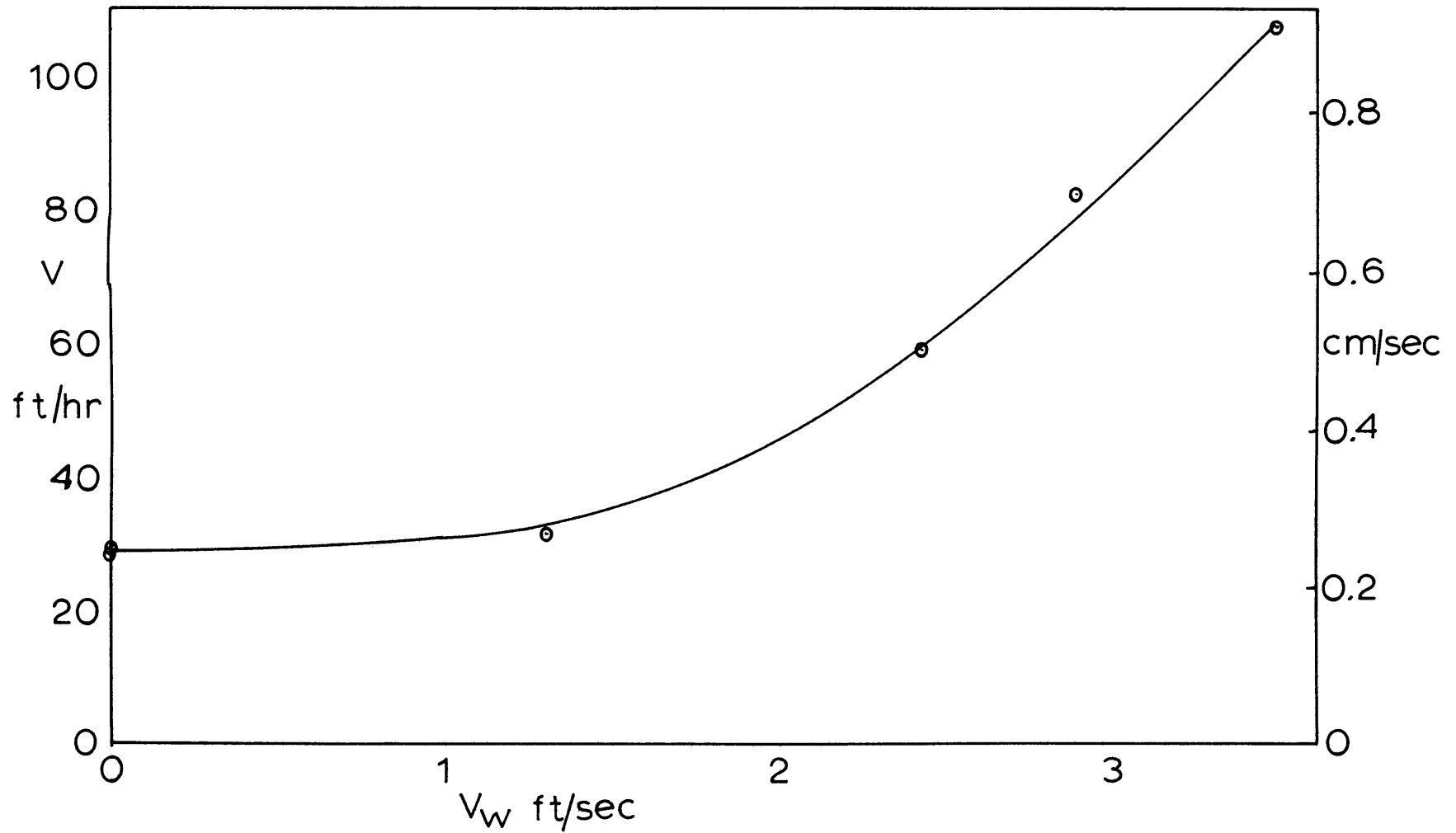


Figure 3-12 Effect of Wind Velocity on the Rate of Fire Spread for Shredded Newspaper (Humidity 73-77%)

Let the two-inch flame height of the newspaper fire become a 20-foot forest fire. A 3.5 ft/sec (2.38 mile/hr) wind velocity on the newspaper fire is equivalent to 38.4 ft/sec (26.2 mile/hr) in the forest fire. The small two-inch newspaper fire is certainly not a well-developed turbulent fire, but the above analysis shows that the 3.5 ft/sec wind velocity is a strong wind for that size fire.

Recall equation 3-18

$$Q/L)_C = h l' (T_f - T_i) \quad 3-18$$

and 3-2

$$V Q_i = Q/L)_C - Q/L)_L \quad 3-2$$

with the radiation heat transfer neglected. Since there is no significant radiation, all heat transferred to and away from the fuel is produced by convection and occurs very near the flame front. If the $Q/L)_C$ is considered the net heat input by convection at the flame front equation 3-2 becomes

$$Q_i V = Q/L)_C \quad 3-28$$

Q_i , the energy required for ignition in the above experiments, remained the same. Therefore, $Q/L)_C$ increases by the same factor as the velocity of spread when the wind is present. The distance over which the flame bathes the fuel, l' appears to increase by approximately 4 - 8 fold for a 3.5 ft/sec wind, (a visual estimate). The heat transfer coefficient between the flame gases and the fuel, h , must increase significantly since the velocity increases. The flame temperature apparently is decreased by the cold wind blowing through the flame.

The above suggests an interesting simple experiment to determine the distance over which the convection heat transfer occurs. A fuel bed could be constructed with line spaces containing no combustibles. The spaces would be widely separated with uniformly distributed fuel. The sizes of the spaces would

increase as their distance from the ignition end increased. The fire would jump the spaces until the convection heat transfer could not heat the fuel across the opening to ignition.

IV. TWO DIMENSIONAL INTERCHANGE FACTORS WITH AN ABSORBING GAS

4.1 Introduction

Systems in which one dimension is very much larger than the other dimensions present an important class of problems in radiant heat transfer. Many industrial furnaces fall into this category. A fire front moving through a forest has effectively an infinite front. This chapter considers some of the two-dimensional view factors with an absorbing gas in part of the system and the remaining space filled by clear gas. It also presents some of the modifications necessary when the "infinite" dimension must be considered finite.

4.2 Interchange Factor Between a Volume Element of Gray Gas Infinite in one Dimension and a Black Strip Separated by a Gray and Clear Gas

The first step in obtaining the intensity profile around an open flame is the solution to the above problem. Consider the geometry in Figure 4-1, where the boundary between the absorbing and clear gas is given by the two dimensional surfaces $f(z)$. The volume element $dV = dx dy dz$ lies a distance $r = \sqrt{x^2 + y^2 + z^2}$ from the surface element dA which is inclined at an angle α with the perpendicular to the xy plane. Radiation leaving dV passes through the absorbing gas for a length s . The volume element emits at a rate $4k'EdV$ with the fraction $\cos \phi_1 dA/4\pi r^2$ heading towards dA . The amount absorbed in its traverse by Beer's Law is e^{-ks} . The interchange area $d^4 \overline{gs}$ is then given by

$$d^4 \overline{gs} = \frac{k' \cos \phi_1 e^{-k's} dA dV}{\pi r^2} \quad 4-1$$

where

$$\cos \phi = (z/r) \cos \alpha + (x/r) \sin \alpha \quad 4-2$$

$$dA = L dx \quad 4-3$$

Substitution of 4-2 and 4-3 into 4-1 gives

$$d^4 \overline{gs} = \frac{k' e^{-k's} (z \cos \alpha + x \sin \alpha) dz dx^2 dy}{\pi (z^2 + y^2 + x^2)^{3/2}} \quad 4-4$$

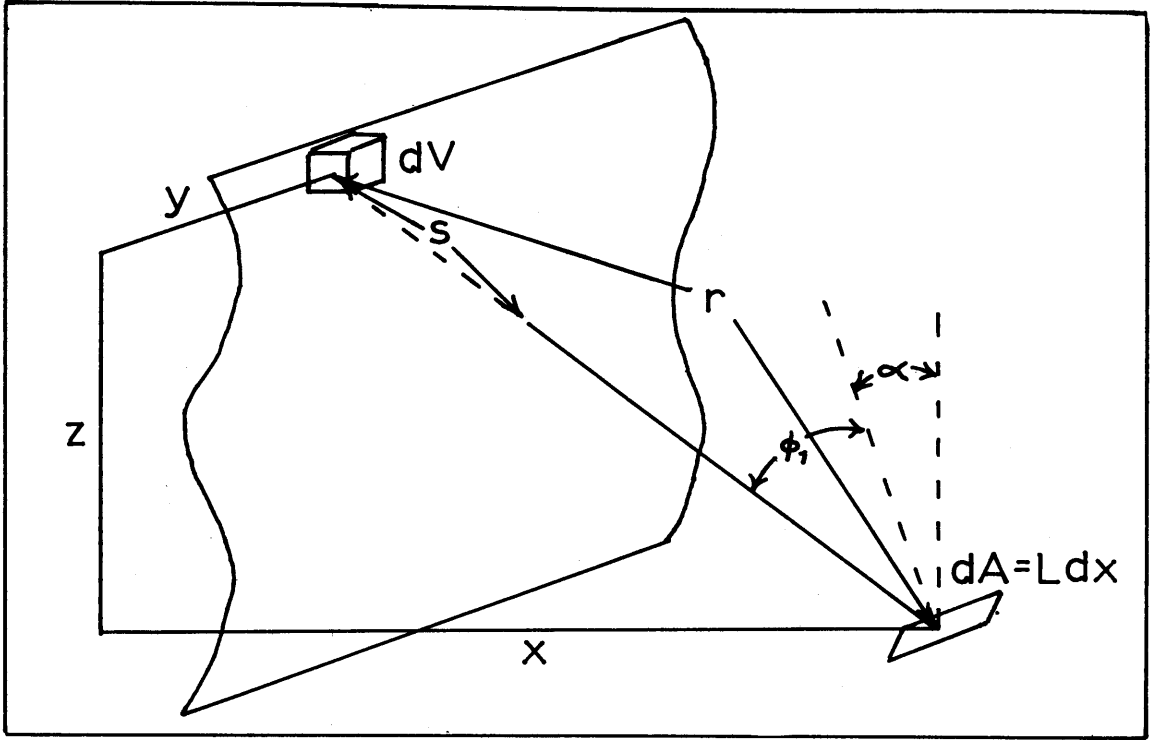


Figure 4-1 Interchange Between a Gray Gas Volume and a Black Spot Separated by Gray and Clear Gas

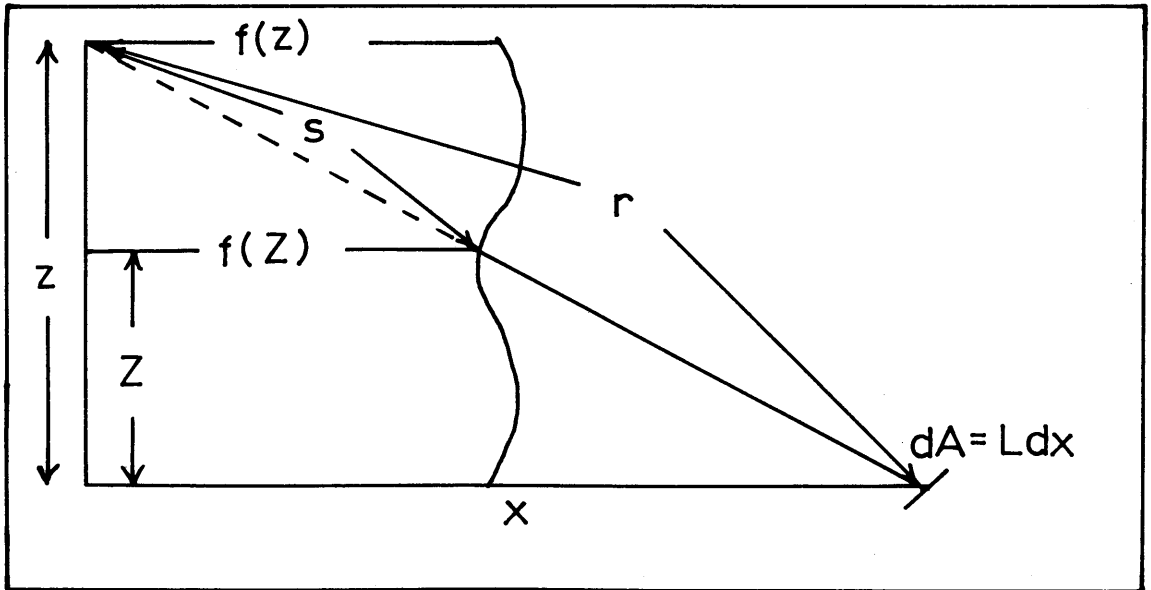


Figure 4-2 Fraction of Path in Gray Gas Between Gray Gas Volume and Black Spot

Since the fraction of the path over which absorption occurs is independent of y the relationship can be obtained by considering the problem in two dimensions as shown in Figure 4-2. The radiation headed for the area dA intersects the gray-clear gas interface at a height Z and a horizontal distance $f(Z)$. The ratio of the absorbing path to the total path is then $f(Z)/x$ and s is given by

$$s = \frac{f(Z)}{x} r \quad 4-5$$

where Z can be found from the relation of similar triangles

$$\frac{x}{f(Z)} = \frac{z}{(z - Z)} \quad 4-6$$

Equation 4-4 becomes

$$\frac{d^4_{gs}}{L dx^2 dz} = \frac{k' e^{-(k' f(Z)/x)(z^2 + x^2 + y^2)^{1/2}}}{\pi (z^2 + y^2 + x^2)^{3/2}} (z \cos \alpha + x \sin \alpha) dy \quad 4-7$$

Substituting the dimensionless variables

$$z' = k'z, \quad x' = k'x, \quad \text{and } y' = k'y \quad 4-8$$

and integrating over y from $-\infty$ to ∞ , noting the symmetry about $y = 0$ gives

$$\frac{d^3_{gs}}{L dx' dz' dx} = \int_0^{\infty} \frac{2 e^{-(k' f(Z)/x')(z'^2 + x'^2 + y'^2)^{1/2}}}{\pi (z'^2 + x'^2 + y'^2)^{3/2}} (z' \cos \alpha + x' \sin \alpha) dy' \quad 4-9$$

Making the substitutions

$$\begin{aligned} v'^2 &= z'^2 + x'^2 & s' &= \frac{k' f(Z)}{x'} v' \\ y' &= v' \sinh \theta & y'^2 + v'^2 &= v'^2 \cosh^2 \theta \end{aligned} \quad 4-10$$

The interchange factor between a volume element infinite in length by $(dx dz)$ and the area element $L dx$ becomes

$$\frac{\overline{d^3_{gs}}}{L dx' dz' dx} = \frac{2(z' \cos \alpha + x' \sin \alpha)}{\pi v'^2} \int_0^{\infty} \frac{e^{-s' \cosh \theta} d\theta}{\cosh^2 \theta} \quad 4-11$$

Now consider the same system but assume no radiation is absorbed as it traverses from the volume element to the area $L dx$. The exchange factor for "no gas absorption" is given by equation (9) with the exponential term deleted. Therefore,

$$\left. \frac{\overline{d^3_{gs}}}{L dx' dz' dx} \right)_{\text{No absorption}} = \frac{2(z' \cos \alpha + x' \sin \alpha)}{\pi} \int_0^{\infty} \frac{dy'}{(y'^2 + x'^2 + z'^2)^{3/2}} \quad 4-12$$

which upon integration gives

$$\left. \frac{\overline{d^3_{gs}}}{L dx' dz' dx} \right)_{\text{No Absorption}} = \frac{2(z' \cos \alpha + x' \sin \alpha)}{\pi v'^2} \quad 4-13$$

The transmissivity of a gas is defined as the ratio of the intensity of radiation passing through the gas to the incident intensity of radiation. Beer's Law gives $\mathcal{T} = e^{-k'l}$ where l is the distance through the absorbing gas which the radiation passes. In the case of interest, the radiation traverses an infinite number of different absorbing paths. Define a transmissivity in this instance as $\mathcal{T} = e^{-Bs'}$ where s' is the shortest dimensionless path between the radiating volume and receiving surface and B is the ratio of the mean beam length (used many times by Hottel (10)) to the shortest absorbing distance. The mean beam length is physically the dimensionless distance a beam of radiation which properly weights all the beams must travel through an absorbing gas. The ratio of the true exchange factor to the no-absorption factor, (4-11)/(4-13), is equal to the transmissivity giving

$$e^{-Bs'} = \int_0^{\infty} \frac{e^{-s' \cosh \theta} d\theta}{\cosh^2 \theta} \quad 4-15$$

and

$$B = -\frac{1}{s'} \ln \left[\int_0^{\infty} \frac{e^{-s' \cosh \theta} d\theta}{\cosh^2 \theta} \right] \quad 4-16$$

Thus, the mean beam length to shortest absorbing distance ratio is only a function of the minimum absorbing path length s' and is shown as the top curve in Figure 4-3. It approached $\pi/2$ as s' goes to zero and unity as s' goes to infinity. The above solution is general for any arbitrary boundary between a gray and clear gas which extends to infinity.

4.3 Interchange Factor Between a Volume Element of Gray Gas and a Black Spot Centrally Located Between the Ends, Separated by Gray and Clear Gas

The derivation for the system with all dimensions finite proceeds in an identical fashion as the case with one dimension infinite. However, the limits for integration on y are finite. Taking the symmetrical case where the element of area lies a dimensionless distance $k'Y = Y'$ from both ends of the absorbing gas volume, equation 4-9 becomes

$$\frac{d^3 \overline{gs}}{dx'dz'dx} = \frac{2(z' \cos \alpha + x' \sin \alpha)}{\pi} \int_0^{Y'} \frac{e^{-(k'f(Z)/x')(x'^2 + z'^2 + y'^2)^{1/2}} dy}{(z'^2 + x'^2 + y'^2)^{3/2}} \quad 4-17$$

Using the substitutions from 4-10 gives

$$\frac{d^3 \overline{gs}}{dx'dz'dx} = \frac{2(z' \cos \alpha + x' \sin \alpha)}{\pi v'^2} \int_0^{\theta} \frac{e^{-s' \cosh \theta} d\theta}{\cosh^2 \theta} \quad 4-18$$

where

$$\theta = \sinh^{-1} Y'/v' \quad \theta = \ln \left[\frac{Y'}{v'} + \sqrt{\frac{Y'^2}{v'^2} + 1} \right] \quad 4-19$$

The omission of the exponential function gives the exchange factor for "no-absorption". This is given by equation 4-12 with a finite limit of integration Y' . Therefore,

$$\left. \frac{d^3 \overline{gs}}{dx'dz'dx} \right|_{\text{No Absorption}} = 2(z' \cos \alpha + x' \sin \alpha) \int_0^{Y'} \frac{dy'}{\pi (y'^2 + x'^2 + z'^2)^{3/2}} \quad 4-20$$

which gives on integration

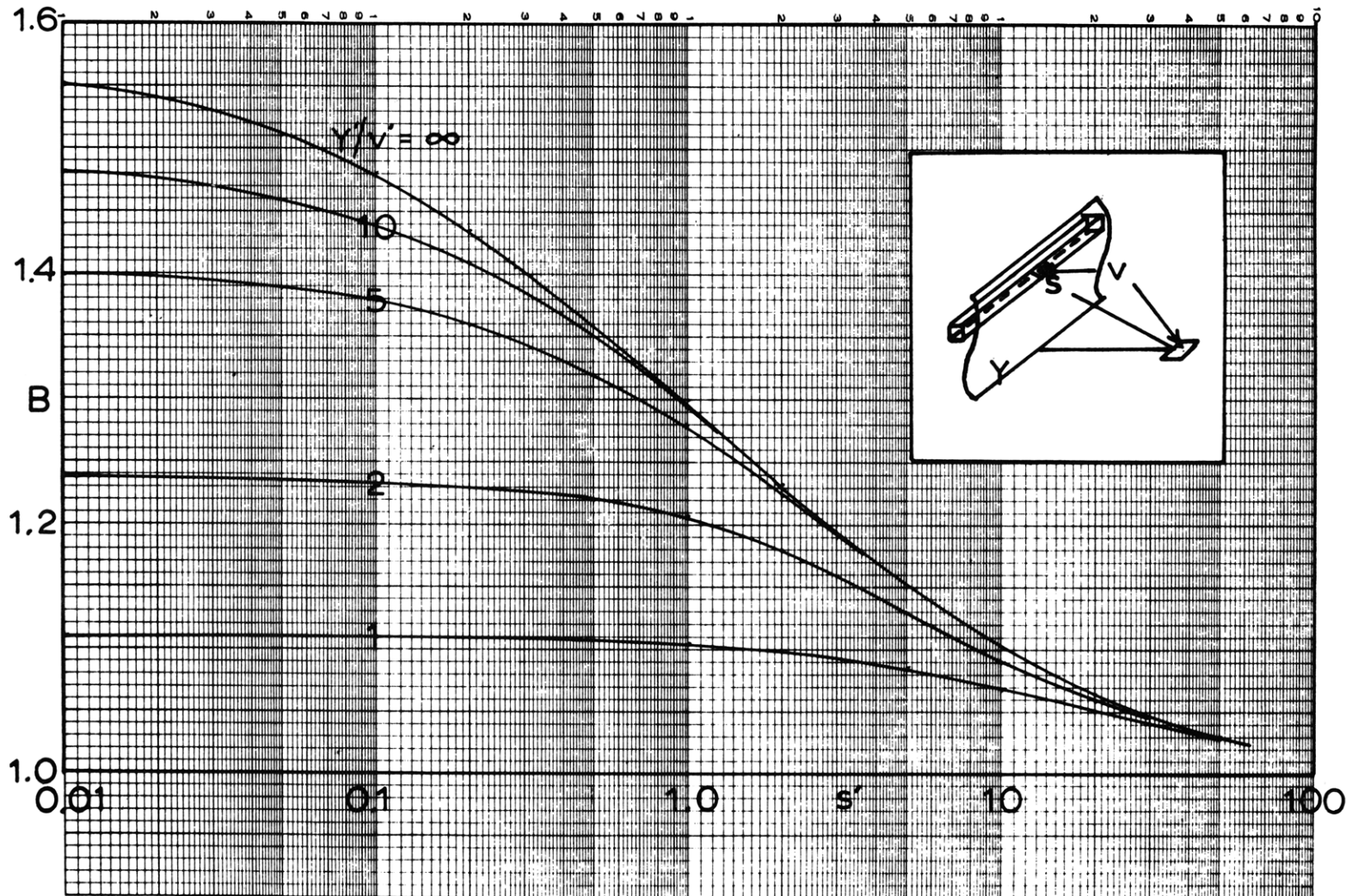


Figure 4-3 Mean Beam Length to Shortest Absorbing Distance Ratio Between a Two Dimensional Gray Gas Volume of Length $2Y$ and a Black Spot Centrally Located as a Function of the Shortest Dimensionless Absorbing Distance

$$\frac{d^3_{gs}}{L dx' dz' dx} = \frac{2(z' \cos \alpha + x' \sin \alpha)}{\pi v'^2} \frac{Y'}{(Y'^2 + v'^2)^{1/2}} \quad 4-21$$

no absorption

The mean beam length to shortest absorbing distance ratio is therefore

$$B = -\frac{1}{s'} \ln \left[\frac{\int_0^{\theta} \frac{e^{-s' \cosh \theta} \cosh \theta \, d\theta}{\cosh^2 \theta}}{\frac{Y'/v'}{\sqrt{(Y'/v')^2 + 1}}} \right] \quad 4-22$$

B is given in Figure 4-3 as a function of the shortest absorbing distance s' with a family of curves for Y'/v' .

4.4 Interchange Factor Between Two Infinite Parallel Strips with a Gray and Clear Gas Intervening

This problem has been previously solved in the report of the Summer Combustion Woods Hole Study Group (32) for the special case when only gray gas is present. Consider the system in Figure 4-4. The planes zy and xy intersect at an angle α and form the y axis. The two strips dx and dz extend to infinity. The region of absorbing gas is bounded by the two dimensional surface curve $f(z)$ with clear gas to the right. ϕ_1 and ϕ_2 are the angles between the connecting line r and the perpendiculars to dA_1 and dA_2 respectively. Radiation leaving the area element $dA_2 = dydz$ and headed for the area $dA_1 = Ldx$ is absorbed over a length s . The interchange factor between the two areas is given by

$$d^3_{ss} = \frac{\cos \phi_1 \, dA_1 \cos \phi_2 \, dA_2 \, e^{-k's}}{\pi r^2} \quad 4-23$$

where

$$\begin{aligned} \cos \phi_1 &= \frac{z}{r} \sin \alpha & \cos \phi_2 &= \frac{x}{r} \sin \alpha \\ r^2 &= x^2 + z^2 - 2xz \cos \alpha + y^2 \end{aligned} \quad 4-24$$

Substituting and integrating over y from $-\infty$ to ∞ gives

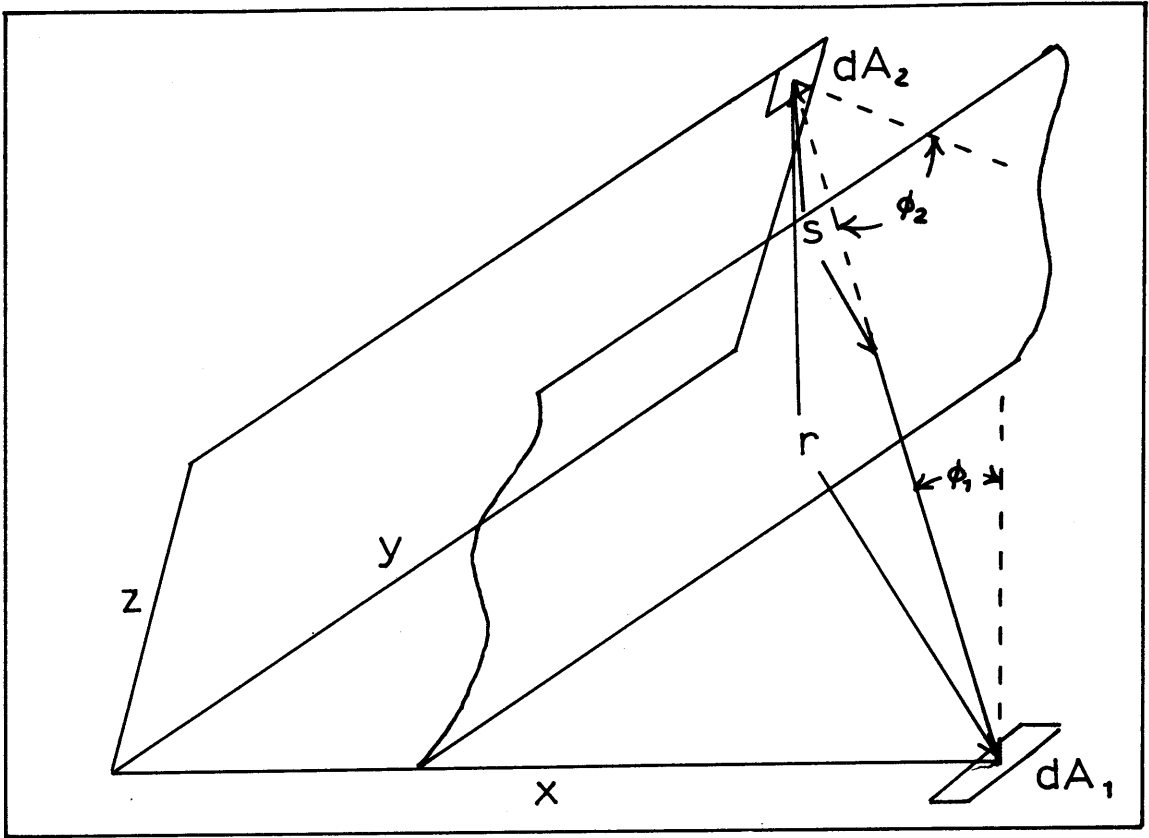


Figure 4-4 Interchange Between Two Black Spots Separated by a Gray and Clear Gas

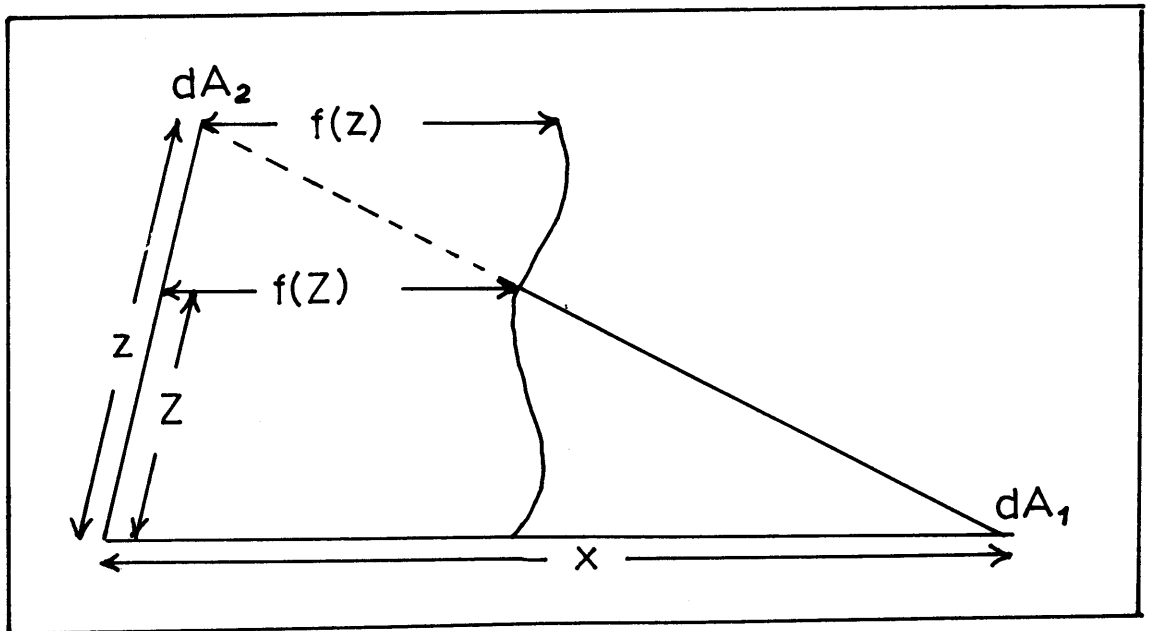


Figure 4-5 Fraction of Path in Gray Gas Between Two Black Spots

$$\frac{d^2 ss}{L dx dz} = \int_0^{\infty} \frac{2 zx \sin^2 \alpha e^{-k's} dy}{\pi(x^2 + z^2 + y^2 - 2 xz \cos \alpha)^2} \quad 4-25$$

The fraction of the path in which absorption occurs can again be considered in two dimensions and is obtained from Figure 4-5, where Z is the height at which the connecting line intersects the boundary between gray and clear gas. Therefore s is given by

$$s = \frac{f(Z) - (z - Z) \cos \alpha}{x - z \cos \alpha} (x^2 + y^2 + z^2 - 2 xz \cos \alpha)^{1/2} \quad 4-26$$

Where Z can be obtained from

$$\frac{x}{f(Z)} = \frac{z}{z - Z} \quad 4-27$$

Using the substitutions

$$\begin{aligned} x' &= k'x & v'^2 &= z'^2 + x'^2 - 2 x'z' \cos \alpha \\ y' &= k'y & y'^2 + v'^2 &= v'^2 \cosh^2 \theta \\ z' &= k'z & s' &= \frac{k'f(Z) - (z' - Z) \cos \alpha}{x' - z' \cos \alpha} v' \end{aligned} \quad 4-28$$

and integrating over y from zero to infinity gives

$$\frac{d^2 ss}{L dx dz'} = \frac{2 z' x' \sin^2 \alpha}{\pi v'^3} \int_0^{\infty} \frac{e^{-s' \cosh \theta} d\theta}{\cosh^3 \theta} \quad 4-29$$

Once again the mean beam length discussed in Section 4-2 can be used. The exchange factor between the black strips with no absorbing gas can be found either by excluding the exponential term in 4-29 and integrating or by the cross strings method described by Hottel (10). In either case one obtains

$$\left. \frac{d^2 ss}{L dx dz'} \right)_{\text{No Absorption}} = \frac{x' z' \sin^2 \alpha}{2 v'^3} \quad 4-30$$

Then

$$e^{-Bs'} = \frac{4}{\pi} \int_0^{\infty} \frac{e^{-s' \cosh \theta} d\theta}{\cosh^3 \theta} \quad 4-31$$

and

$$B = -\frac{1}{s'} \ln \left[\frac{4}{\pi} \int_0^{\infty} \frac{e^{-s' \cosh \theta} d\theta}{\cosh^3 \theta} \right] \quad 4-32$$

The mean beam length to shortest absorbing distance ratio is again only a function of the shortest absorbing distance s' , and is given by the top curve in Figure 4-6. B approaches $4/\pi$ as s' goes to zero and unity as s' goes to infinity.

4.5 Interchange Factor Between a Finite Black Strip and a Black Spot Centrally Located with a Gray and Clear Gas Intervening

The derivation for obtaining the mean beam length between a finite black strip and a black spot centrally located separated by gray and clear gas proceeds in the same manner as the infinite one in Section 4-4. The symmetrical case with the element of the area a distance Y' from both ends of the strips is considered. The "no-absorption" exchange factor is obtained from equation 4-25 by dropping the exponential term and integrating over the finite dimensionless distance Y' . The mean beam length to shortest absorbing distance ratio is given by

$$B = -\frac{1}{s'} \ln \left[\frac{2 \int_0^{\infty} \frac{e^{-s' \cosh \theta} d\theta}{\cosh^3 \theta}}{\frac{Y'/v'}{(Y'/v')^2 + 1} + \tan^{-1} \frac{Y'}{v'}} \right] \quad 4-33$$

B is plotted vs. the shortest absorbing distance, s' , with the Y'/v' family of curves in Figure 4-6.

The above four derivations are important because they replace a numerical

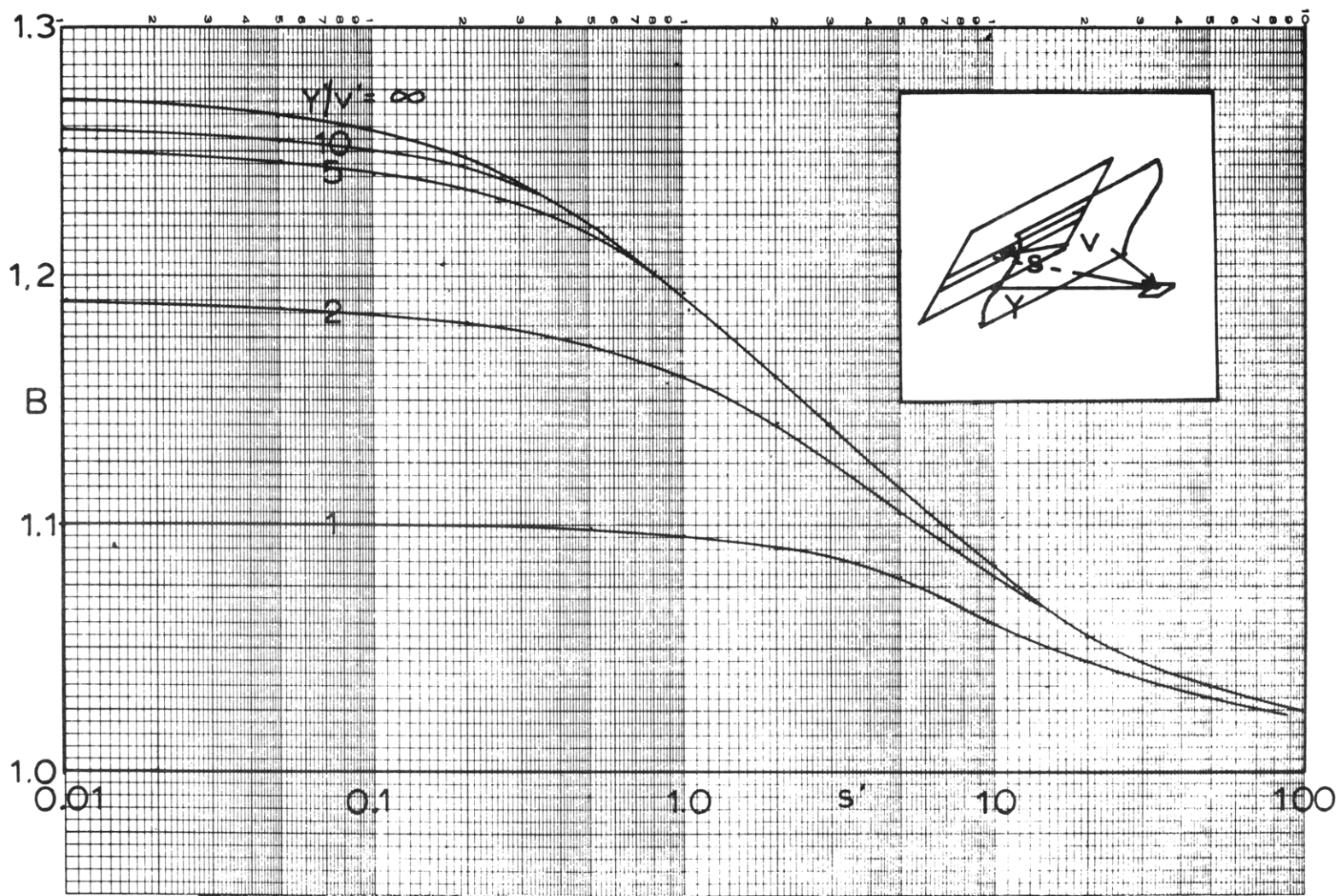


Figure 4-6 Mean Beam Length to Shortest Absorbing Distance Ratio Between a Black Strip of Length $2Y$ and a Black Spot Centrally Located as a Function of the Shortest Dimensionless Absorbing Distance

integration with a very simple graph. Although the two integrals could be tabulated as well, the replacement of these integrals with the mean beam length is believed to have the advantages of both physical meaning and easier use.

4.6 Interchange Factors Between a Gray Gas Rectangular Parallelepiped of Height Z, Width W, and Infinite Length and a Black Infinite Parallel Strip dx Wide on a Surrounding Horizontal Surface

This problem has been solved in the report of the Combustion Summer Study Group (32). Notice that it is a special case of Section 4-2. Considering Figure 4-7 the element of volume $dV = dw dz dy$ is located a distance w from the front gray gas face, at a height z and displaced a distance y from the xz plane. The area element $L dx$ is a distance x from the front gray gas face. Notice the integration over y' in Section 4-2 can be applied directly. Relating the above nomenclature with that in Section 4-2

$$\begin{aligned} \alpha &= 0 & f(z) &= w \\ \sin \alpha &= 0 & v' &= \sqrt{z'^2 + (x' + w')^2} \\ \cos \alpha &= 1 & & \\ x &= x + w & & \end{aligned} \quad 4-34$$

Equation 4-11 and 4-15 gives

$$\frac{d \bar{g}_s}{L dx} = \int_0^{z'} \int_0^{w'} \frac{2z' e^{-(Bw'/(w'+x'))(z'^2 + (x'+w')^2)^{1/2}}}{\pi(z'^2 + (x' + w')^2)} dz' dw' \quad 4-35$$

Integration over W' gives the exchange factor between a volume of gray gas of infinite length, W' dimensionless width, and dz' height and the element Ldx' at a dimensionless distance x' . A second integration over Z' gives the interchange factor between the rectangular parallelepiped and the element Ldx' at a dimensionless distance x' from its base.

It is possible to solve the above integral analytically only in the limit when the gas does not absorb. The double integration without the

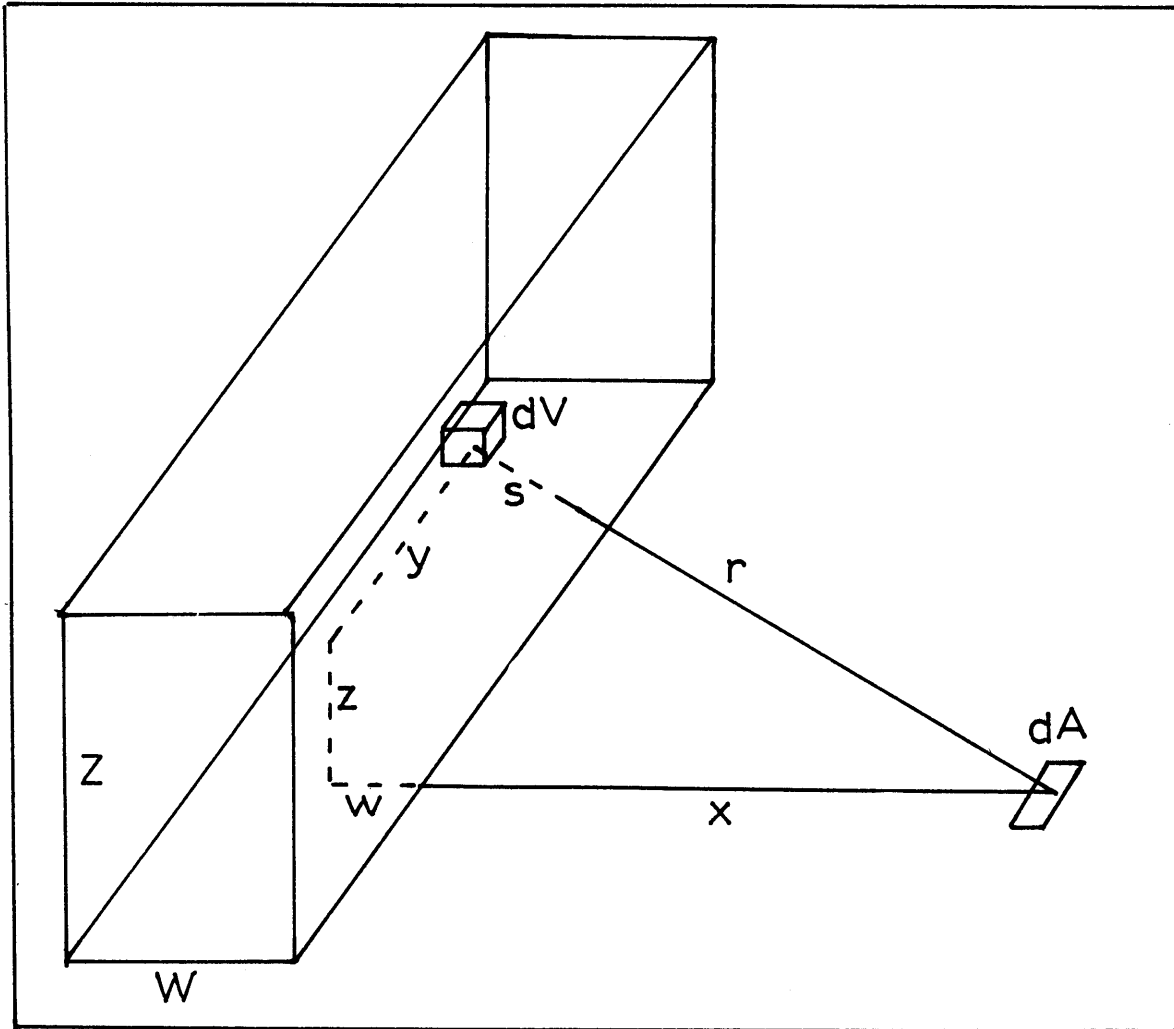


Figure 4-7 Interchange Between a Rectangular Parallelepiped of Gray Gas and a Black Strip

exponential term gives

$$\frac{d \bar{g}_s}{Z' dx} = \frac{2}{\pi} \left[\tan^{-1} \frac{W' + x'}{Z'} - \tan^{-1} \frac{x'}{Z'} + \frac{W' + x'}{2Z'} \ln \left[1 + \left(\frac{Z'}{W' + x'} \right)^2 \right] - \frac{x'}{2Z'} \ln \left[1 + \left(\frac{Z'}{x'} \right)^2 \right] \right] \quad 4-36$$

The other limit of $k = \infty$ (or a black wall to a black strip) is obtained by the cross strings method.

$$\frac{d \bar{g}_s}{dx} = \frac{1}{2} \left(1 - \frac{x/Z}{\sqrt{1 + (x/Z)^2}} \right) \quad 4-37$$

In order to obtain the exchange factors between the two limits the double numerical integration of equation 4-35 must be completed. Since numerical integration is a laborious process a semi-integration process with good accuracy is used. Note that, except very near the front face of the gray parallelepiped, s' , the shortest absorption path, and therefore B , change slowly with w' . Equation 4-35 is well approximated by

$$\frac{d^2 \bar{g}_s}{dx dz} = \frac{2}{\pi} \sum_1^m \exp - \left[\frac{B \frac{W'_n + W'_{n-1}}{2}}{x' + \frac{W'_n + W'_{n-1}}{2}} \right] \left[z'^2 + \left(x' + \frac{W'_n + W'_{n-1}}{2} \right)^2 \right]^{1/2} \int_{W'_{n-1}}^{W'_n} \frac{z' dw'}{z'^2 + (x' + w')^2} \quad 4-38$$

where $m = W'/\Delta w'$, the number of increments into which W' is divided. Integration over W'_{n-1} to W'_n gives

$$\frac{d^2 \overline{gs}}{L dx dz'} = \frac{2}{\pi} \sum_1^m \exp - \left[\frac{B \frac{(W'_n + W'_{n-1})}{2}}{x' + \frac{W'_n + W'_{n-1}}{2}} \right] \left[z'^2 + \left(x' + \frac{W'_n + W'_{n-1}}{2} \right)^2 \right]^{1/2} \\ \left(\tan^{-1} \frac{W'_n + x'}{z'} - \tan^{-1} \frac{W'_{n-1} + x'}{z'} \right)$$

4-39

Use of equation 4-39 reduces numerical work considerably. Values for \tan^{-1} can be tabulated and used repeatedly while B is read directly from Figure 4-3. As an example, take $x' = 0.1$, $z' = 1.0$ and $W' = 1.0$. Numerical integration gives $(d^2 \overline{gs} / L dx dz') = 0.16376$. Equation 4-39 with $m = 10$ or $\Delta w' = 0.1$ gives $(d^2 \overline{gs} / L dx dz') = 0.16056$ which is about 2% low. Most of the error is in the first two intervals. Dividing these two intervals in half again so that $\Delta w' = 0.05$ for $w' < 0.2$ and $\Delta w' = 0.1$ for $w' > 0.2$ gives $(d^2 \overline{gs} / L dx dz') = 0.16409$ which is 0.2% high. The numerical integration is only good to about 0.5%. By using equation 4-39 the double integration of equation 4-35 was carried out on the 709 and 7090 computers at the M.I.T. Computation Center for a wide range of heights and widths. The results are given in Figure 4-8 (a - h). $(d \overline{gs} / Z' L dx)$ is plotted vs. x'/Z' with a family of curves for different Z' 's. Values for an intermediate W'/Z' can be obtained to within 5% by arithmetic averaging.

If an analytical expression is desired

$$\frac{d \overline{gs}}{L dx} = \frac{(1 - e^{-BZ'})}{2} \left(1 - \frac{x/z}{\sqrt{1 + (x/z)^2}} \right) \quad 4-40$$

The bracketed term represents twice the exchange factor between an infinitely long black surface of height Z' and a black strip on a horizontal plane. The exponential term, $(1 - e^{-BZ'})$, is the effective emissivity of the gray gas rectangular parallelepiped where B is given in Figures 4-9 and bears the burden of making the simplified equation give the rigorous answer.

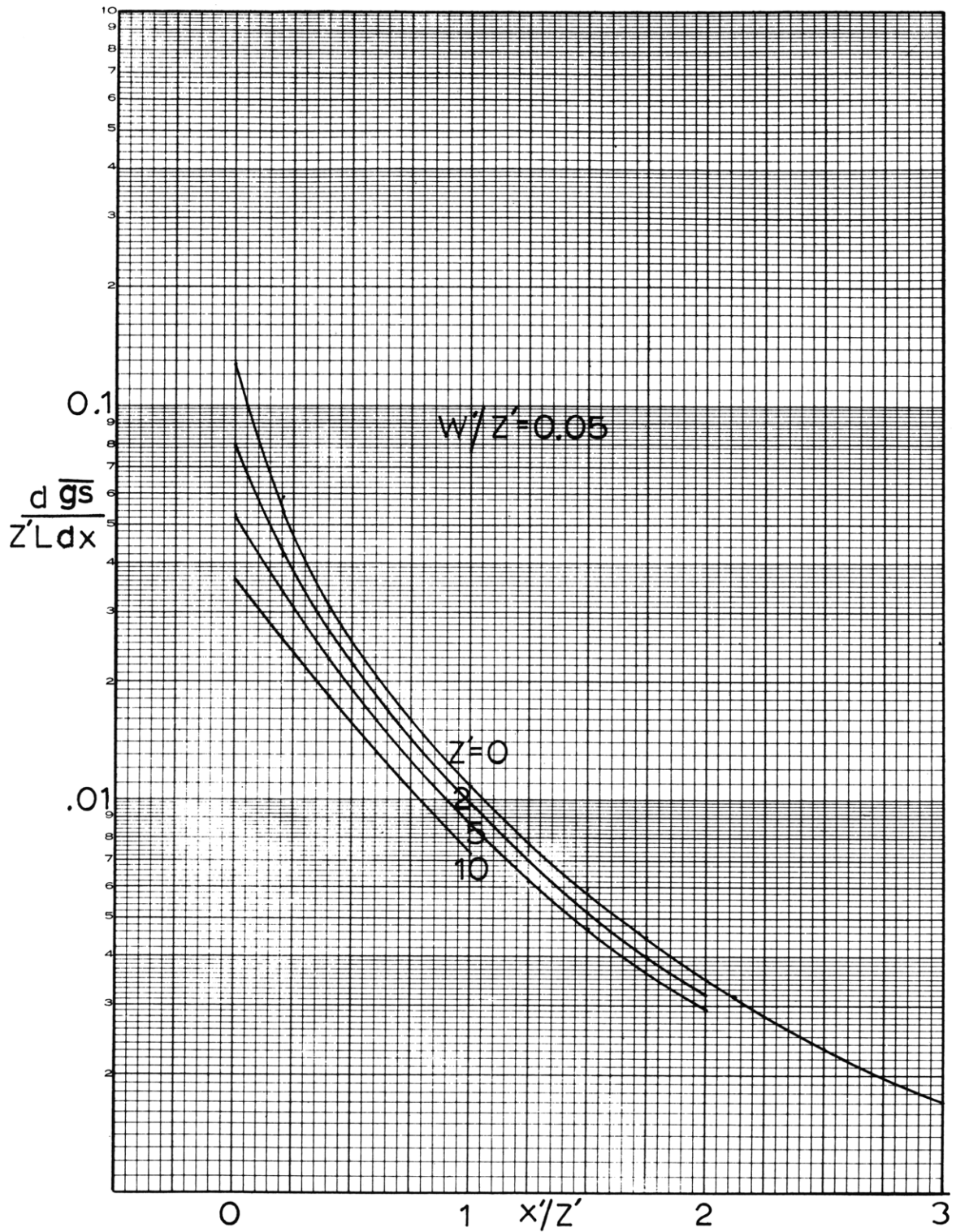


Figure 4-8a Interchange Factors for an Infinite Gray Gas Rectangular Parallelepiped of Height Z' and Width W' and the Surrounding Surface as a Function of the Distance from the Front Face to Height Ratio

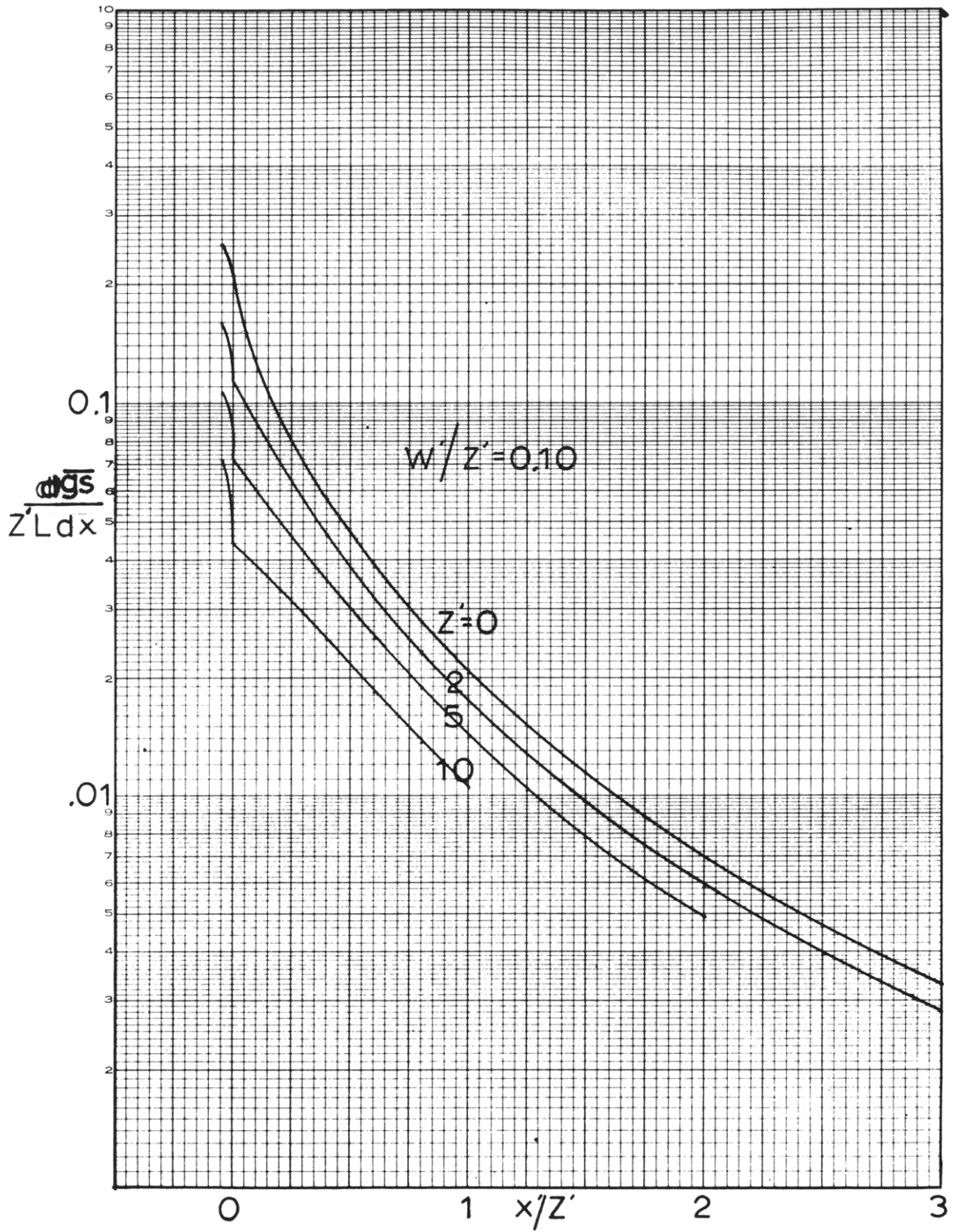


Figure 4-8b

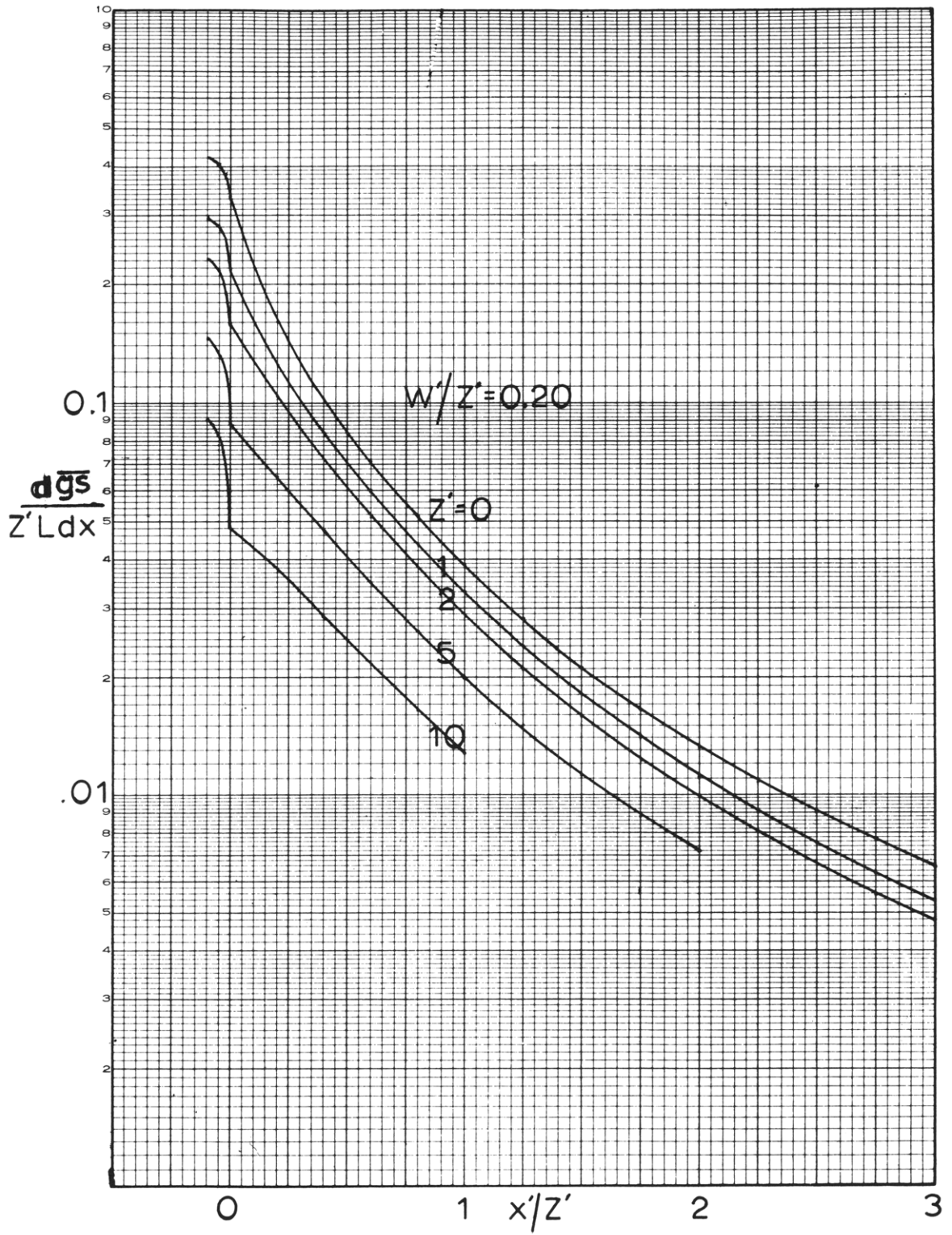


Figure 4-8a

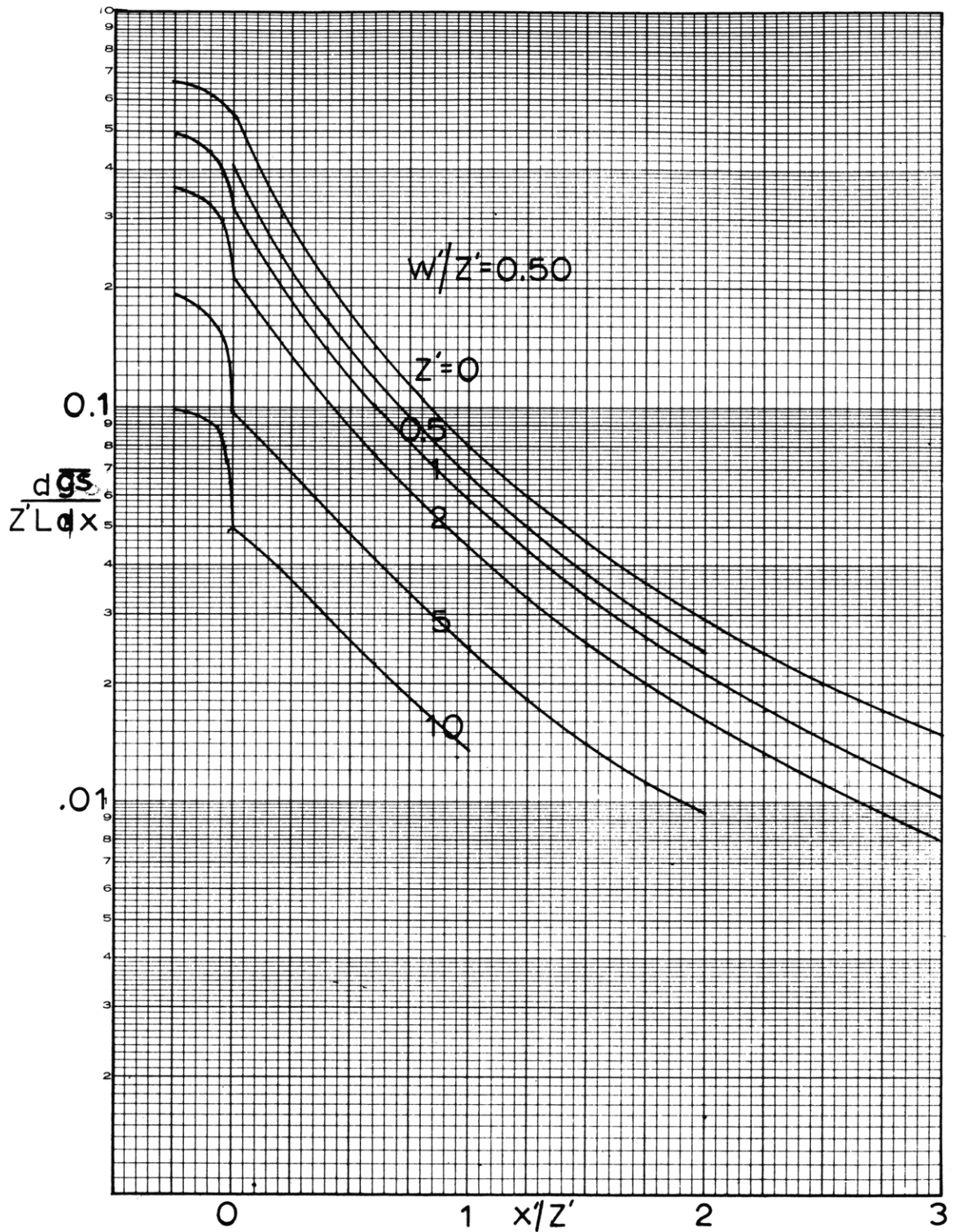


Figure 4-8d

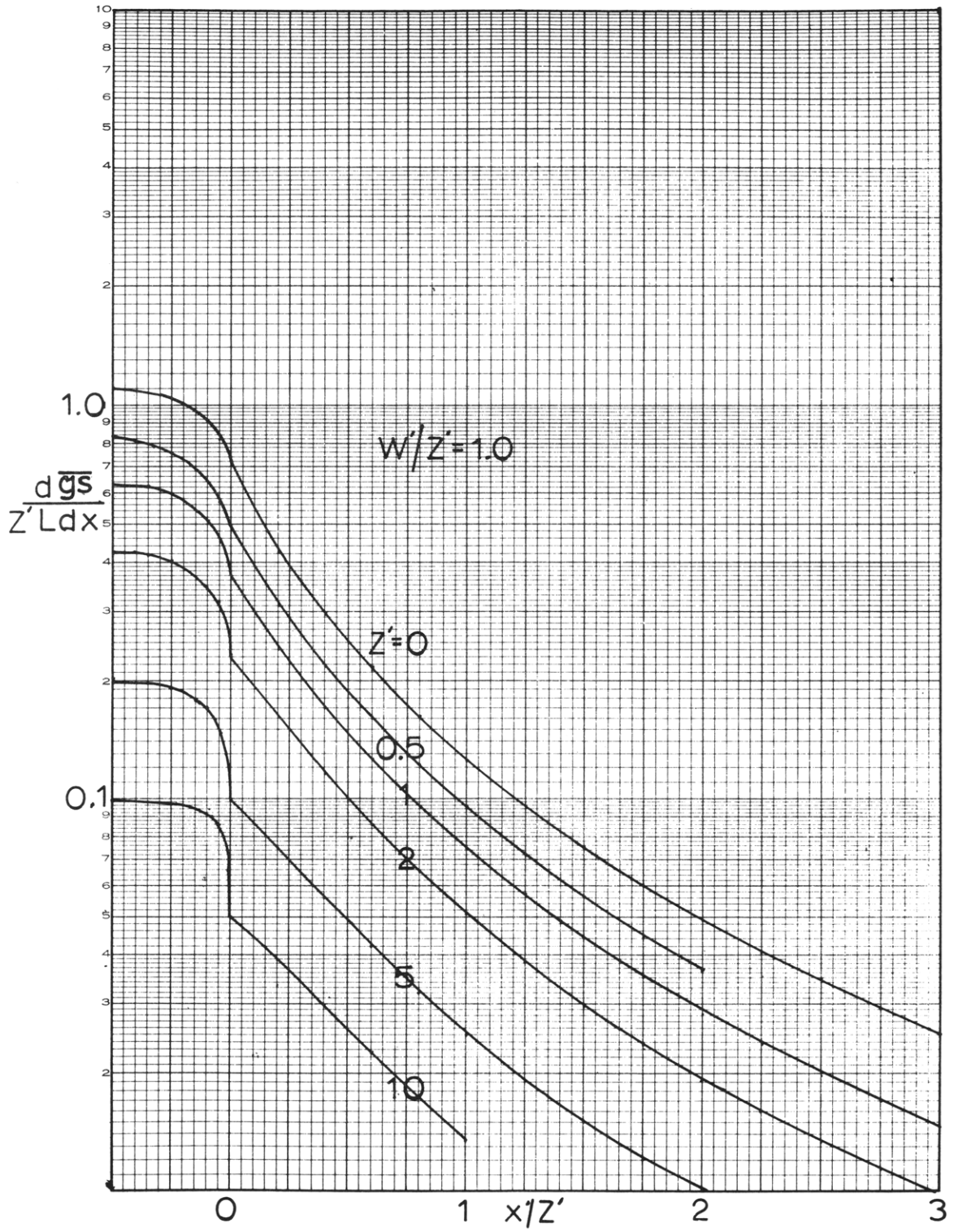


Figure 4-8e

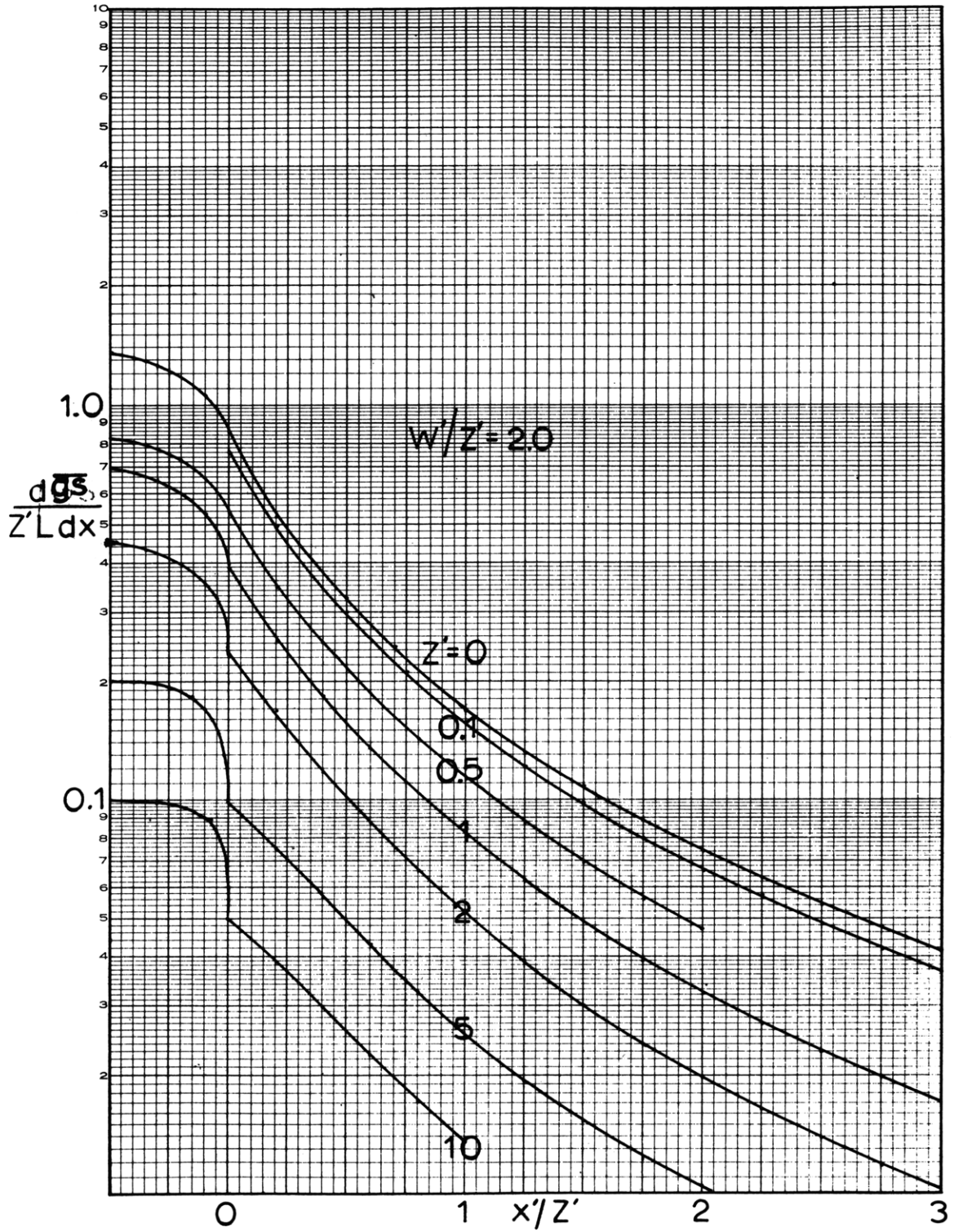


Figure 4-8f

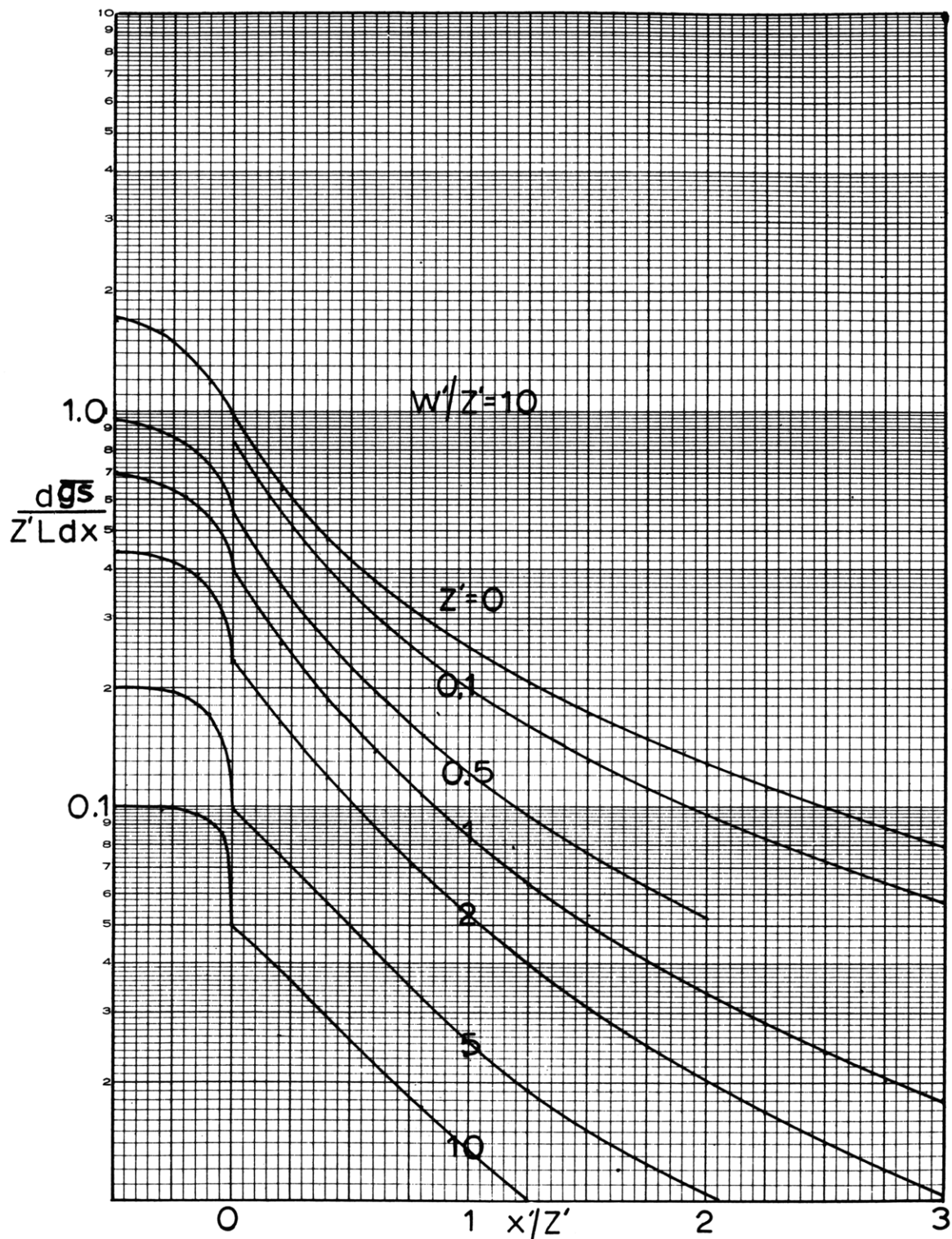


Figure 4-8g

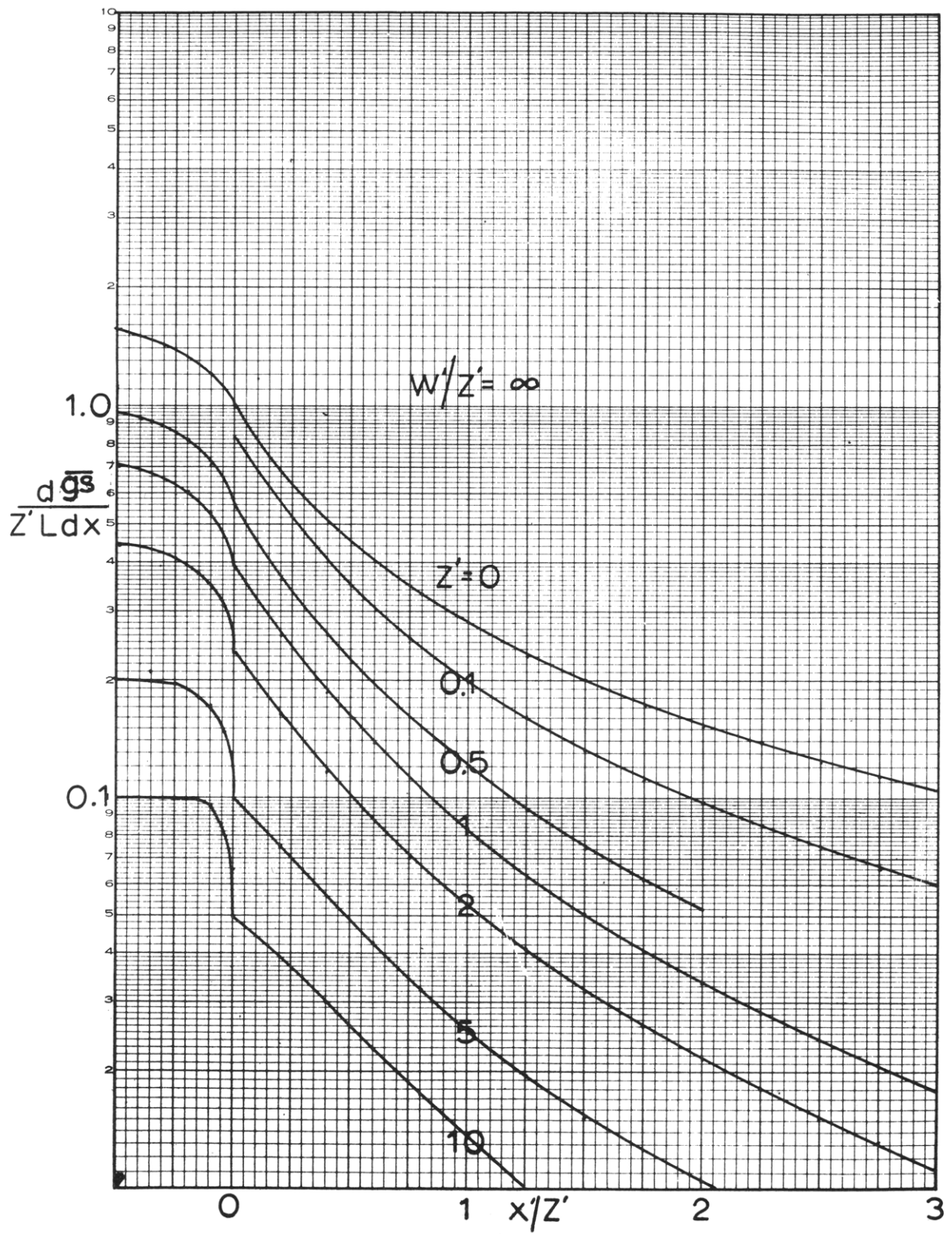


Figure 4-8h

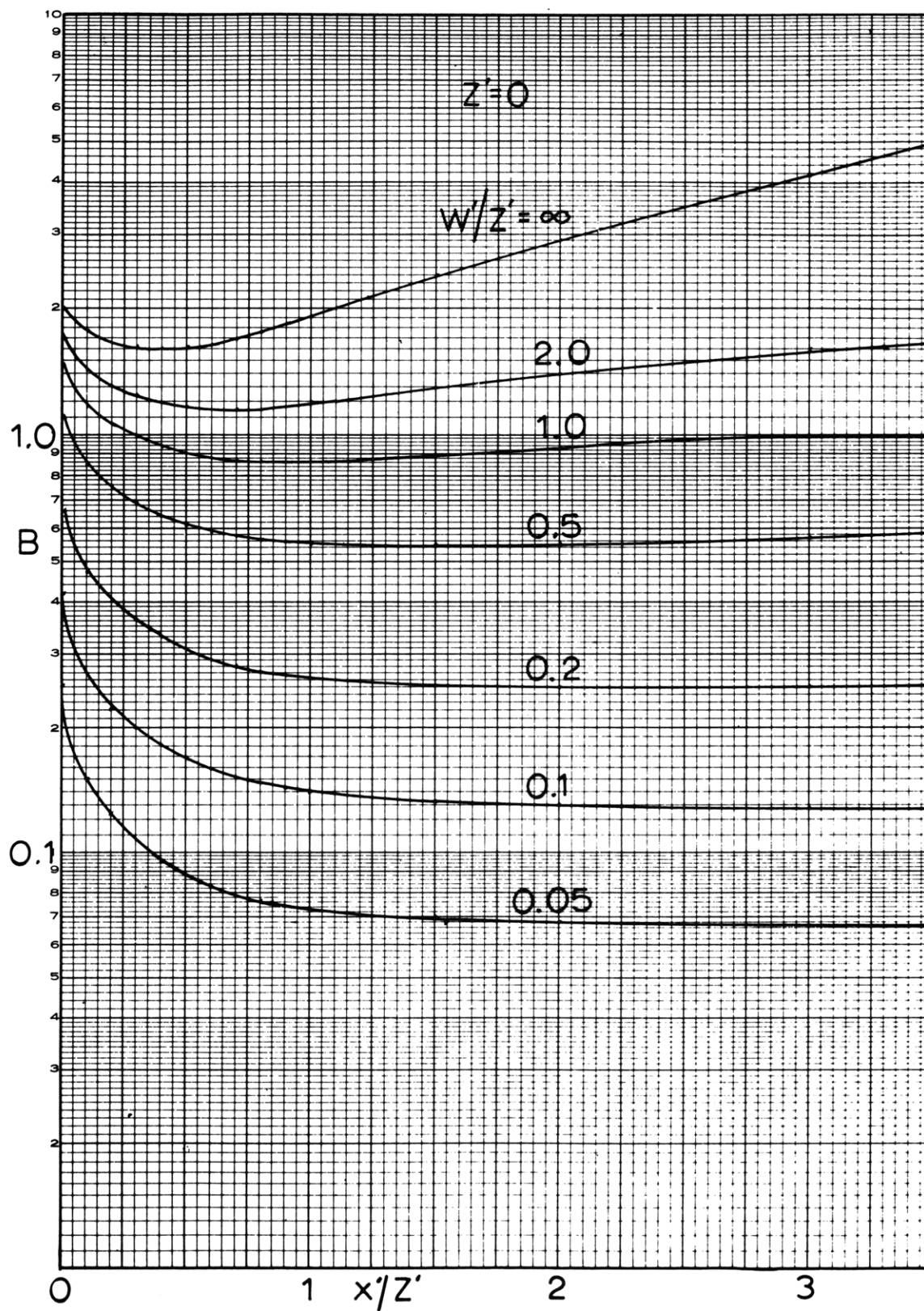


Figure 4-9a Mean Beam Length for Equation 4-40 as a Function of the Ratio of the Distance from the Front Face to the Height

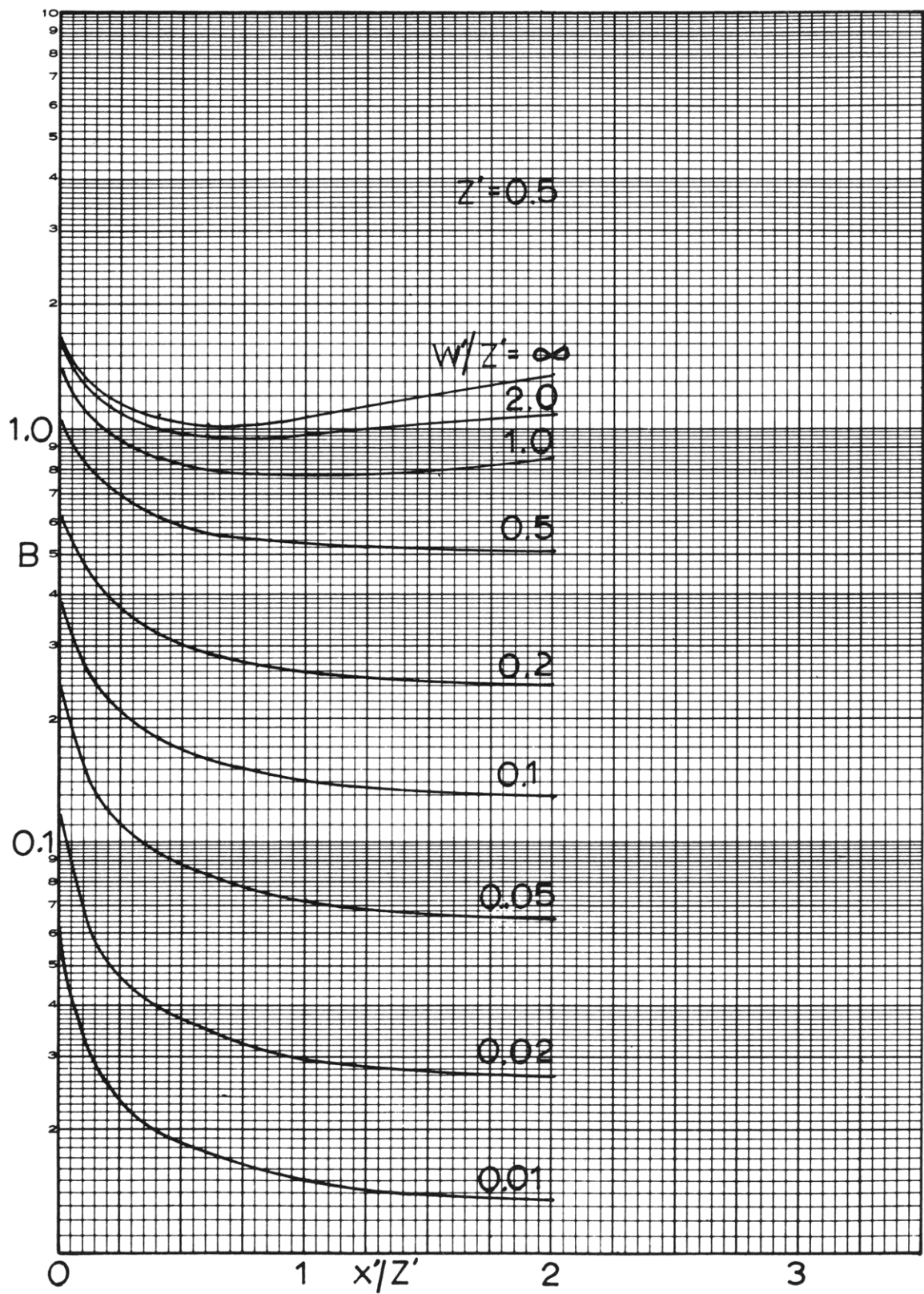


Figure 4-9b

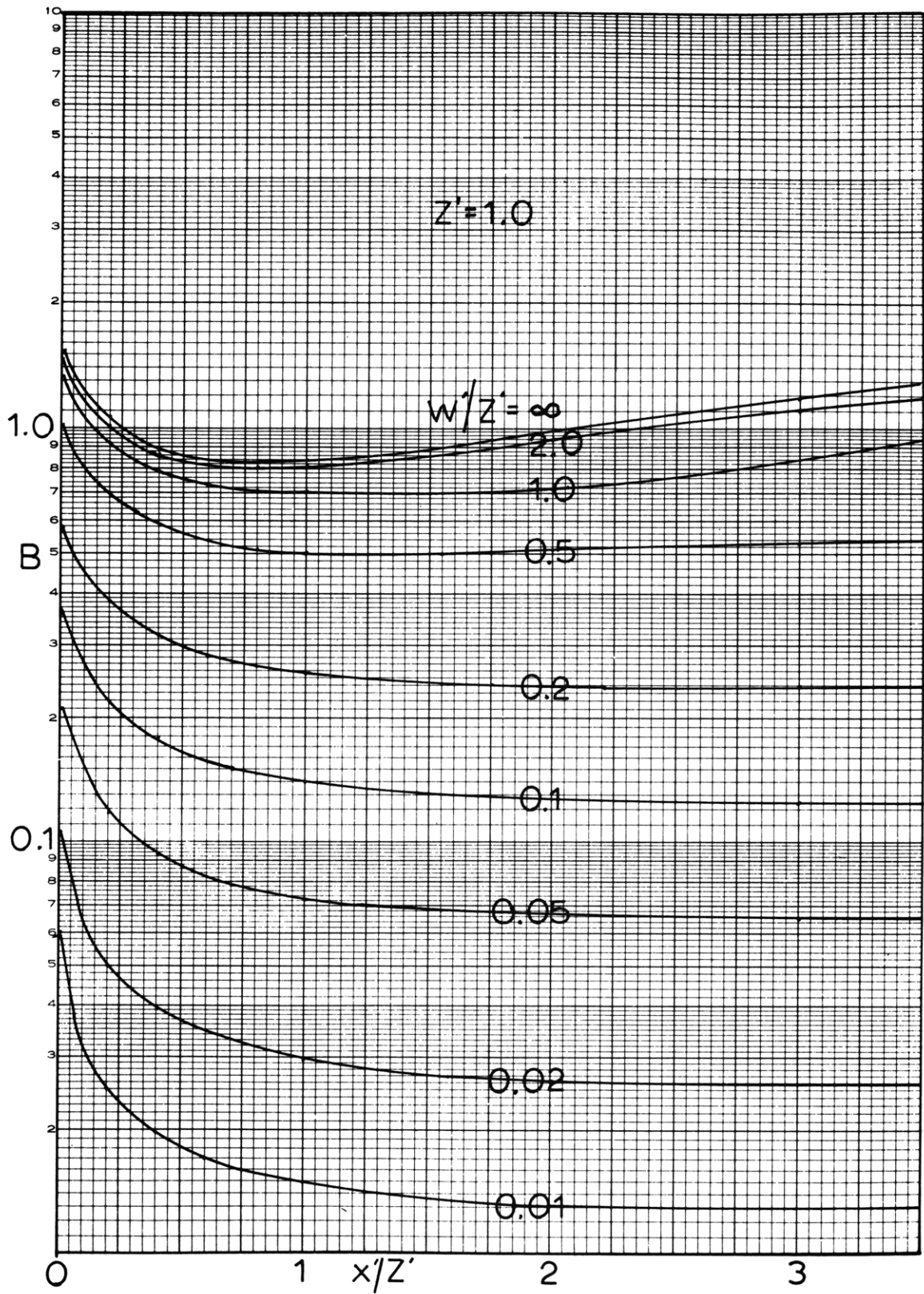


Figure 4-9c

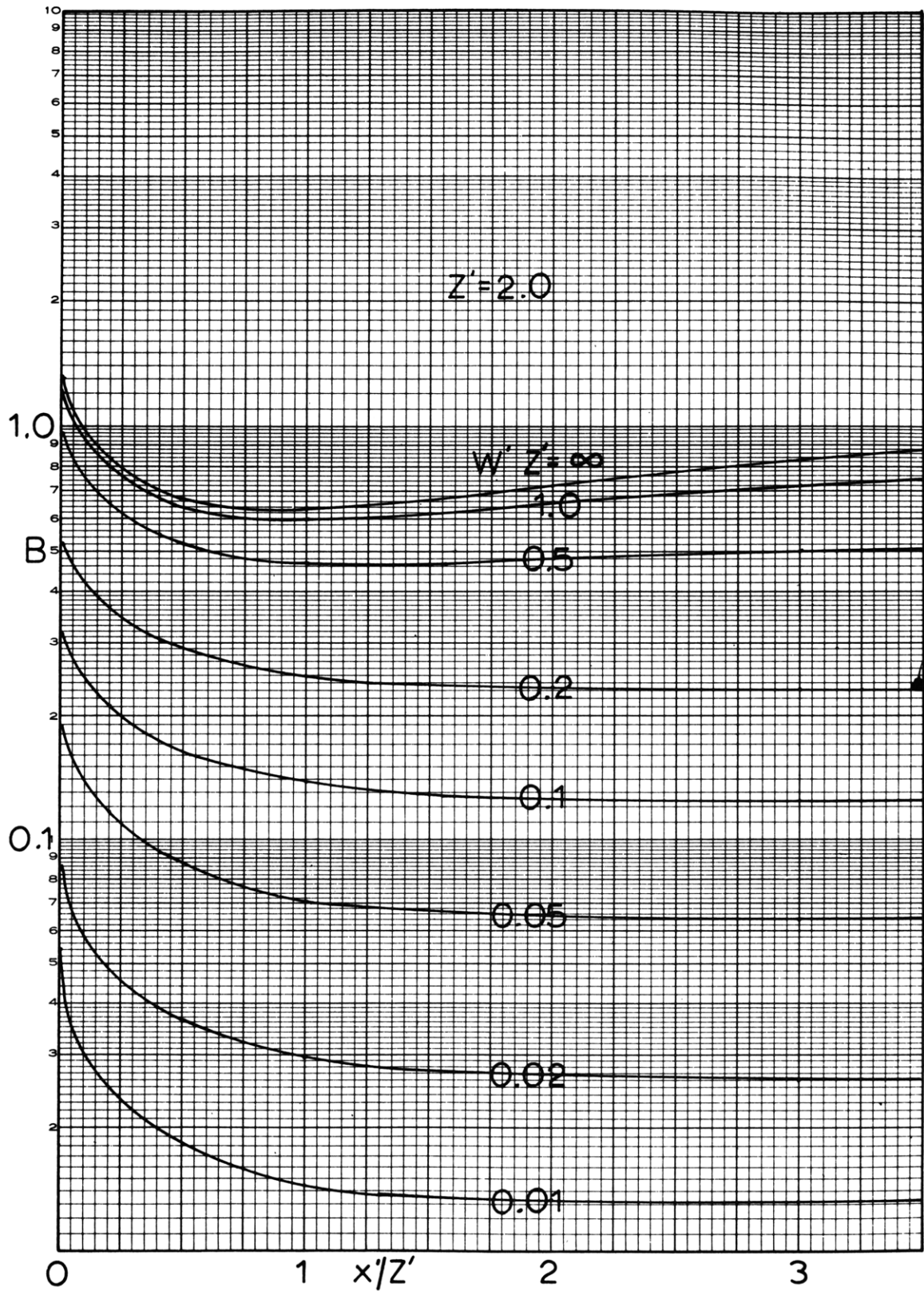


Figure 4-9d

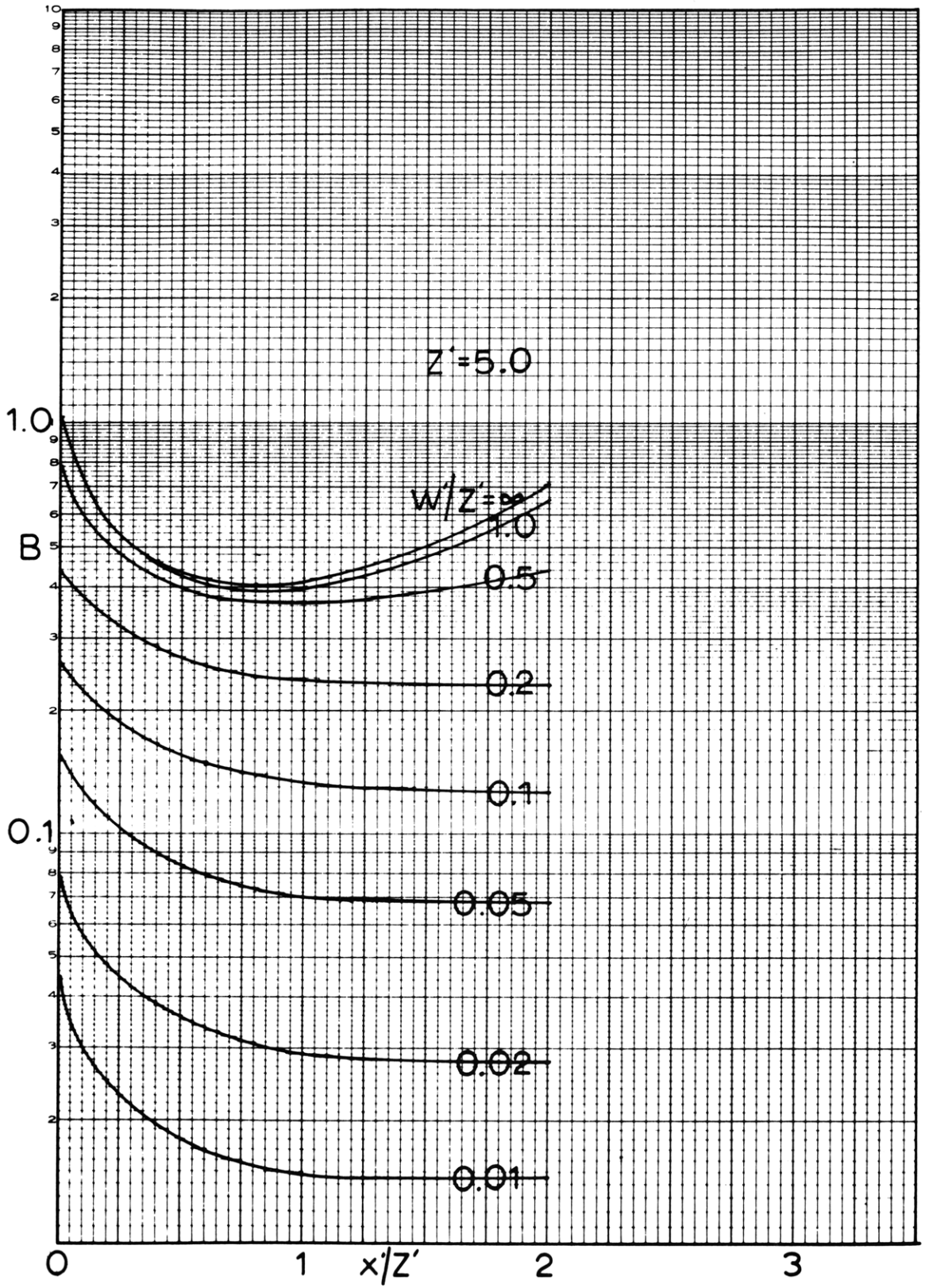


Figure 4-9e

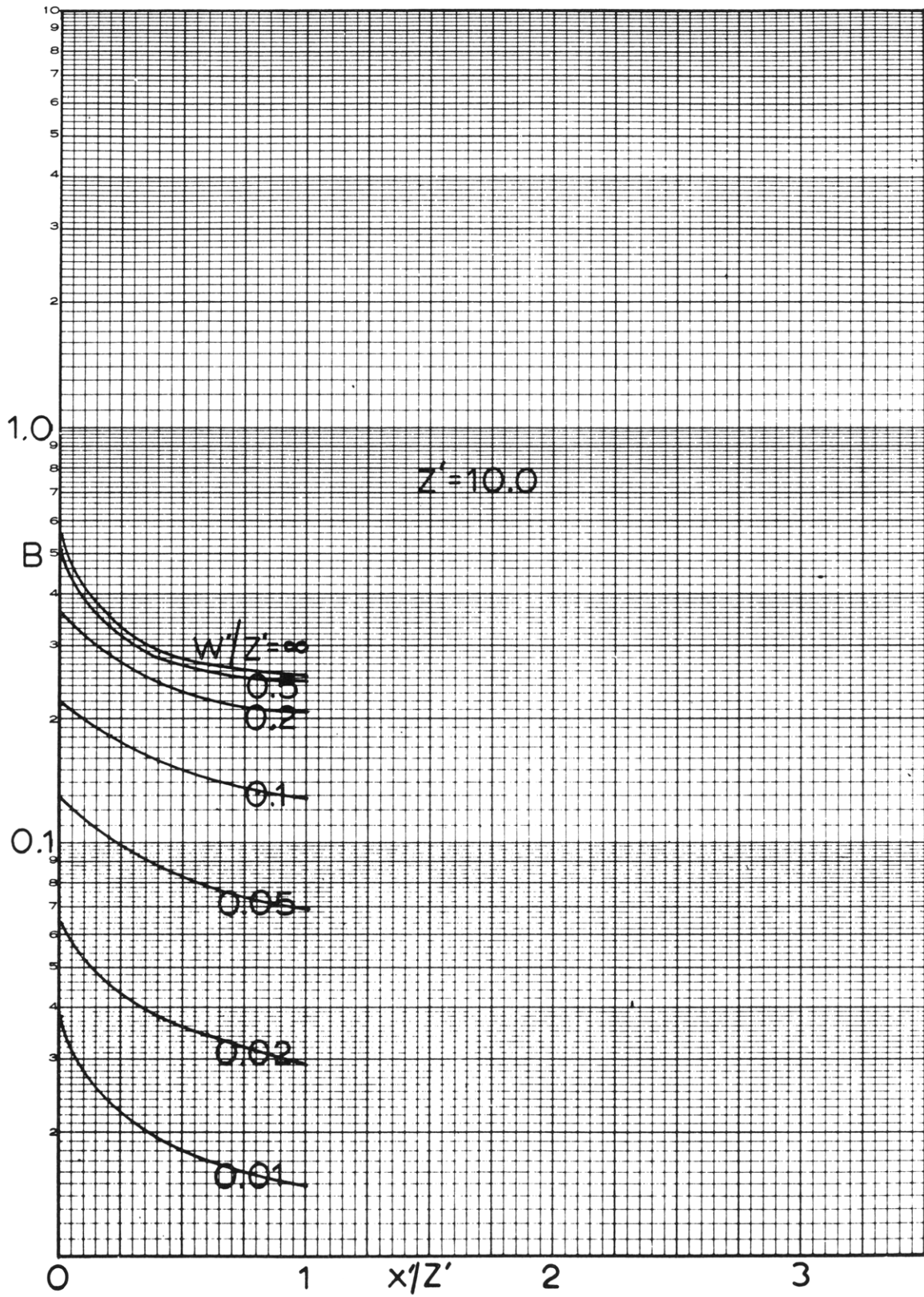


Figure 4-9f

Notice how the mean beam length varies in Figure 4-9a where $Z' = 0$. Consider the curve $W'/Z' = 1.0$, for instance. B starts at a value greater than Z' for $x' = 0$, since the shortest possible path is Z' . As x'/Z' increases the mean beam length decreases since the short distance through the upper corner of the parallelepiped becomes important. Finally as $x'/Z' \rightarrow \infty$ the mean beam length must return to unity since the absorbing path length becomes equal to W' for all traces.

4.7 Interchange Factors Between an Infinite Gray Gas Wedge and an Infinite Black Strip on the Horizontal Surface Surrounding its Base

The element of volume $dV = dz dw dy$ in Figure 4-10 is located a distance w from the axis of symmetry of the wedge, a height z above the horizontal surface z and displaced a distance y from the xz plane. The area element Ldx is a distance x from the axis of symmetry. The base of the wedge is of half width b and the boundary of the gray gas wedge is given by $W = az + b$. Note that this is again a special case of Section 4-2 and therefore the integration over y can be applied directly. Thus, equation 4-11 with proper numerical substitution of B in the integral becomes

$$\frac{\overline{dgs}}{Ldx} = \frac{2}{\pi} \int_0^{Z'} Z' dZ' \int_{-(az'+b)}^{az'+b} \frac{e^{-Bs'} dw'}{[z'^2 + (x' - w')^2]} \quad 4-41$$

where s' , given by 4-5 and 4-6 is

$$s' = \left(\frac{az' + b' - w'}{az' + x' - w'} \right) \sqrt{z'^2 + (x' - w')^2} \quad 4-42$$

The approximate formula suggested in Section 4-6 applies giving

$$\frac{\overline{dgs}}{Ldx dz'} = \frac{2}{\pi} \sum_1^m \exp - \left[\frac{B \left(az' + b' - \left(\frac{W'_n + W'_{n-1}}{2} \right) \right)}{\left(az' + x' - \left(\frac{W'_n + W'_{n-1}}{2} \right) \right)} r'_{ave} \right] \left(\tan^{-1} \frac{x' - W'_n}{Z'} - \tan^{-1} \frac{x' - W'_{n-1}}{Z'} \right) \quad 4-43$$

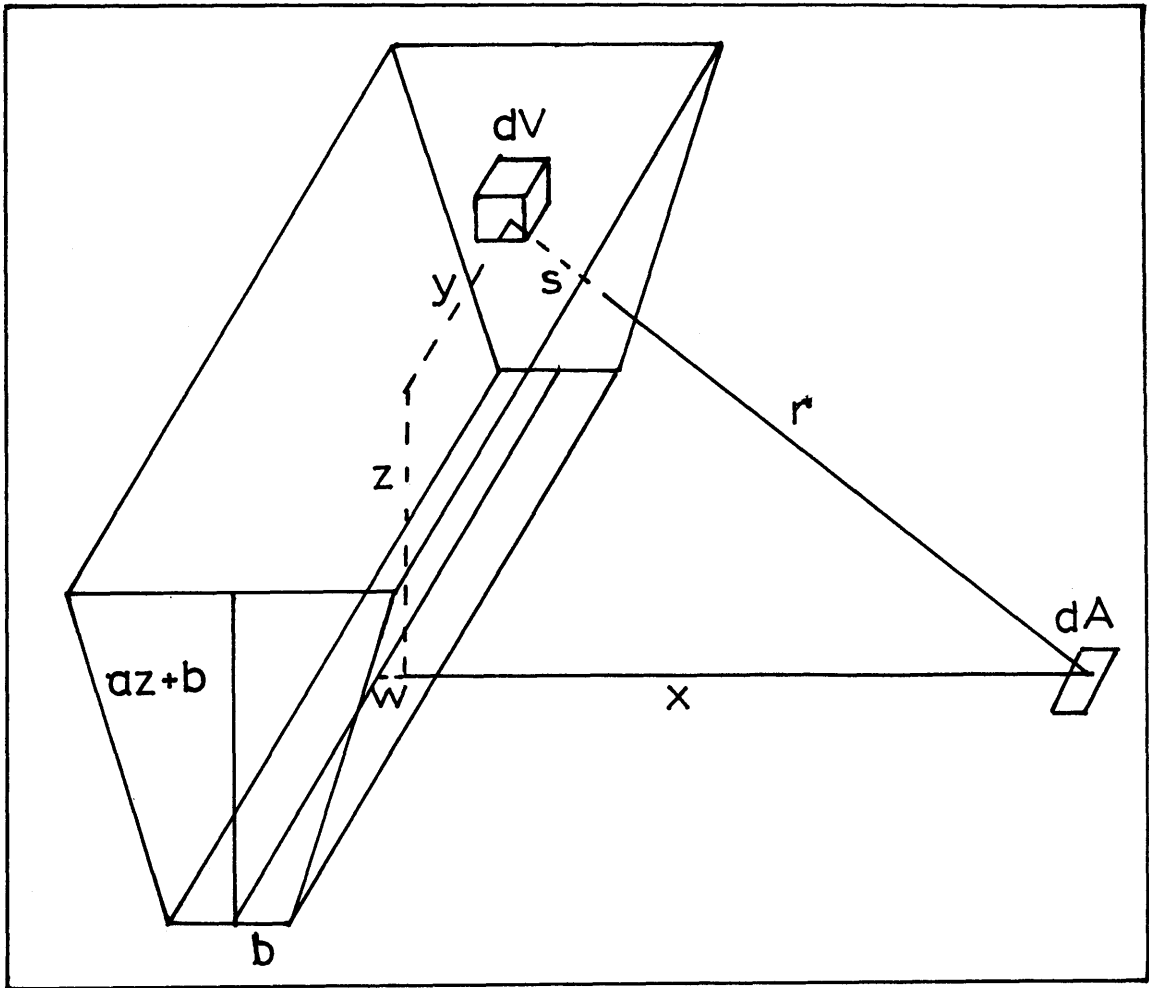


Figure 4-10 Interchange Between a Gray Gas Wedge and a Black Strip

where

$$r'_{ave} = \sqrt{z'^2 + \left(x' - \frac{W'_n + W'_{n-1}}{2}\right)^2}$$

and $m = 2 az'/\Delta w'$. The same $\Delta w'$ is recommended as in Section 4-6. It is possible to solve equation 4-41 only in the limit $k = 0.0$ by deleting the exponential term. The solution is

$$\begin{aligned} \frac{\overline{dgs}}{Z' L dx} = & \frac{2}{\pi} \left\{ \tan^{-1} \left(\frac{x' + aZ' + b'}{Z'} \right) - \tan^{-1} \left(\frac{x' - (aZ' + b')}{Z'} \right) \right. \\ & + \frac{(x' + b')}{2Z'(1 + a^2)} \ln \left[\frac{(1 + a^2)Z'^2 + 2a(x' + b')Z' + (x' + b')^2}{(x' + b')^2} \right] \\ & - \frac{(x' - b')}{2Z'(1 + a^2)} \ln \left[\frac{(1 + a^2)Z'^2 - 2a(x' + b')Z' + (x' - b')^2}{(x' - b')^2} \right] \\ & - \frac{(x' + b')a}{Z'(1 + a^2)} \left[\tan^{-1} \left(\frac{(1 + a^2)Z' + a(x' + b')}{(x' + b')} \right) - \tan^{-1} a \right] \\ & \left. - \frac{a(x' - b')}{Z'(1 + a^2)} \left[\tan^{-1} \left(\frac{(a^2 + 1)Z' - a(x' - b')}{(x' - b')} \right) + \tan^{-1} a \right] \right\} \quad 4-44 \end{aligned}$$

The solution for $k = \infty$ by cross strings is

$$\frac{\overline{dgs}}{L dx} = \frac{1}{2} \left[1 - \frac{(x/Z) - a}{\sqrt{1 + \left(\frac{x}{Z} - a\right)^2}} \right] \quad 4-45$$

Some values for other absorption coefficients have been obtained on the 709 and 7090 computers for a base $b' = 0$ and a wedge slope of $a = 0.25$, and are given in Figure 4-11. The slope 0.25 corresponds approximately to the slope of a buoyant line flame given by the analysis in Chapter 6. The equation recommended for analytical use is

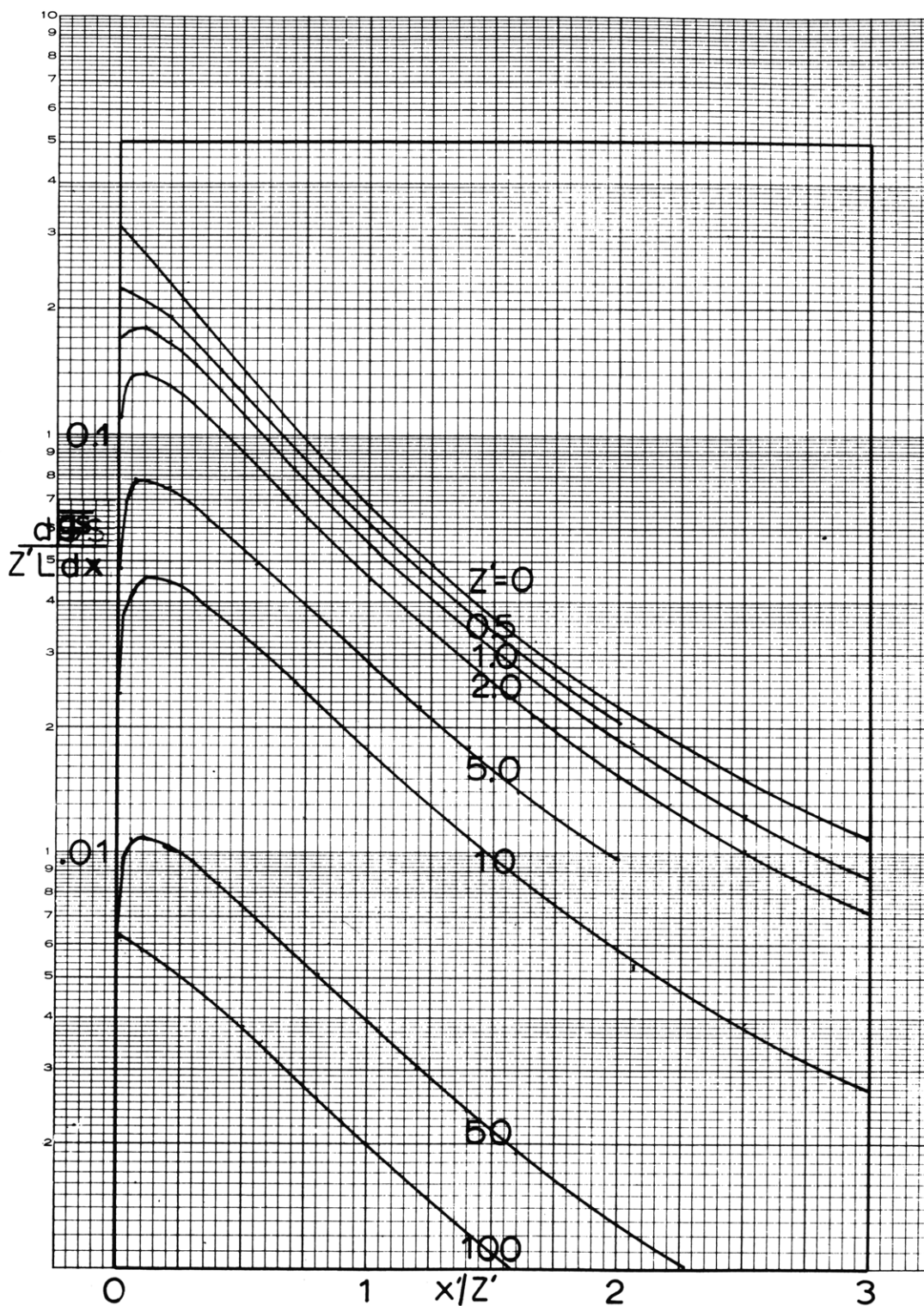


Figure 4-11. Interchange Factors for an Infinite Gray Gas Wedge of Height Z' and Slope 0.25 and the Surrounding Surface as a Function of the Distance from the Center Line to Height Ratio

$$\frac{d \overline{gs}}{L dx} = \frac{(1 - e^{-BZ'})}{2} \left[1 - \frac{((x/Z) - a)}{\sqrt{1 + (\frac{x}{Z} - a)^2}} \right] \quad 4-46$$

where the bracketed term represents twice the exchange between an infinitely long black plane of height Z inclined at a slope "a" and a black strip on a horizontal plane. The exponential term, $(1 - e^{-BZ'})$, represents the effective emissivity of the gray gas wedge. B is given in Figure 4-12 and supplies the correct values to make the simplified equation give the rigorous answer.

The method for correcting the data of Chapter V was based on the above infinite wedge exchange factors, along with the required finite ones calculated manually. The radiation from a line fire can be given, to a first approximation, by the assumption of a uniform temperature wedge for a very narrow-base fire, or a uniform temperature rectangular parallelepiped for a wide-base fire. The data in Chapter V suggest that a uniform temperature of approximately 1200°F be used.

4.8 Total Interchange Areas

In many engineering problems involving radiative transfer, it is advantageous to divide the system into finite zones. Once the interchange between each zone and all the other zones is known it is not difficult to obtain the heat transfer to and from various parts of the system. The zoning technique used before has usually been for small regularly shaped areas. However, it is possible to apply the same technique to the system which is infinite in one dimension.

It is apparent that the interchange between a rectangular volume of gray gas and a finite surrounding surface in a system of infinite length is given by the integration of equation 4-35.

$$\frac{\overline{gs}}{L} = \int_{x_1}^{x_2} \left(\frac{d \overline{gs}}{L dx} \right) dx \quad 4-47$$

where $d \overline{gs}/L dx$ can be obtained from Figure 4-8 as a function of x .

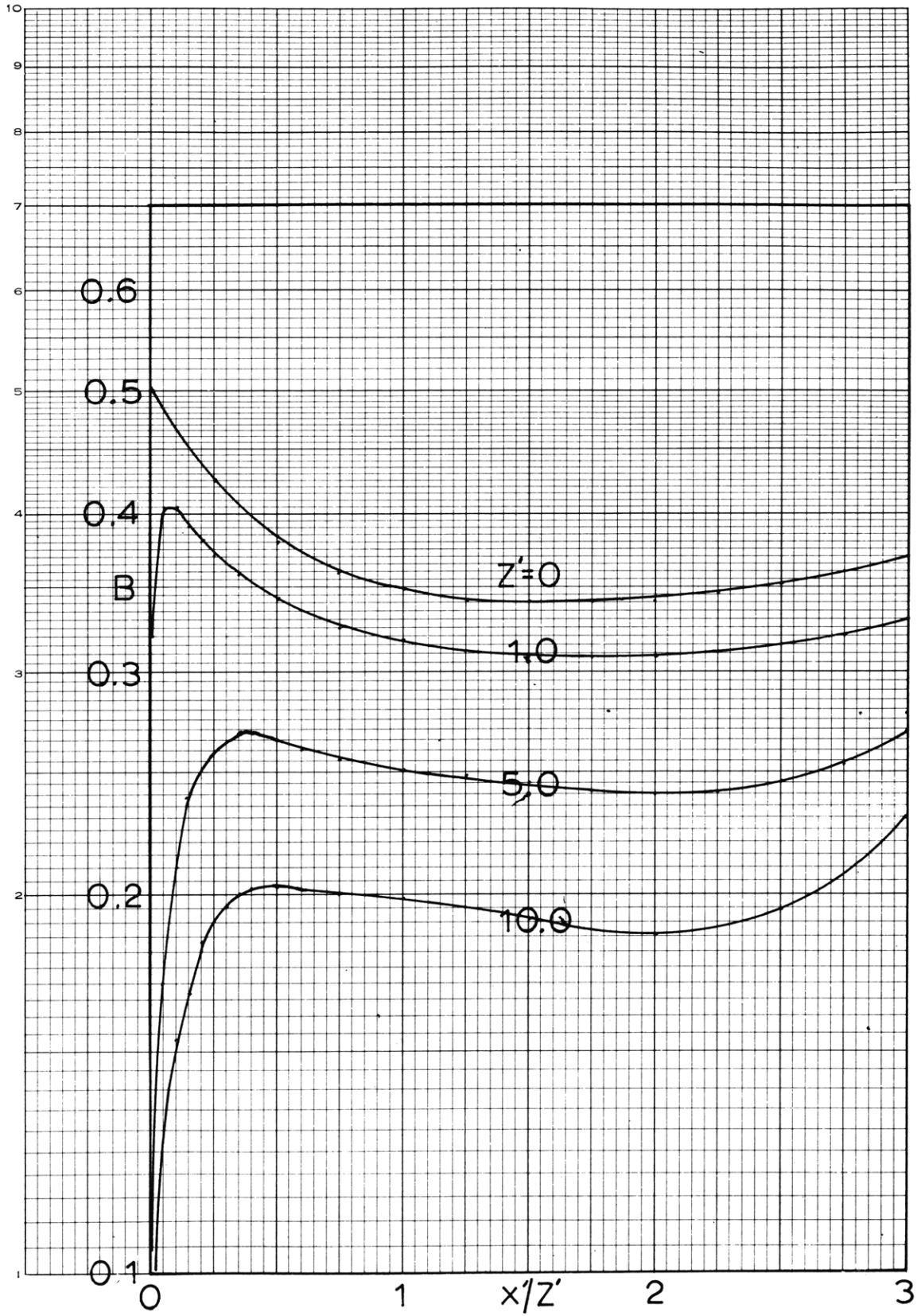


Figure 4-12 Mean Beam Length for Equation 4-46 as a Function of the Ratio of the Distance from the Center Line to the Height

Consider the simple system in Figure 4-13 where it is desired to obtain the interchange between the gas volumes and the various surfaces. $\overline{G1 - S1}$ can be obtained directly from 4-47 and is the same as $\overline{G1 - S8}$, $\overline{G2 - S2}$, etc. $\overline{G4 - S1}$, is found by

$$\overline{G4 - S1} = \overline{G4 + G1 - S1} - \overline{G1 - S1} \quad 4-48$$

where $\overline{G4 + G1 - S1}$ is obtained from 4-47. In like manner

$$\overline{G2 - S1} = \overline{G2 + G1 - S1} - \overline{G1 - S1} \quad 4-49$$

$$\overline{G3 - S1} = \overline{G3 + G2 - S1} - \overline{G2 - S1} \quad 4-50$$

Therefore, it is necessary to obtain only four interchange factors by numerical integration to find all the gas-to-surface exchange factors.

In order to obtain the surface-to-surface interchange factors it would be necessary to perform two more integrations of equation 4-29. It appears that it may be desirable to pursue this system to completion, and it is recommended that evaluation of these interchange factors be made a part of future studies.

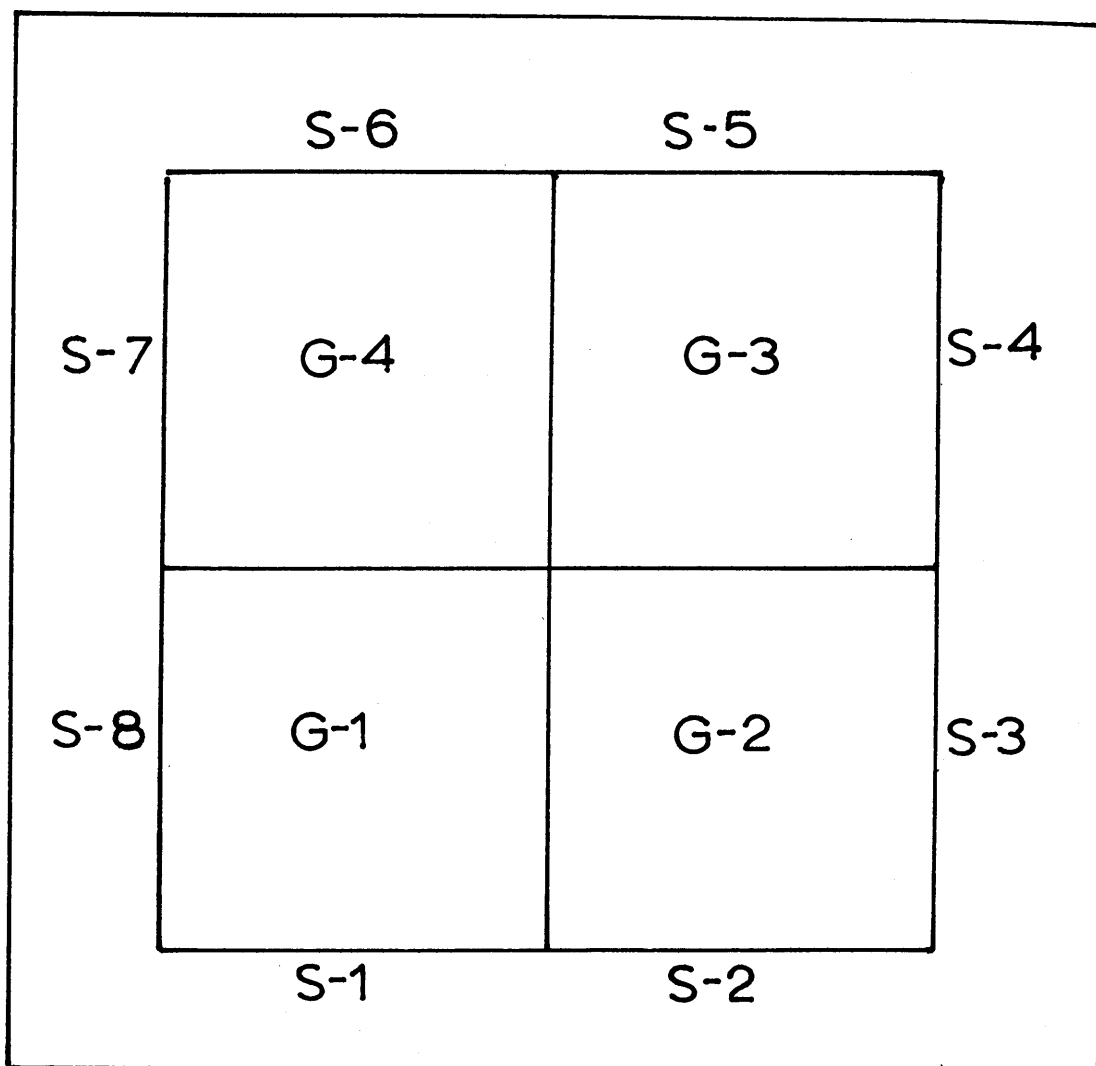


Figure 4-13 Total Gas-to-Surface Interchange Factors

V. RADIATION FROM A LINE FIRE

5.1 Introduction

The two-dimensional exchange factors in Chapter 4 give the intensity profiles around a uniform temperature gray gas wedge and rectangular parallelepiped. It seemed desirable to establish how well these profiles approximate the distribution of the flux density of radiation on a surface surrounding an actual fire. Some measurements of radiation flux density around a line fire were made by de Rochechouart (24) using methane flames. The present author used propane flames.

5.2 Apparatus

The apparatus is discussed in more detail by de Rochechouart (24). It consisted of a 2" by 24" slot surrounded by a flat surface of 3 feet on both sides. Fuel was fed at a measured rate through a one inch pipe with numerous small holes throughout its length, into the bottom of a metal chimney to obtain a uniform velocity profile. The flow rate of the fuel issuing from the slot was so low that the fuel momentum was negligible compared to the buoyancy produced by the flame. The resulting fire is shown in Figure 5-1. The radiation flux density was measured at several distances from the flame with a thermopile consisting of a flat chromel-constantan strip soldered at the ends to 2-inch copper cubes. The thermopile is described fully by de Rochechouart (24). For each measurement the e m f was recorded continuously for several minutes on a Sanborn 150 Recorder. The recorded data oscillated rather randomly by about 5%. The radiation flux densities were evaluated by drawing the best straight line through the recorded data.

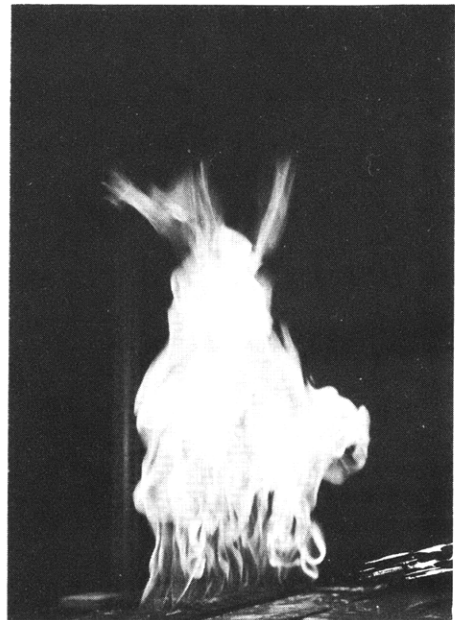


Figure 5-1 Line Fires (Methane)

5.3 Data on Line Fire Radiation

The data of de Rochechouart (24) of radiation flux densities around methane flames is given in Figure 5-2 and tabulated in Appendix F. The heat liberation rates reported originally were wrong, due to an error for which this author is partially responsible. The values given are based on the low heating value of the fuels. The data for radiation around propane flames is given in Figure 5-3 and is tabulated in Appendix^{ces} F-2 and F-3. The data cover a range of heat liberation rates from 72,000 to 231,000 Btu/hr-ft. The measurements were made at distances of 0.2 to 1.2 feet from the center of the slot.

Inspection of Figure 5-1 shows that the fires were nearly laminar at the base and developed large scale turbulence at the top of the flame. This was also observed by Blinov and Kludihov (2) in large pan fires. The photographs and visual observation indicate that this turbulence is quite spectacular with whole sections of luminous gas separating itself from the rest of the flame. This is believed to be responsible for the oscillations in the measured radiation flux density. It was also observed that propane flames tended to wander out over the surface. This is undoubtedly because propane has a higher density than air and will be discussed more fully in section 6.4.

5.4 Correction of Data to an Infinitely Long Flame

The fires in these experiments were only two feet long because it was unfeasible to liberate a large amount of heat in the small test cell. Some of the larger fires raised the temperature of the air near the ceiling to 150°F in less than 10 minutes. The experimenters were forced to make one measurement over several minutes, stop the fire, and resume after the room had

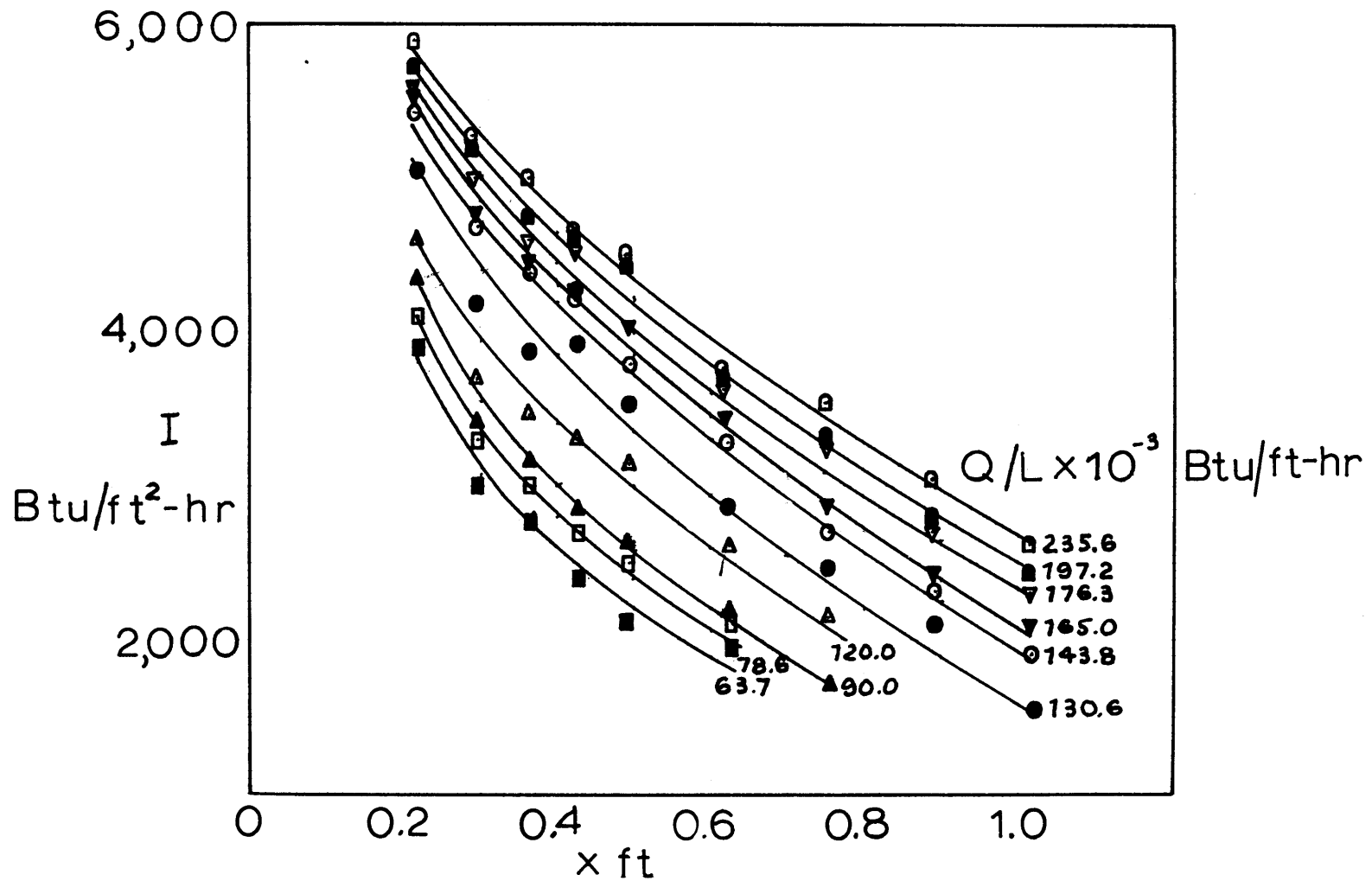


Figure 5-2 Flux Density of Radiation on a Horizontal Surface Surrounding a Line Methane Flame for Different Heat Liberation Rates (data by De Rochechouart⁽²⁴⁾)

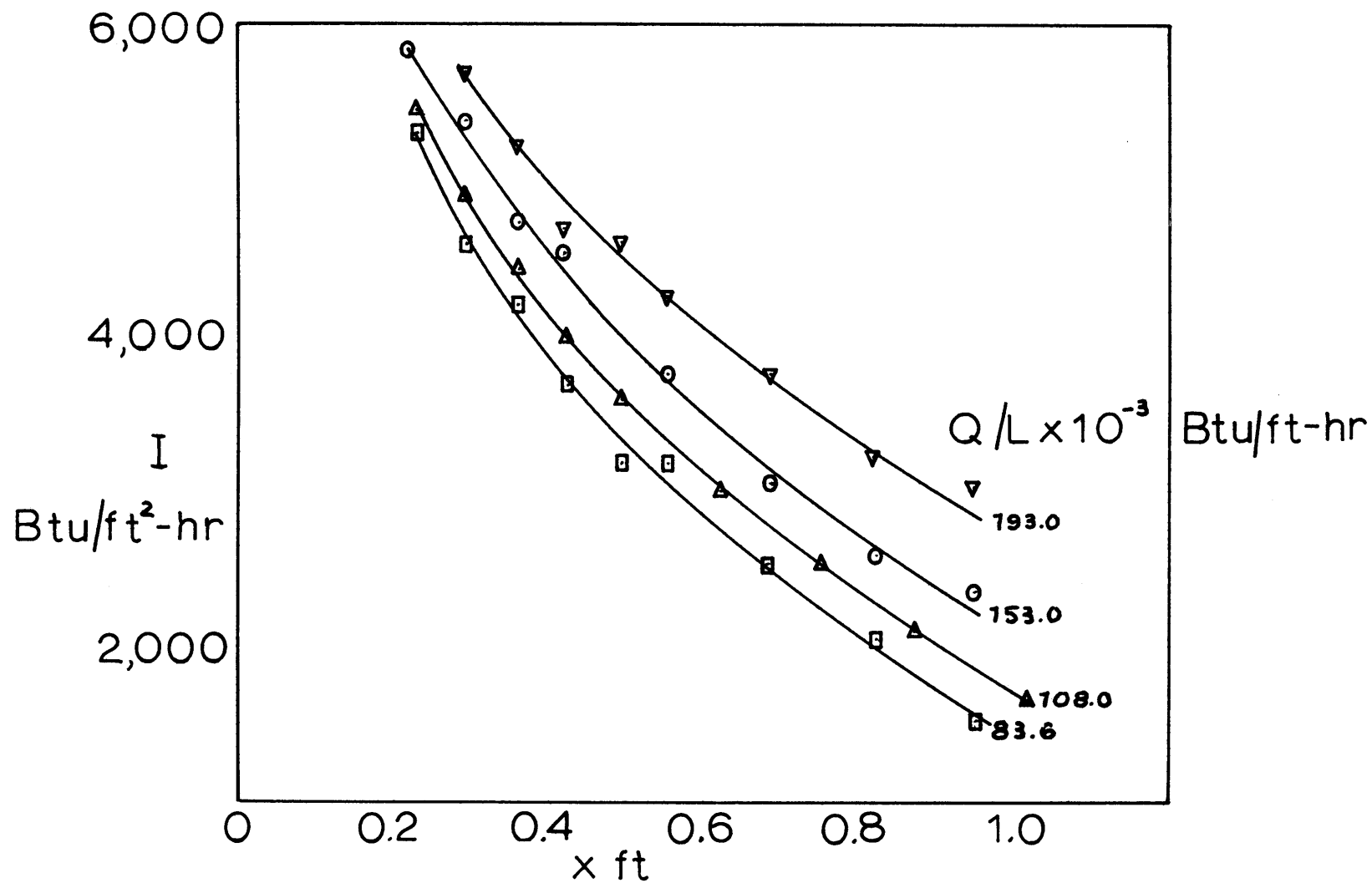


Figure 5-3 Flux Density of Radiation on a Horizontal Surface Surrounding a Line Propane Flame for Different Heat Liberation Rates

cooled. Propane flames also provided a problem because the air in the cell rapidly filled with soot. Therefore, the physical inconvenience of a long fire led to the theoretical inconvenience of a short one, since a two-foot line fire is considerably shorter than an infinite one. To overcome these circumstances the following method was used to predict the intensity patterns from an infinitely long line fire.

It is apparent that equation 4-21 multiplied by $e^{-Bs'}$ with B given by equation 4-22 or Figure 4-3 is the solution for the exchange factors between a finite gray gas wedge and a black element of area $L dx$ located a dimensionless distance x' from the base of the wedge and half way between the ends. By obtaining the proper substitution of variables from Figure 4-10 one obtains the following equation

$$\frac{d \overline{gs}}{L dx} = \frac{2}{\pi} \int_0^{Z'} z' \int_{-(az' + b')}^{az' + b'} \frac{Y' e^{-Bs'} dw'}{(z'^2 + (x' - w')^2)^{\frac{1}{2}} (z'^2 + (x' - w')^2 + Y'^2)^{\frac{1}{2}}} \quad 5-1$$

where s' is given by equation 4-42

$$s' = \frac{(az' + b' - w')}{(az' + x' - w')} \sqrt{z'^2 + (x' - w')^2} \quad 4-42$$

The double integration of equation 5-1 was performed graphically for three Z'/Y' at several x'/Z' for $k' = 0 \text{ ft}^{-1}$ and $k' = 1.0 \text{ ft}^{-1}$. The solution for $k' = \infty$ can be obtained analytically and is given in Appendix D. The exchange factors for wedges of infinite length are given in Figure 4-11. The ratio of the exchange factor at infinity to the exchange factor at Y' is given as the ratio of the distance from the wedge to the wedge height for three length-to-height ratio's and three absorption coefficients in Figure 5-4.

Unfortunately the absorption coefficient for the actual fires is not known. In general the absorption coefficient will be a function of the

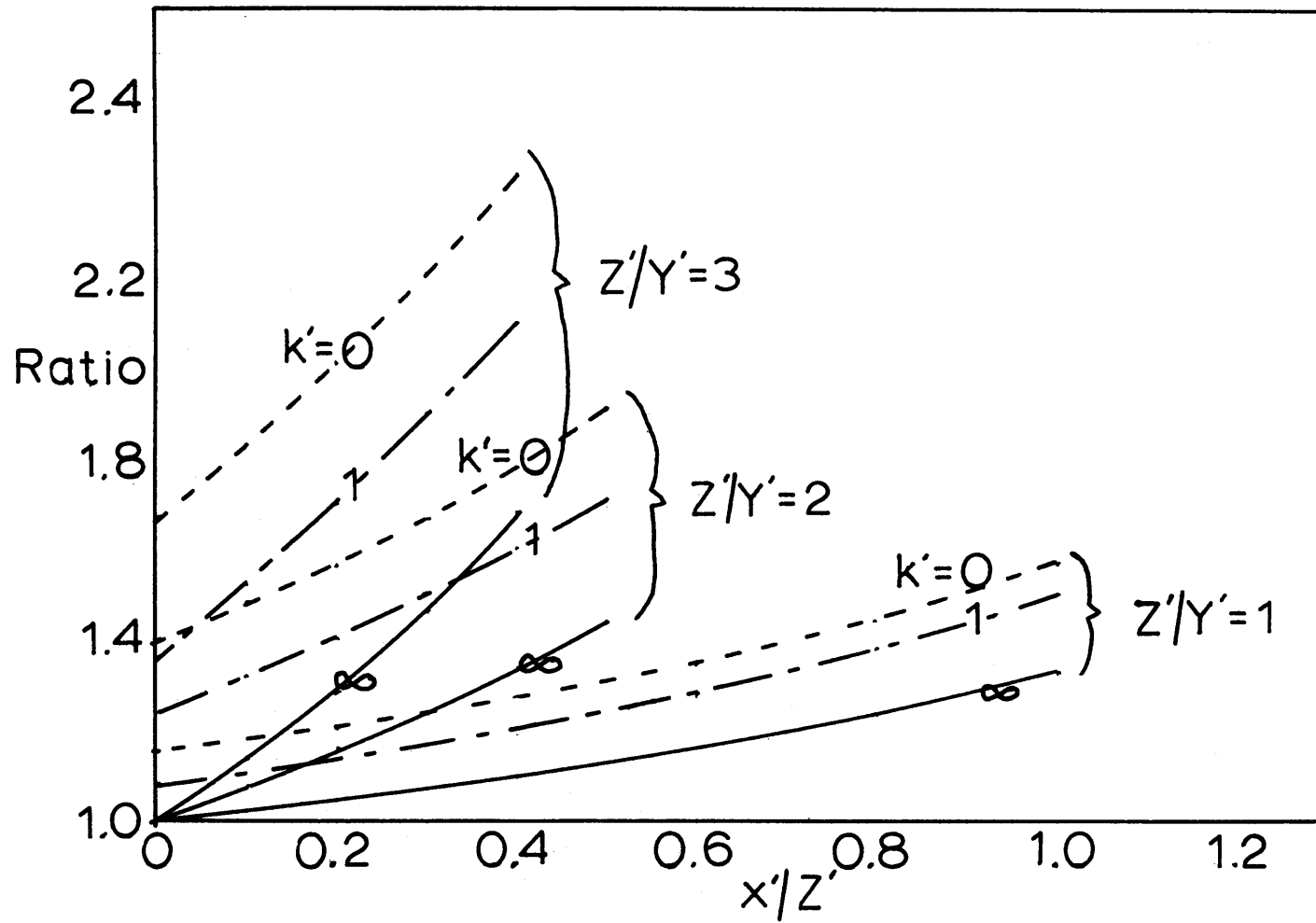


Figure 5-4 Ratios of Exchange Factors for Infinite and Finite Line Wedges

position in the flame since it is a function of carbon and gas concentration and temperature. Attempts to measure this absorption coefficient in the actual flame would be made difficult by the great turbulence in the flame. However, single- and double-path measurements were made on small laminar line flames of methane and propane. The absorption coefficients obtained were approximately $k' = 2.0 \text{ ft}^{-1}$ for methane and $k' = 10.0 \text{ ft}^{-1}$ for propane. With the flame heights given in Figure 6-2, it is now possible to correct the data to an infinite flame using Figure 5-4. The corrected data are shown in Figure 5-5 and 5-6.

A reconsideration of the analysis of Section 4-7 is helpful. The exchange factors around a gray gas wedge are given by equation 4-46

$$\frac{d \overline{gs}}{L dx} = \frac{(1-e^{-BZ'})}{2} \left[1 - \frac{\left(\frac{x}{Z} - a\right)}{\sqrt{1 + \left(\frac{x}{Z} - a\right)^2}} \right] \quad 4-46$$

where B is obtained from Figure 4-12. Therefore a plot of the flux density divided by $(1-e^{-BZ'})$ vs. the distance from the center of the flame base by the flame height, should give a single curve. This plot is shown in Figure 5-7.

Note that if the data for a particular fuel do not fall on a single curve in Figure 5-7 either the measured absorption coefficient is in error or the approximation of the flame by a uniform temperature gray gas wedge is not a good one. The correlation of the data in Figure 5-7 seems to support both the measured absorption coefficients and the assumption.

The solid curves in Figure 5-7 are those of gray wedges with temperatures of 1260°F and 1120°F . These values do not seem unreasonable since they are based on the entire luminous flame region. Although propane has a higher heating value and a slightly higher adiabatic flame temperature

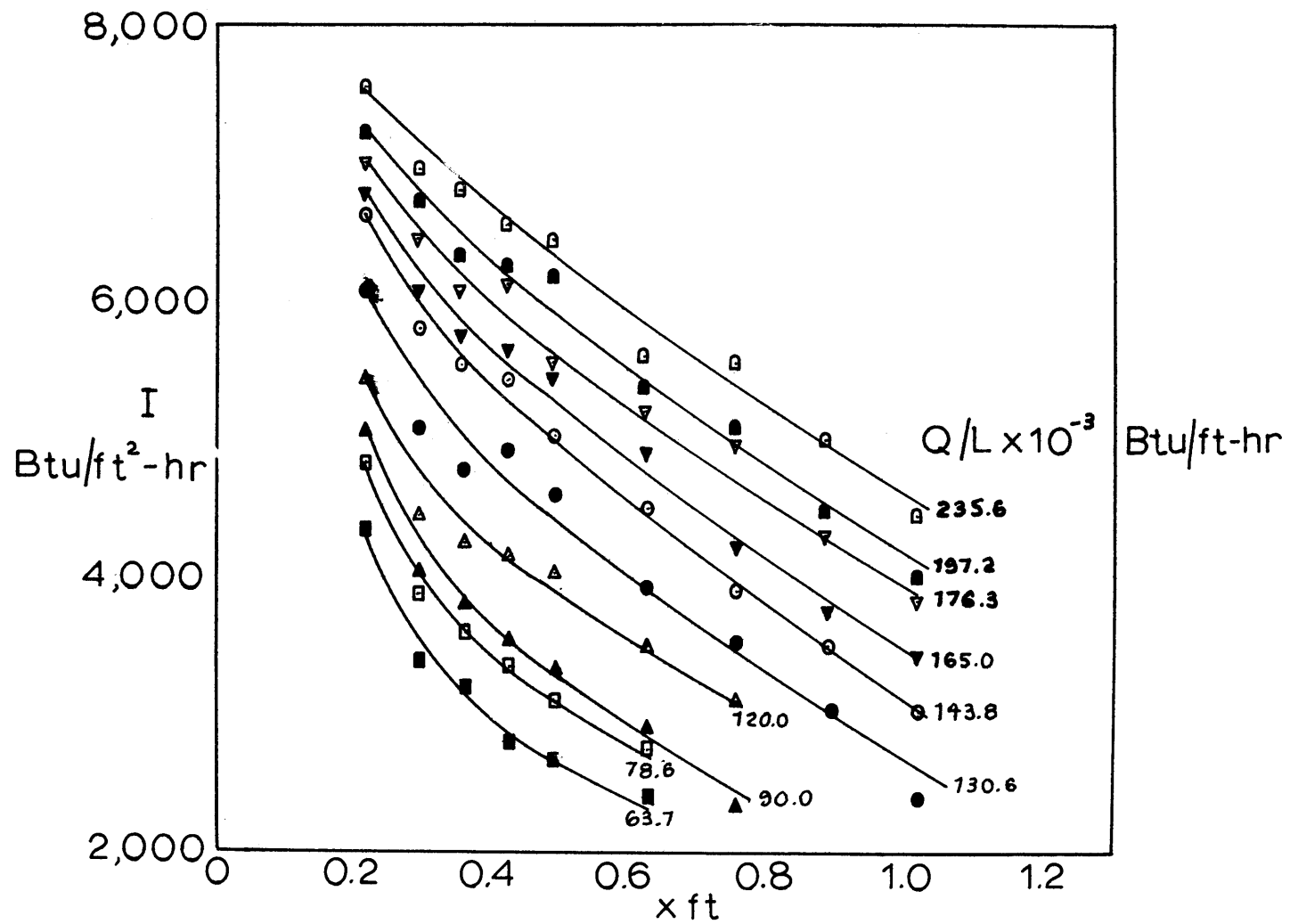


Figure 5-5 Flux Density of Radiation on a Horizontal Surface Surrounding an Infinite Line Methane Flame for Different Heat Liberation Rates (Corrected)

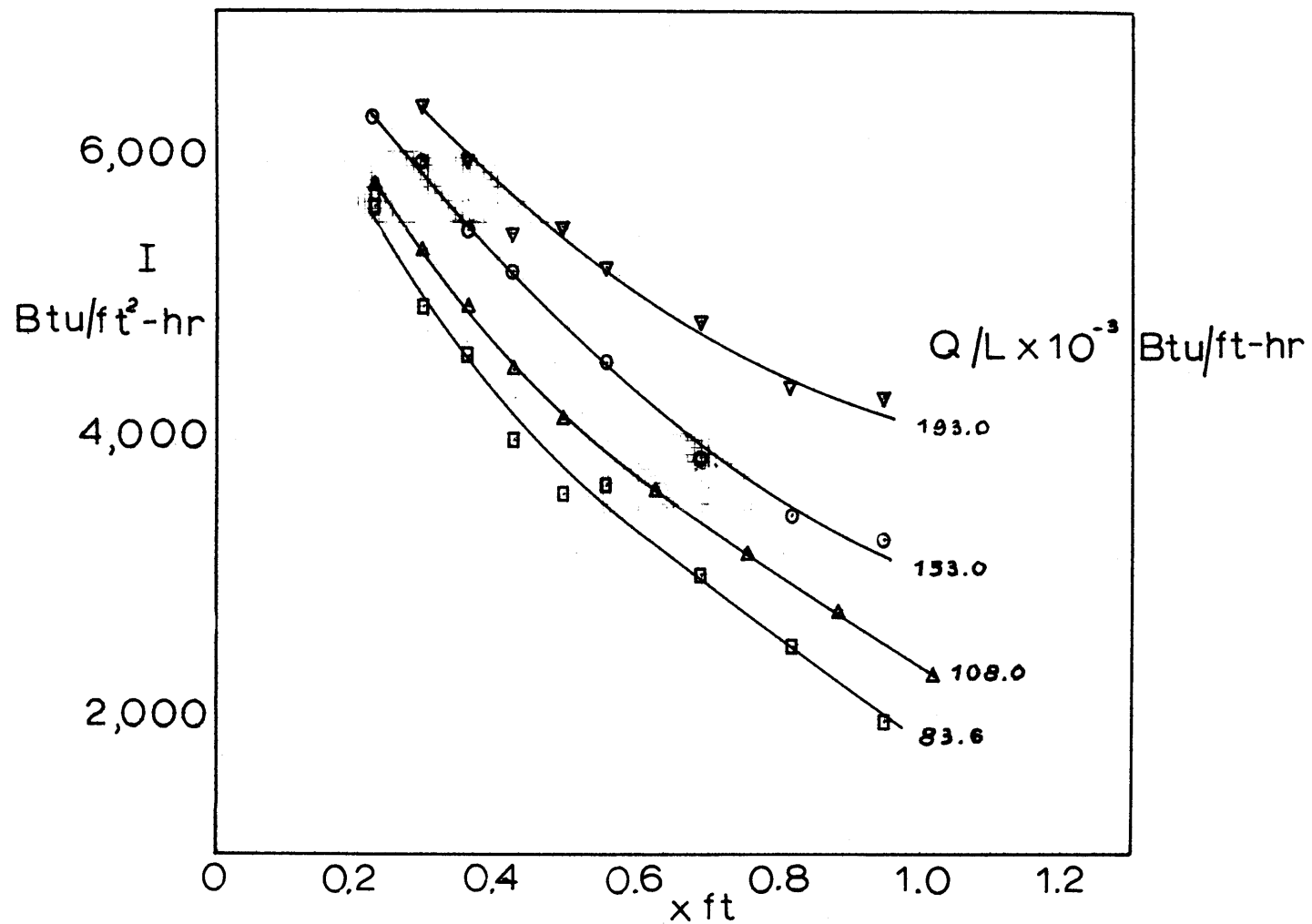


Figure 5-6 Flux Density of Radiation on a Horizontal Surface Surrounding an Infinite Line Propane Flame for Different Heat Liberation Rates (Corrected)

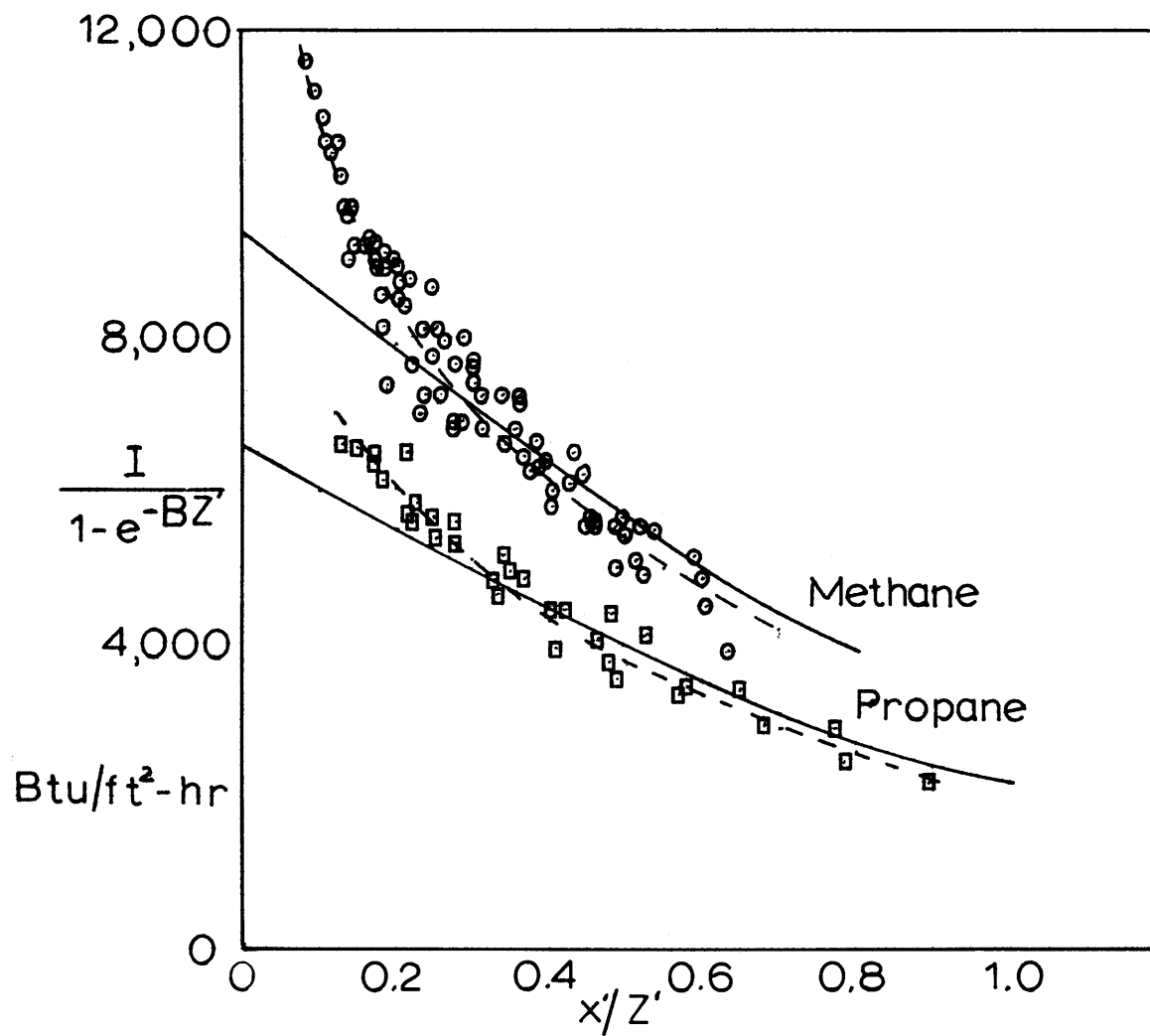


Figure 5-7 Radiation Flux Density to Flame Emissivity Ratio as a Function of the Ratio of the Distance from the Center of the Flame to the Flame Height

for a stoichiometric mixture, the propane flame is considerably blacker and radiates more of its heat.

The data indicate that a gray gas wedge of slope 0.25 with a uniform temperature and constant absorption coefficient is a good approximation for flames of a narrow base. A rectangular parallelepiped of uniform temperature and uniform absorption coefficient is recommended for calculating the radiation flux density around a wide-base fire.

VI. THE FLAME AND RESULTING CONVECTION COLUMN

6.1 Introduction

An understanding of the fluid dynamics of a buoyant plume is important in the analysis of fire spread. The flame supplies radiation to the unburned and burning fuel, and the buoyant plume above the fire influences combustion to an unknown extent. The data on the distribution of radiation around buoyant flames in Chapter V indicates that the approximation of the flame by a gray gas wedge of uniform temperature is a rather good one. However, it may be possible to improve the analysis by allowing for temperature and concentration variations in the flame.

Although it is apparent that disturbances in the convection columns above small fires do not greatly influence the fire itself, it is possible that once a fire attains a magnitude where it can compete with normal meteorological forces, conditions in the convection column may greatly affect the fire below. This is where the almost completely undetermined influence of weather plays its parts. Schaefer (26) reports that "wild fires" nearly always occur in a very unstable atmosphere (super adiabatic) with a jet stream in the upper atmosphere. However, there is no quantitative knowledge of the effect of weather on large fires.

6.2 Buoyant Plumes

Buoyant plumes can be defined as currents of rising fluid produced by a difference in density of the plume and the surrounding fluid. Although this density difference can be a low density source, such as a low density liquid (water) issuing into higher density liquid (salt solution), the most important applications involve a density difference produced by a heat source establishing an upward flow in the atmosphere. This heat source may be a chimney, sand heated by the sun, a lake on a cool summer night, or a fire. Our primary interest is in the latter.

The problem was first considered analytically by Schmidt (28). Schmidt made the following assumptions which are general to all other investigators:

1. Turbulent flow fully developed and molecular processes neglected.

2. Transverse forces small compared with those in the vertical direction.
3. Mixing in the vertical direction neglected.
4. No horizontal pressure variation.

Schmidt used Prandtl's mixing length theory and similarity but not equality of eddy viscosity and eddy conduction.

$$\text{Rate of lateral momentum transfer} \propto \rho b^2 \left(\frac{du}{dy}\right)^2$$

$$\text{Rate of lateral heat transfer} \propto c \rho b^2 \left(\frac{du}{dy}\right) \left(\frac{d\theta}{dy}\right)$$

where

ρ = density

b = distance of transfer

u = velocity perpendicular to transfer

c = heat capacity

θ = temperature

Using the above assumptions Schmidt writes the equations of continuity, vertical motion (force balance), and an energy balance. With the additional assumptions of uniform density at infinity and density variations small compared to absolute density he obtains a solution which (1) predicts the form of the temperature and velocity distributions and in addition calls for (2) the normalized distributions of temperature and upward velocity to be self preserving at all heights (although the distributions of temperature and of velocity are different). By making measurements above an electrically heated coil he found (2) well verified and (1) approximately so.

Rouse, Yih, and Humphreys (25) wrote the same equations as Schmidt independently, but assumed his second conclusion of similar profiles instead of Prandtl's mixing length. Their solution gives the variation of center line properties with height but leaves the profiles to be determined experimentally. The profiles above both point and line sources were obtained by measuring physical properties over small gas burners.

Later work by Priestley and Ball (33) and Morton, Tayler, and Turner (22) extend the analysis to an atmosphere in which density changes with height

above the source, but make slightly different assumptions regarding boundary conditions.

Priestley and Ball assume effectively that the plume is straight-sided which is strictly true only if the ambient density does not vary with height. They apply boundary conditions at a finite source. Morton applies all boundary conditions at a virtual source of zero radius and momentum flux and assumes a weight deficiency (or heating rate) is known. The significant difference occurs when the density decreases with height. In this case the plume has a finite height, and will spread horizontally as it stops. Priestley and Ball's assumption of linear spread is certainly not good in this instance and although Morton's does not include entrainment from the top of the plume it seems to be more realistic.

Morton (19) extends his previous paper to include the effect of a moist atmosphere and predicts when condensation will occur and its effect on the flow. He assumes a simple linear decrease in humidity with height and no effects on physical properties due to water vapor.

Morton (20) adapts his previous treatment to finite sources with finite flow by relating them to the virtual point source in his previous paper.

Schmidt (27) reviews the findings of Priestley and Ball (33) and suggests a new axial velocity distribution to replace the standard Gaussian function. However, the new distribution does not seem justified and predicts a reverse flow region the existence of which seems rather dubious.

Murgai and Emmons (23) give a very useful method of calculating a plume for any arbitrary lapse rate by making the calculation over several heights of constant lapse rate. No assumption of virtual source is made and the previous final conditions become the initial conditions of the next step, i.e., all boundary conditions are applied at a finite source.

Lee and Emmons (15) give the treatment of a finite line source issuing into a constant density atmosphere. No virtual source is assumed and the

boundary conditions are applied at a finite source.

Morton (21) extends his previous papers on buoyant jets to include wakes. He also introduces a very simple momentum-mass flux diagram which is very helpful in clarifying the meaning of the solutions for various cases.

Homsy (9) has obtained the solution for a plume originating at a finite circular source without the assumption of small density variations. The boundary conditions are applied at the finite source and the assumptions of a constant density atmosphere and reproducing profiles are made. This method of solution can easily be applied to a finite line source.

The above solutions are now at a state where the convection column above a fire can be described with confidence since the results have been well supported by data.

6.3 A Model of a Burning Jet

The solutions for buoyant jets reported in the previous section, except for Homsey (9), assume the density difference between the jet and the surrounding fluid to be small compared to the absolute density of the fluid. This will be true in the upper section of the convection column of a fire. Homsey's solution does not require the assumption of small density variations and can, therefore, be used with confidence near the fire. However, Homsey (9) also finds a solution for a circular buoyant or forced jet in which combustion occurs. It is easy to extend this to a line source.

In addition to the assumptions made by Schmidt and listed in Section 6-2, the following assumptions are made.

5. Normalized density and velocity profiles are independent of height.
6. The rate of entrainment is proportional to the local velocity of the jet.
7. The inspired air mixes with the fuel and burns to stoichiometric completion instantaneously.
8. The ambient fluid is of uniform density.
9. The heat capacity is independent of temperature and the molecular weight of the jet is uniform.
10. Radiation from the flame is neglected.

The assumptions 1 through 4 have been discussed by previous workers and are well justified by experiment.

Although assumption 5 of self-preserving profiles is well established when the density variations are small it is undoubtedly casual for a flame. The fuel at the edge of the flame mixes with air more rapidly than the fuel at the center of the jet. Therefore, the more rapid combustion at the edge of the flame causes the temperature to rise more quickly. The velocity and density profiles must take on the appearance of a camel's humps, which diminish higher in the jet. It is thus doubtful that this humped pattern is maintained for a great distance in a turbulent flame.

Once again assumption 6 is reasonably well established when the density differences are small. Inadequate data are available to give firm support to this assumption for buoyant flames.

The instantaneous mixing of fuel and air to burn to stoichiometric completion does not occur in buoyant jets with large scale turbulence. If this were true the camel hump velocity profile described above would be quite pronounced. However, any attempt to describe the burning pattern in the flame introduces at least one additional parameter.

An ambient density variation could be included in the same manner employed by Murgai and Emmons (23), but most flames occur in a substantially constant density medium.

A mean heat capacity and molecular weight is considered sufficient in view of other approximations.

The inclusion of radiation makes an analytical solution impossible since the energy balance would depend on a fourth power temperature relation.

The analysis is not affected by the assumption of the type of velocity and density profiles. For simplicity a rectangular or top hat profile will be assumed.

In Figure 6-1 fuel at a density ρ_0 is released at a velocity u_0 through a slot of half-width y_0 . The flame entrains air at a density ρ_a which is mixed with fuel producing combustion. At a height x the density is ρ , the velocity u , and the half-width y_x .

The characteristics of the buoyant flame are given by a force balance, an energy balance, continuity, the equation of state, and the postulated burning law. It is apparent that the change in momentum across the element is equal to the buoyant force acting on the volume $2y_x dx$. The force balance is given by

$$\frac{d(\rho u^2 y_x)}{dx} = (\rho_a - \rho) g y_x \quad \text{Force Balance} \quad 6-1$$

By assumptions 7 and 8 the change in sensible energy across the element dx is equal to the energy released by the combustion produced by the inspired air.

$$\frac{c d(\rho u y_x T)}{dx} = \frac{k'' Q_c}{r_f} u \rho_a \quad \text{Energy Balance} \quad 6-2$$

where k'' is the entrainment coefficient, dimensionless, c is the heat capacity of the gas, Btu/lb-°F, Q_c is the heat of combustion per pound of fuel, Btu/lb-fuel, r_f is the lbs of air per lb of fuel for stoichiometric combustion, lb/lb. Combining the energy balance with the equation of state for a perfect gas,

$$\frac{P}{\rho_a} = \frac{RT_a}{M_a} \quad \text{Equation of State} \quad 6-3$$

gives

$$\frac{d(u y_x)}{dx} = \frac{k'' Q_c}{r_f c T_a} u \quad 6-4$$

The mass flux in the flame at a height x is equal to the mass entering the base of the flame plus the mass entrained up to height x .

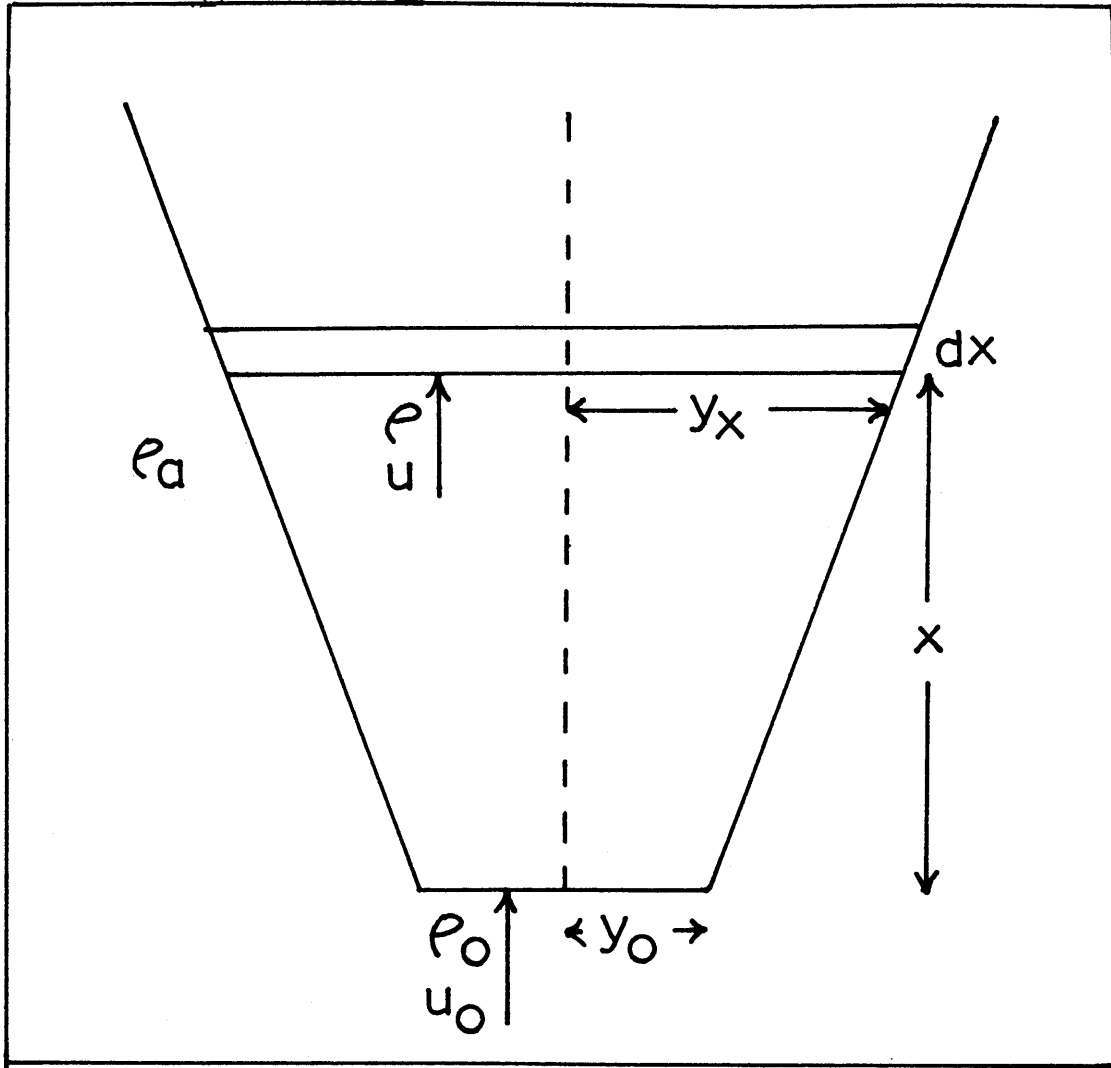


Figure 6-1 Line Jet

$$\rho V_x = \rho_o V_o + \rho_a V_a \quad \text{Mass Balance} \quad 6-5$$

where

V_x is the volumetric flow per unit length at height x , $\text{ft}^3/\text{hr-ft}$
 V_o is the volumetric flow per unit length at the origin, $\text{ft}^3/\text{hr-ft}$
 V_a is the volume per unit length ^{per unit time} inspired up to height x , $\text{ft}^3/\text{hr-ft}$

Defining

$$\omega = \frac{V_a}{V_x - V_o} \quad 6-6$$

gives

$$\rho u y_x = \rho_o u_o y_o + \omega \rho_a (u y_x - u_o y_o) \quad 6-7$$

Since it was assumed that the burning goes to stoichiometric completion an energy balance on the fluid passing up to height x can be written by equating the energy at height x , to the energy input from incoming fuel and air. Neglecting radiation and taking T_a as the base temperature

$$nMc (T - T_a) = n_o M_o c (T_o - T_a) + \frac{Q_c M_a n_a}{r_f} \quad 6-8$$

where

n is the molal flow rate at height x
 n_o is the molal flow rate of fuel at $x = 0$
 n_a is the molal flow rate into the flame up to height x

Since the heat capacity and molecular weight are assumed to be constant equation 6-8 can be rearranged to

$$\frac{nT - n_o T_o}{n_a T_a} = \frac{n - n_o}{n_a} + \frac{Q_c}{r_f c T_a} \quad 6-9$$

The right hand side being equivalent to $(V_x - V_o)/V_a$. Therefore

where

$$F = u_o^2 / g y_o \quad \text{and} \quad K' = \frac{k'' Q_c}{r_f c T_a} \quad 6-16$$

Solving for ρ' in 6-15 and introducing it into 6-13 gives

$$\frac{d[u' \rho'_o + \omega u' (u' y'_x - 1)]}{dx''} = \frac{y'_x}{F} \left[1 - \frac{\rho'_o}{u' y'_x} - \omega \left(1 - \frac{1}{u' y'_x} \right) \right] \quad 6-17$$

Let

$$v'_x = u' y'_x \quad 6-18$$

and equations 6-14 and 6-17 become

$$\frac{dv'_x}{dx''} = K' u' \quad 6-19$$

and

$$\frac{d[u'(\rho'_o + \omega(v'_x - 1))]}{dx''} = \frac{1}{Fu'} [(\omega - \rho'_o) + v'_x(1 - \omega)] \quad 6-21$$

respectively. Dividing 6-17 by 6-20 gives

$$\frac{d[u'(\rho'_o + \omega(v'_x - 1))]}{dv'_x} = \frac{1}{K' Fu'^2} [(\omega - \rho'_o) + v'_x(1 - \omega)] \quad 6-22$$

Let

$$t' = u'(\omega(v'_x - 1) + \rho'_o) \quad 6-23$$

Equation 6-22 becomes

$$\frac{dt'}{dv'_x} = \frac{1}{K'F\omega^2} [(\omega(v'_x - 1) + \rho'_0)^2((\omega - \rho'_0) + v'_x(1 - \omega))]$$

or

$$\int_{e'_0}^{t'} dt' = \frac{1}{K'F} \int_1^{v'_x} [(\omega(v'_x - 1) + \rho'_0)^2((\omega - \rho'_0) + v'_x(1 - \omega))] dv'_x$$

6-24

Solution of the integral on the right hand side is given by Burington (5).

Therefore t' is given by

$$t' = \left[\frac{1}{4K'F\omega^2} \left[(\omega v'_x + \rho'_0 - \omega)^3(3\omega(1 - \omega)v'_x + (\omega - \rho'_0)(3\omega + 1)) - \rho'_0^3(\omega(4 - 3\rho'_0) - \rho'_0) \right] + \rho'_0^3 \right]^{1/3}$$

6-25

u' is obtained from t' by equation 6-22 and y'_x is given by 6-18. It is necessary to obtain x'' from a numerical integration of equation 6-19 or

$$x'' = \int_1^{v'_x} \frac{dv'_x}{K'u'} \quad 6-26$$

Notice that for a buoyance-controlled line fire $\rho'_0{}^3$ is small compared to the other term in equation 6-25 at a very small v'_x . Thus

$$t' = \left[\frac{1}{4K'F\omega^2} (f_1(v'_x, \omega, \rho'_0)) \right]^{1/3} \quad 6-27$$

Since

$$u' = \frac{t'}{[\omega(v'_x - 1) + \rho'_0]} \quad 6-28$$

Therefore

$$x'' = \frac{(K'F\omega^2)^{1/3}}{K'} f_2(v'_x, \omega, \rho'_0) \quad 6-29$$

If a single fuel is considered

$$\frac{(K'F\omega^2)^{1/3}}{K'} = \left[\frac{u_o^2}{gy_o} \left[\frac{1 + \frac{Q_c}{r_f c T_a}}{\frac{Q_c}{r_f c T_a}} \right]^2 \right]^{1/3} \quad 6-30$$

Since $Q_c/r_f c$ is equal to the adiabatic flame temperature minus the ambient temperature $T_f - T_a$,

$$\frac{(K'F\omega^2)^{1/3}}{K'} = \left[\frac{u_o^2}{gy_o} \left[\frac{T_a^2}{(T_f - T_a) T_f} \right]^2 \right]^{1/3} \quad 6-31$$

Since the energy flux at the origin is given by

$$(Q/L) = 2 Q_c \rho_o u_o y_o \quad 6-32$$

Equation 6-31 becomes

$$\frac{(K'F\omega^2)^{1/3}}{K'} = \left[\left[\frac{T_a^2}{(T_f - T_a) T_f} \right]^2 \frac{(Q/L)^2}{4(Q_c \rho_o)^2 gy_o^3} \right]^{1/3} \quad 6-33$$

and the flame height H is given by 6-29 and 6-33.

$$H \left[\frac{T_a^2}{(T_f - T_a) T_f} \frac{(Q/L)}{2Q_c \rho_o g^{1/2}} \right]^{2/3} \quad 6-34$$

The flame height is proportional to $(Q/L)^{2/3}$ for a single type of fuel.

This result was deduced by Hottel (11) from dimensional analysis. Hottel points out that his solution does not depend on the assumption of similar temperature and velocity profiles.

6.4 Flame Heights

One reason for developing a theoretical model for burning jets is to predict flame heights. The fire spread model in Chapter II requires

knowledge of the relation between the flame height and other variables. This section reviews the analyses of other authors and gives some new data.

Thomas, Webster, and Raftery (31) considered the flame heights of circular burning fires and obtained

$$\frac{H}{D} = f_1 \left[\frac{F_v^2}{D^5} \right] \quad 6-35$$

where

H is the flame height, ft.

D is the diameter of the base, ft.

F_v is the volumetric flow rate from the base, ft³/hr

This equation was obtained from the following argument where the line source will be used as the example.

In a flow system containing viscous, inertial and buoyant forces the ratio of the velocity anywhere in the system to a reference velocity (e.g., the velocity at the base) is a function of the Grashof and Reynolds Numbers and the distance above the source. Thus

$$\frac{u}{u_0} = f_2 \left(\frac{g B' \mathcal{W}^3 \Delta T \rho^2}{\mu^2}, \frac{u_0 \mathcal{W} \rho}{\mu}, \frac{x}{\mathcal{W}} \right) \quad 6-36$$

where

u_0 is the velocity of the fuel at the base, ft/hr

B' the coefficient of thermal expansion, °F⁻¹

ΔT the excess temperature in the flame, °F

ρ the density of the gas, lbs/ft³

μ the viscosity of the gas, lbs/ft-hr

\mathcal{W} the width of the base, ft

By definition the volumetric flow rate is given by

$$\frac{F_v}{L} \propto u_0 \mathcal{W} \quad 6-37$$

It is assumed possible to neglect the viscous forces. Therefore equation 6-36 can be replaced by

$$\frac{u}{u_0} = f_3 \left[\frac{gB' \mathcal{W} \Delta T}{u_0^2}, \frac{x}{\mathcal{W}} \right] \quad 6-38$$

The surface area per unit length of a line flame is readily seen to be given by

$$S = \mathcal{W} f_4 \left[\frac{H}{\mathcal{W}} \right] \quad 6-39$$

The rate of air entrainment per unit area is assumed to be directly proportional to the local stream velocity. This is a common assumption for non-burning jets. The total air entrainment through out the flame is then proportional to the product of an average value of the entrainment velocity and the surface area of the jet. The average entrainment velocity is given by equation 6-38 with x replaced by H . This product is also proportional to the volumetric fuel flow rate at the base. Eliminating u from equations 6-37, 6-38, and 6-39, gives

$$\frac{F_v}{L} \propto u_0 \mathcal{W} \propto f_4 \left(\frac{H}{\mathcal{W}} \right) u_0 f_5 \left(\frac{gB' \Delta T \mathcal{W}}{u_0^2}, \frac{H}{\mathcal{W}} \right) \quad 6-40$$

Therefore

$$\frac{H}{\mathcal{W}} = f_6 \left[\frac{(F_v/L)^2}{gB' \Delta T \mathcal{W}^3} \right] \quad 6-41$$

Most buoyancy controlled flames of interest are large compared to their source width and can be considered a line source. Therefore, the flow conditions at the base have little influence in the flame and the entrainment velocity would become independent of the base width as well as the base velocity. Equation 6-40 would then give

$$v_e \propto x^{1/2} \quad 6-42$$

where v_e is the entrainment velocity.

The surface area per unit length given by equation 6-39 will be directly proportional to the flame height H when the flame is a large wedge and directly proportional to W when the flame is small and just covers the surface. Therefore,

$$S \propto W \left(\frac{H}{W} \right)^n \quad 6-43$$

where n goes from zero to unity as H/W increases. If the mean entrainment velocity is taken proportional to $H^{1/2}$ (equation 6-42), then from equations 6-40 and 6-43

$$\frac{H}{W} \propto \left[\frac{(F_v/L)^2}{W^3} \right]^{1/(2n+1)} \quad 6-44$$

The above equation calls for H/W to increase with $(F_v/L)^2/W^3$, but with a decreasing power since n goes from 0 to 1.

Hottel (11) obtained the relation for a line source

$$\frac{(Q/L)^2 T_a}{(\rho c)^2 (T - T_a)^3 g H^3} = f \left(\frac{x}{H} \right) \quad 6-45$$

from dimensional analysis. However, if the width of the line source becomes finite it is apparent that

$$\frac{(Q/L)^2 T_a}{(\rho c)^2 (T - T_a)^3 g H^3} = f \left(\frac{x}{H}, \frac{H}{W} \right) \quad 6-46$$

Replacing the H^3 on the left hand side by W^3 and defining the flame height as the height at which a temperature T_f is reached

$$\frac{H}{W} = f \left[\frac{(Q/L)^2 T_a}{W^3 (\rho c)^2 (T_f - T_a)^3 g} \right] \quad 6-47$$

or for a single fuel

$$\frac{H}{W} = f \left[\frac{(Q/L)^2}{W^3} \right] \quad 6-48$$

The analysis of Thomas, Webster and Raftery gives the same result if the volumetric flow rate per unit length is replaced by the heat liberation per unit length. Notice that the treatment by Hottel is for heat liberated at the origin but does not include combustion. The derivation in the preceding section includes combustion of a special type (combustion occurs on mixing and goes to stoichiometric completion; (assumption 8)). The relation for the flame height can be derived from equation 6-29 and is

$$\frac{H}{W} = f \left[\frac{(Q/L)^2}{W^3 (q_c \rho_o)^2 g} \left[\frac{T_a^2}{(T_f - T_a) T_f} \right]^2, W, \rho_o / \rho_a \right] \quad 6-49$$

is equal to T_a/T_f and nearly constant for all fuels. Therefore,

$$\frac{H}{W} = f \left[\frac{(Q/L)^2}{W^3}, \rho_o / \rho_a \right] \quad 6-50$$

The effect of the parameter (ρ_o / ρ_a) is quite significant near the base of the flame. If the fuel gas issuing forth is heavier than air the small amount of momentum will soon be dissipated. The gas will then flow in a horizontal direction, or possibly in a reverse direction. When enough combustion has occurred to make the fluid lighter than the surrounding air, the flow continues upward. This caused the experimental propane flames to wander across the surface.

Some flame heights for line fires of methane and propane, measured visually, are given in Figure 6-2 vs. the square of the heat liberation rate divided by the cube of the source width. The lines recommended by Thomas, Webster, and Raftery for their data on approximately circular fires are shown based on a heating value of wood of 6000 Btu/lb. The radius is used as the characteristic circular dimension to give a comparison with the line fires at an equivalent mean hydraulic radius.

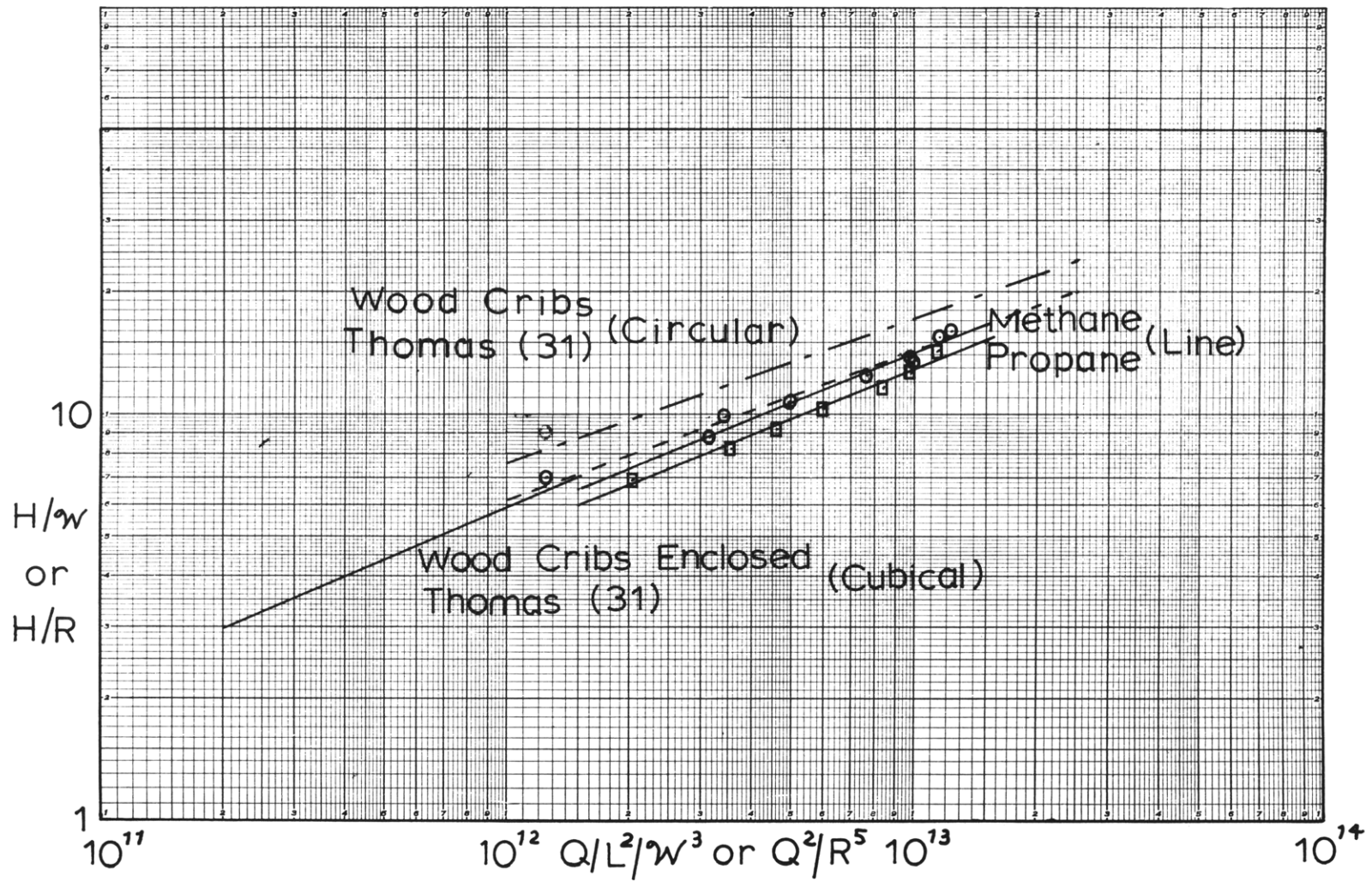


Figure 6-2 Effect of the Normalized Burning Rate on the Flame Height to Flame Base Ratio

The slope of the curves for the line propane and methane fires are approximately 0.4 with methane having a slightly higher flame height than propane for the same $(Q/L)^2/\mathcal{W}^3$. The data nearly coincide with the lines recommended by Thomas, Webster, and Raftery (31) for wood crib fires of nearly circular dimension when the coordinates H/R and Q^2/R^5 are used. It is believed that the heat liberation is a more significant quantity than the volumetric velocity at the origin when different types of fuels are considered since the heat liberation rate is a better indication of the available buoyancy. The close correspondence of the data for line methane and propane fires and circular wood crib fires indicate this to be true. One would expect a lower slope for the circular fire data than for the line fire data since in the circular case as R goes to zero the slope approaches $1/5$ and in the line case as \mathcal{W} approaches zero, the slope approaches $1/3$. Although the slope is slightly less for circular fires in Figure 6-2 (0.3 opposed to 0.4 for line fires) the scatter of the data is too great for firm conclusions.

The base flow rate for the larger flames was approximately $1/3$ ft/sec. The bases of the flames were definitely laminar, particularly for methane (see Figure 5-1). The flame broke into turbulence at a height of about three or four slot widths, the larger flames being turbulent nearer the base. If the base were made $1/10$ as wide the flow rate would be 3.33 ft/sec. and presumably H/\mathcal{W} approximately 10 times larger or 150. This base velocity of 3.33 ft/sec is large enough for one to expect it to influence the flame height. When the base velocity becomes great enough H/\mathcal{W} becomes a constant and equal to approximately 600 for propane (assuming H/R for circular flames corresponds to H/\mathcal{W} for line flames). It appears that all the data in Figure 6-2 are nearly three orders of magnitude in $(Q/L)^2/\mathcal{W}^3$ or Q^2/R^5 from any influence of entering momentum. The data of Thomas, Webster and Raftery (31) indicate that this is an important range for natural fires.

It appears that a good approximation for line flame heights, to be used in the model in Chapter II, would be

$$\frac{H}{\mathcal{W}} = \gamma \left[\frac{(Q/L)^2}{\mathcal{W}^3} \right]^c \quad 6-53$$

where c is 0.33 to 0.4 in the range of interest.

VII. DISCUSSION OF RESULTS

7.1 Introduction

It is apparent that this work has been concerned with numerous aspects of the fire problem over a wide area not entirely related. In order to take full advantage of this work in planning future studies it is necessary to take cognizance of the results as it applies to the general problem of fire spread in a real situation.

7.2 Results of This Thesis Work Applied to Actual Fire Spread

It is believed that the Woods Hole Summer Study Model discussed in Section 2-4 offers the best analysis for fire spread at the present time. The form is general enough that any new observations can be included. It can also be used as a basis for determining future work to supply the missing information for a more thorough understanding of fire phenomena.

The three final equations for the Woods Hole Summer Study Model are:

1. An energy balance on the unburned fuel,

$$v = \frac{1}{Q_1} \left[(Q/L)_B + (Q/L)_R + (Q/L)_C - (Q/L)_L \right] \quad 2-23$$

which states that the velocity of fire spread is directly proportional to the various mechanisms of integrated heat transfer rates to the unburned fuel and inversely proportional to the energy required to produce piloted ignition.

2. A burning law

$$\xi \eta Q_c v = \theta \left[(Q/L)_R + (Q/L)_I \right] \quad 2-28$$

which says that the heat liberation rate by combustion (l. h. s.) is proportional to the heat input rate to the burning solid fuel bed.

3. A determination of the flame height

$$\frac{H}{W} = f \left[\frac{(Q/L)^2}{W^3} \right] \quad 2-29$$

The heating of unburned fuel by radiation from the embers in the fuel bed beneath the gas flame $(Q/L)_B$, is readily amenable to theory.

It was shown in Section 2-4 to be

$$(Q/L)_B = \int_{-\infty}^0 q_1(x) dx = \int_0^{\infty} a' b \sigma T_f^4 e^{-a'x} dx = b \sigma T_f^4 \quad 7-1$$

Obtaining the radiation from the overhead flame, $(Q/L)_R$, has been one of the major endeavors of this thesis. When no wind is present to bend the flame the data of Chapter 5 indicate the flame radiation can be well approximated by

$$(Q/L)_R = \int_0^{\infty} \sigma T_f^4 \left(\frac{d \bar{g}s}{L dx} \right) dx \quad 7-2$$

where $\frac{d \bar{g}s}{L dx}$ is the exchange factor given by either the gray gas wedge or parallelepiped exchange factors discussed in Sections 4-7 and 4-6 respectively. T_f is the average gray gas temperature which propane and methane flame data of Chapter 5 indicate to be approximately 1200°F. It would not be difficult to calculate exchange factors for bent wedges using a similar method to the ones used for straight wedges in Section 4-7. However, a wind will not only bend the flame but can also pass through it. How this affects the combustion pattern, and therefore, the temperature pattern is unknown but certainly significant. Exchange factors for gray gas bent wedges is certainly the first step in analyzing the effect of wind on the overhead radiation.

The convection heat transfer at the flame front, $(Q/L)_C$ is undoubtedly the most elusive for quantitative treatment. In this work

values of 94.0 Btu/hr-ft for shredded newspaper fuel and close to zero for the computer punch out fuel were found in the absence of wind. In an exploratory experiment a wind velocity of 3.5 ft/sec caused nearly a three fold increase in this number. An experiment is recommended in Section 3-7 which could determine the distance over which this heat transfer may occur for different wind velocities. However, the effect of fuel type on this method of heat transfer presents a difficult problem. In a natural fire it is believed that this heat transfer is of primary importance.

The heat loss from the fresh fuel as it preheats, $Q/L)_L$, is also a strong function of fuel type. However, it is believed that the treatment of this term in Section 3-4, by relating it to the other heat transfers, is a promising start. Although fuel beds with significant air spaces would complicate matters a workable relation may still be obtained.

The energy required to produce ignition, Q_i , has been determined in this work for fuel beds of newspaper and computer cutouts. For the newspaper it was found to decrease with humidity by approximately 10% for a 10% decrease in humidity. This is about one third more than would be expected if the change is based on the increase in heat necessary to reach a fixed ignition temperature. However, until other data over a wider range of humidities become available it is recommended that the following relation be used:

$$Q_i = K'' \left(\frac{V_o}{V} \right)^{\frac{1}{4}} Q_o (c_p (T_i - T_a) + M H) \quad 7-3$$

where Q_o is the ignition energy at V_o , Btu/ft²

T_i is the ignition temperature, °F

M is the moisture content of the fuel, lb/lb

ΔH is the latent plus sensible heat of water, Btu/lb

K'' is a characteristic of fuel type to be determined by experiment

Finding how K'' varies with fuel type, other than its variation with thermal properties for flat surfaces, is another difficult problem. An independent experiment under more controlled conditions than is possible when measuring fire spread, may be advisable. However, there is merit in obtaining the ignition energy from measurement of fire spread rates even though the method is not as accurate.

The radiative heat transfer to burning fuel, $(Q/L)_R'$, can be handled in the same manner as the flame radiation to fresh fuel. The heat generation in the bed itself, $(Q/L)_I'$, has not been studied in this work.

The relation between the flame height and the burning base width and the heat liberation recommended in Section 6-4 is

$$\frac{H}{w} = \gamma \left[\frac{Q/L^2}{w^3} \right]^c \quad 6-53$$

where c is between 0.33 and 0.4 and γ is a slight function of fuel type. This relation seems well enough established to be used with confidence.

It is believed that the functions for equations 2-23, 2-28 and 2-29 are sufficiently well-known to justify their numerical solution on a computer.

There are still many problems to be studied, particularly the evaluations of the shift in relative importance of the different terms which appear in the equations of the model when full-scale fuel beds (forests or cities) are of interest.

7.3 Conclusions

1) The energy required to produce piloted ignition in shredded newspaper at a humidity of 48% and a burning rate 60 ft/hr was found to be 2.40 Btu/ft² (0.65 cal/cm²).

2) The energy required to produce piloted ignition in computer card cutouts (1/16" x 1/8"x 0.007") at a humidity of 44% and a burning rate of 60 ft/hr was found to be 9.0 Btu/ft² (2.4 cal/cm²). The required energy to produce piloted ignition for similar fuel cut in approximately 1/2" squares at a humidity of 47% was found to be 7.5 Btu/ft.² (2.0 cal/cm²).

3) A ten per cent decrease in humidity produced approximately a ten per cent decrease in the ignition energy of shredded newspaper.

4) A wind velocity of 3.5 ft/sec produced nearly a three-fold increase in the rate of fire spread over that for no wind, for shredded newspaper.

5) The intensity pattern around a constant temperature gray gas wedge is a good first approximation for the radiation flux density distribution around line flames of propane and methane.

6) The flame heights for line fires of propane and methane is best fitted by the equation

$$\frac{H}{w} = \gamma \left[\frac{Q/L^2}{w^3} \right]^{.4} \quad 6-53$$

where γ is a slight function of the fuel type.

7.4 Recommendations

1) A detailed study of the convection heat transfer at the flame front as a function of the wind velocity should be made.

2) An independent experiment should be designed to determine a more exact value for the net piloted ignition energy of the fuels used.

3) The Summer Study Model should be programmed and solved numerically in the light of the new information available.

VII. APPENDIX

A SOLUTION OF DIFFERENTIAL EQUATIONS

A-1 The Solution of the Differential Equation of Atallah's Model (1)

The heat balance for the model suggested by Atallah on a small element of fuel dx ahead of the flame was given in Section 2,3 as

$$\begin{aligned}
 kl \frac{d^2 T}{dx^2} + \bar{V} \bar{c}_p \bar{\gamma} \frac{dT}{dx} - \left[U + \frac{\sigma \epsilon (T_i^4 - T_a^4)}{(T_i - T_a)} \right] (T - T_a) \\
 = - \sigma \epsilon_f F(x) (T_f^4 - T_a^4)
 \end{aligned} \tag{2-10}$$

with the boundary conditions

$$\begin{aligned}
 T &= T_a \quad \text{at} \quad x = \infty \\
 T &= T_i \quad \text{at} \quad x = 0 \\
 \frac{dT}{dx} &= 0 \quad \text{at} \quad x = 0
 \end{aligned} \tag{2-11}$$

The temperature of the fuel is the dependent variable and x the independent variable. All other variables are constant for a particular fire. Making a change of variables

$$\theta = \frac{T - T_a}{T_i - T_a} \quad z = x/H \tag{A-1}$$

gives

$$\begin{aligned}
 \frac{d^2 \theta}{dz^2} + \frac{\bar{V} \bar{c}_p \bar{\gamma} H}{k} \frac{d\theta}{dz} - \left[\frac{\sigma \epsilon H^2 (T_i^4 - T_a^4)}{kl (T_i - T_a)} + \frac{UH^2}{kl} \right] \theta \\
 = - \frac{\sigma \epsilon_f H^2 (T_f^4 - T_a^4)}{kl (T_i - T_a)}
 \end{aligned} \tag{A-2}$$

Let

$$\begin{aligned}
 A &= \frac{\bar{V}_c \bar{\gamma} H}{k} & B &= \frac{\sigma \epsilon H^2 (T_i^4 - T_a^4)}{k_1 (T_i - T_a)} + \frac{UH^2}{k_1} \\
 C &= \frac{\sigma \epsilon_f H^2 (T_f^4 - T_a^4)}{k_1 (T_i - T_a)} & & \text{A-3}
 \end{aligned}$$

which gives

$$\frac{d^2 \theta}{dz^2} + A \frac{d\theta}{dz} - B \theta = -C F(z) \quad \text{A-4}$$

with the boundary conditions

$$\begin{aligned}
 \theta &= 0 & \text{at } z &= \infty \\
 \theta &= 1 & \text{at } z &= 0 \\
 \frac{d\theta}{dz} &= 0 & \text{at } z &= 0
 \end{aligned} \quad \text{A-5}$$

The general solution for this equation is given by Martin and Reissner (17) as

$$\theta = C_1(z) \exp(r_1 z) + C_2(z) \exp(r_2 z) \quad \text{A-6}$$

where

$$C_1(z) = - \int_0^z \frac{-C F(z) \exp(r_2 z) dz}{W(\exp(r_1 z), \exp(r_2 z))} + C_1$$

$$C_2(z) = \int_0^z \frac{-C F(z) \exp(r_1 z) dz}{W(\exp(r_1 z), \exp(r_2 z))} + C_2$$

$$W(\exp(r_1 z), \exp(r_2 z)) = \begin{vmatrix} \exp(r_1 z) & \exp(r_2 z) \\ r_1 \exp(r_1 z) & r_2 \exp(r_2 z) \end{vmatrix}$$

$$r_1 = \frac{-A + \sqrt{A^2 + 4B}}{2} \quad r_2 = \frac{-A - \sqrt{A^2 + 4B}}{2} \quad A-7$$

Substitution into equation A-6 gives

$$\Theta = \left[C_1 + \frac{C}{(r_2 - r_1)} \int_0^z \exp(-r_1 z) F(z) dz \right] \exp(r_1 z)$$

$$+ \left[C_2 - \frac{C}{(r_2 - r_1)} \int_0^z \exp(-r_2 z) F(z) dz \right] \exp(r_2 z) \quad A-8$$

The boundary condition $\Theta = 1$ at $z = 0$ gives

$$C_1 + C_2 = 1 \quad A-9$$

To apply the boundary condition $\Theta = 0$ at $z = \infty$ is a little more subtle.

Since r_2 is negative $\exp(r_2 z)$ goes to zero as z goes to infinity. Since r_1 is positive $\exp(r_1 z)$ goes to infinity as z goes to infinity. Therefore, if Θ is to equal zero at $z = \infty$ the section of equation A-8 multiplying $\exp(r_1 z)$ must equal zero at z equal to infinity and

$$C_1 = - \frac{C}{(r_2 - r_1)} \int_0^{\infty} \exp(-r_1 z) F(z) dz \quad A-10$$

Therefore,

$$C_2 = 1 + \frac{C}{(r_2 - r_1)} \int_0^{\infty} \exp(-r_1 z) F(z) dz \quad \text{A-11}$$

and

$$\begin{aligned} \Theta = & \left[1 + \frac{C}{(r_2 - r_1)} \int_0^{\infty} \exp(-r_1 z) F(z) dz \right. \\ & - \left. \frac{C}{(r_2 - r_1)} \int_0^z \exp(-r_2 z) F(z) dz \right] \exp(r_2 z) \\ & + \left[- \frac{C}{(r_2 - r_1)} \int_0^{\infty} \exp(-r_1 z) F(z) dz \right. \\ & + \left. \frac{C}{(r_2 - r_1)} \int_0^z \exp(-r_1 z) F(z) dz \right] \exp(r_1 z) \quad \text{A-12} \end{aligned}$$

Differentiating the above one finds

$$\begin{aligned} \frac{d\Theta}{dz} = & r_2 \exp(r_2 z) \left[1 + \frac{C}{(r_2 - r_1)} \int_0^{\infty} \exp(-r_1 z) F(z) dz \right. \\ & - \left. \frac{C}{(r_2 - r_1)} \int_0^z \exp(-r_2 z) F(z) dz \right] - \frac{C}{(r_2 - r_1)} F(z) \\ & - r_1 \exp(r_1 z) \left[\frac{C}{(r_2 - r_1)} \int_0^{\infty} \exp(-r_1 z) F(z) dz \right. \\ & - \left. \frac{C}{(r_2 - r_1)} \int_0^z \exp(-r_1 z) F(z) dz \right] + \frac{C}{(r_2 - r_1)} F(z) \quad \text{A-13} \end{aligned}$$

and applying the boundary condition $\frac{d\Theta}{dz} = 0$ at $z = 0$ gives

$$r_2 \left[1 + \frac{C}{(r_2 - r_1)} \int_0^{\infty} \exp(-r_1 z) F(z) dz \right] - \frac{r_1 C}{(r_2 - r_1)} \int_0^{\infty} \exp(-r_1 z) F(z) dz = 0 \quad \text{A-14}$$

Simplifying the solution becomes

$$C = \frac{-r_2}{\int_0^{\infty} \exp(-r_1 z) F(z) dz} \quad \text{A-15}$$

where

$$F(z) = 1/2 \left[1 - \frac{z}{\sqrt{1+z^2}} \right] \quad \text{A-16}$$

An explicit solution for the velocity of fire spread can not be obtained.

A-2. The Solution of the Differential Equation of Atallah's Model (1) Neglecting Conduction and Assuming the Exponential View Factor

An important special case of the previous model is one in which conduction along the bed is negligible. It is doubtful that this conduction ever contributes a significant amount of heat transfer in an actual fire.

Neglecting this conduction equation 2-10 becomes

$$\begin{aligned} \bar{v}_p \bar{\gamma} \frac{dT}{dx} &= \left[U + \frac{\sigma \epsilon (T_i^4 - T_a^4)}{(T_i - T_a)} \right] (T - T_a) \\ &= - \sigma \epsilon \epsilon_f F(x) (T_f^4 - T_a^4) \end{aligned} \quad \text{A-17}$$

with the boundary conditions

$$T = T_a \quad \text{at} \quad x = \infty$$

$$T = T_i \quad \text{at} \quad x = 0$$

A-18

Making the same change of variables as in Section A-1

$$\theta = \frac{T - T_a}{T_i - T_a} \quad z = x/H$$

A-1

gives

$$\frac{d\theta}{dz} = \left[\frac{U}{\bar{c}_p \bar{\gamma}} + \frac{\sigma \epsilon (T_i^4 - T_a^4)}{\bar{c}_p \bar{\gamma} (T_i - T_a)} \right] \frac{H\theta}{V_1}$$

$$= \frac{\sigma \epsilon \epsilon_f (T_f^4 - T_a^4)}{\bar{c}_p \bar{\gamma} (T_i - T_a)} \frac{H F(z)}{V_1}$$

A-19

Let

$$A' = \frac{U}{\bar{c}_p \bar{\gamma}} + \frac{\sigma \epsilon (T_i^4 - T_a^4)}{\bar{c}_p \bar{\gamma} (T_i - T_a)}$$

$$B' = \frac{\sigma \epsilon \epsilon_f (T_f^4 - T_a^4)}{\bar{c}_p \bar{\gamma} (T_i - T_a)}$$

A-20

giving

$$\frac{d\theta}{dz} - \frac{A'H}{V_1} \theta = - \frac{B'H}{V_1} F(z)$$

A-21

with the boundary conditions

$$\theta = 0 \quad \text{at} \quad z = \infty$$

$$\theta = 1 \quad \text{at} \quad z = 0$$

A-22

The general solution for equation A-21 is given by Martin and Reissner (17) as

$$\theta = \frac{\int \exp\left(\int P(z) dz\right) Q(z) dz + C}{\exp\left(\int P(z) dz\right)}$$

A-23

where

$$P(z) = -\frac{A'H}{V_1}$$

$$Q(z) = -\frac{B'H}{V_1} F(z)$$

A-24

Substitution gives

$$\theta = \frac{-\int \exp\left(-\frac{A'H}{V_1} z\right) \frac{B'H}{V_1} F(z) dz}{\exp\left(-\frac{A'H}{V_1} z\right)}$$

A-25

Applying the boundary condition $\theta = 1$ at $z = 0$ gives

$$C = 1$$

A-26

and

$$\theta = \frac{-\frac{B'H}{V_1} \int \exp\left(-\frac{A'H}{V_1} z\right) F(z) dz + 1}{\exp\left(-\frac{A'H}{V_1} z\right)}$$

A-27

Let it be assumed that

$$F(z) = 1/2 e^{-z}$$

A-28

The above assumption gives a curve with the same area as the true view factor $1/2 (1 - z/\sqrt{1+z^2})$. It also follows the true curve closely.

Equation A-27 becomes

$$\theta = \frac{-\frac{B'H}{2V \cdot 1} \int \exp(-\frac{A'H}{V \cdot 1} z) e^{-z} dz + 1}{\exp(-\frac{A'H}{V \cdot 1} z)} \quad \text{A-29}$$

which gives upon solution of the integral and applying the boundary condition

$$\theta = 0 \text{ at } z = \infty$$

$$V = (B'/2 - A') H/1 \quad \text{A-30}$$

B MEASUREMENT OF THE RADIATION FROM THE WIRES

B-1 The Flux Density of Radiation Around a Single Wire

The wires used in the flame spread experiments of Chapter III were so small compared to the dimensions of the system that the wires can be assumed to be a line source

A line source of heat with an energy rate per unit length Q_w is shown in Figure B-1 located a distance x from the line perpendicular to the surface which passes through the line source. A line drawn between the element of area and the line source is of length r and makes an angle α with the surface. The flux density of radiation on dx is given by the strength of the source times the solid angle or

$$dE = \frac{Q_w \sin \alpha dx}{2 \pi r} \quad \text{B-1}$$

From Figure B-1

$$\sin \alpha = L/r \quad r = \sqrt{x^2 + L^2} \quad \text{B-2}$$

and equation B-1 becomes

$$\frac{dE}{dx} = \frac{Q_w}{L} \left[\frac{1}{2 \pi (1 + x^2/L^2)} \right] = \frac{Q_w \mathcal{F}(x)}{L} \quad \text{B-3}$$

which gives the distribution of radiation around a single line source of infinite extent.

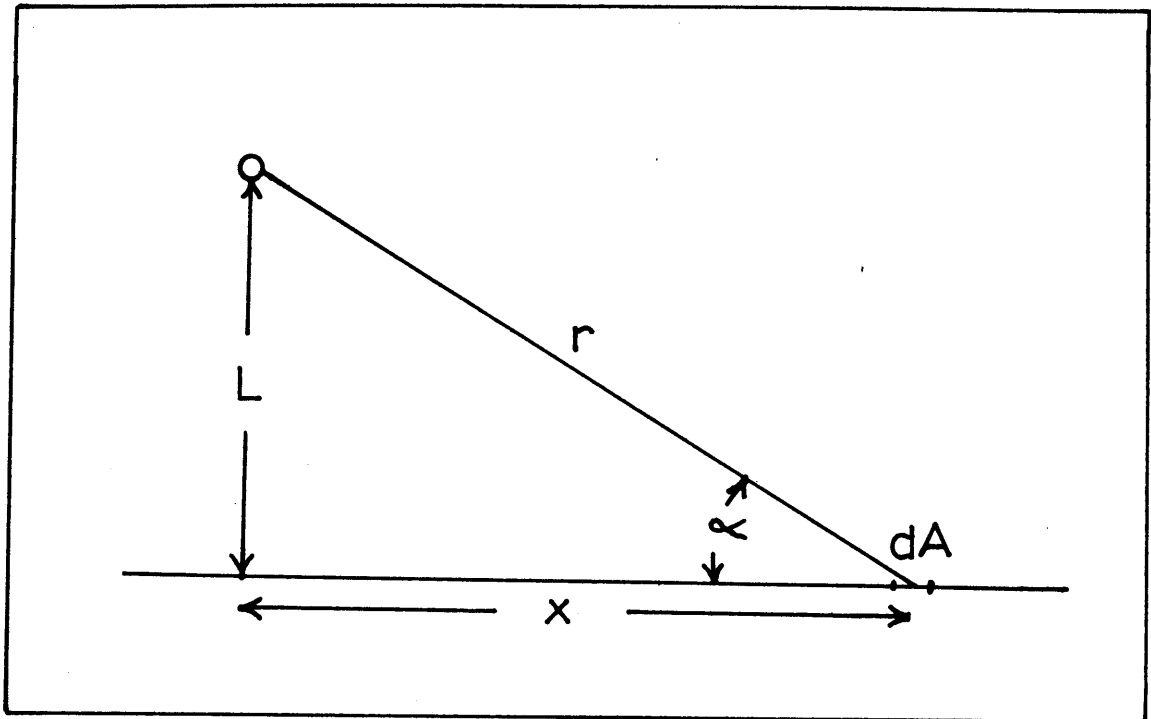


Figure B-1 Line Heat Source

B-2 The Flux Density of Radiation Around Several Wires

The distribution of radiation around several line sources is obtained from adding the contributions from the individual distributions. In order to do this by a simple addition of fluxes it is necessary to assume that the radiation from a single wire is not intercepted by another wire and the amount received from other wires does not raise significantly its emitting power.

The wire arrangements used in the experiments were 1. four wires with a ratio of center-to-center distance to wire diameter of three and 2. eight wires with a ratio of center-to-center distance to wire diameter of 6.

The view factor between two infinitely long wires separated by a distance large compared to their diameter is given approximately by

$$\overline{ss} \approx \frac{d}{2\pi C} \quad \text{B-4}$$

With $C/d = 3.0$, $\overline{ss} = 0.053$, and $C/d = 6.0$, $\overline{ss} = 0.0265$. Most of the runs were made with the eight wire system with a $C/d = 6.0$ to reduce interaction.

The flux density distribution around the four wire and the eight wire systems, $dE/dx/Q_w$, given in Figures B-2 and B-3, were calculated assuming no interaction or interference.

B-3 The Solution for the Integrated Radiation Flux, $(Q/L)_R$, Around Several Wires

Equation B-3 gives the flux density of radiation around a single

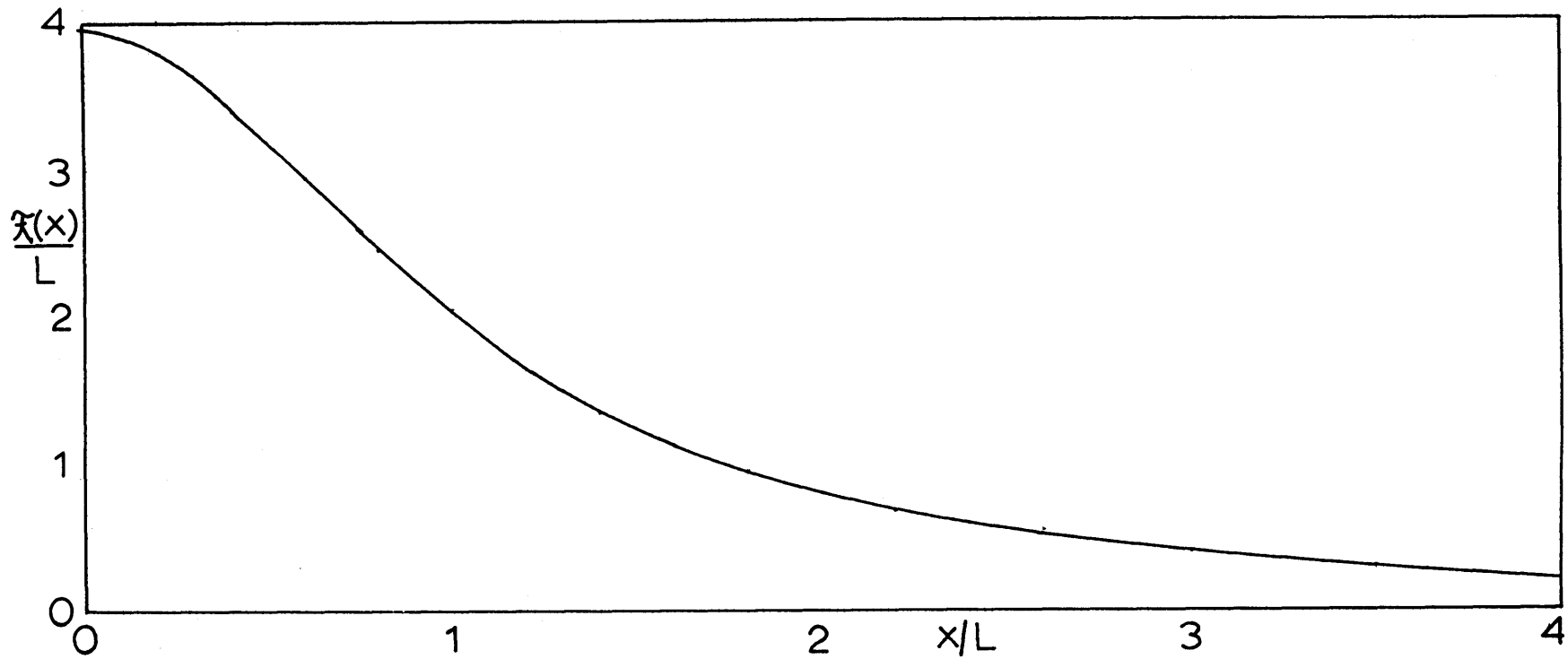


Figure B-2 Distribution of Radiation on a Surface 1.25" Below Four Wires
(Center to Center Distance to Diameter Ratio Equal to 3.0)

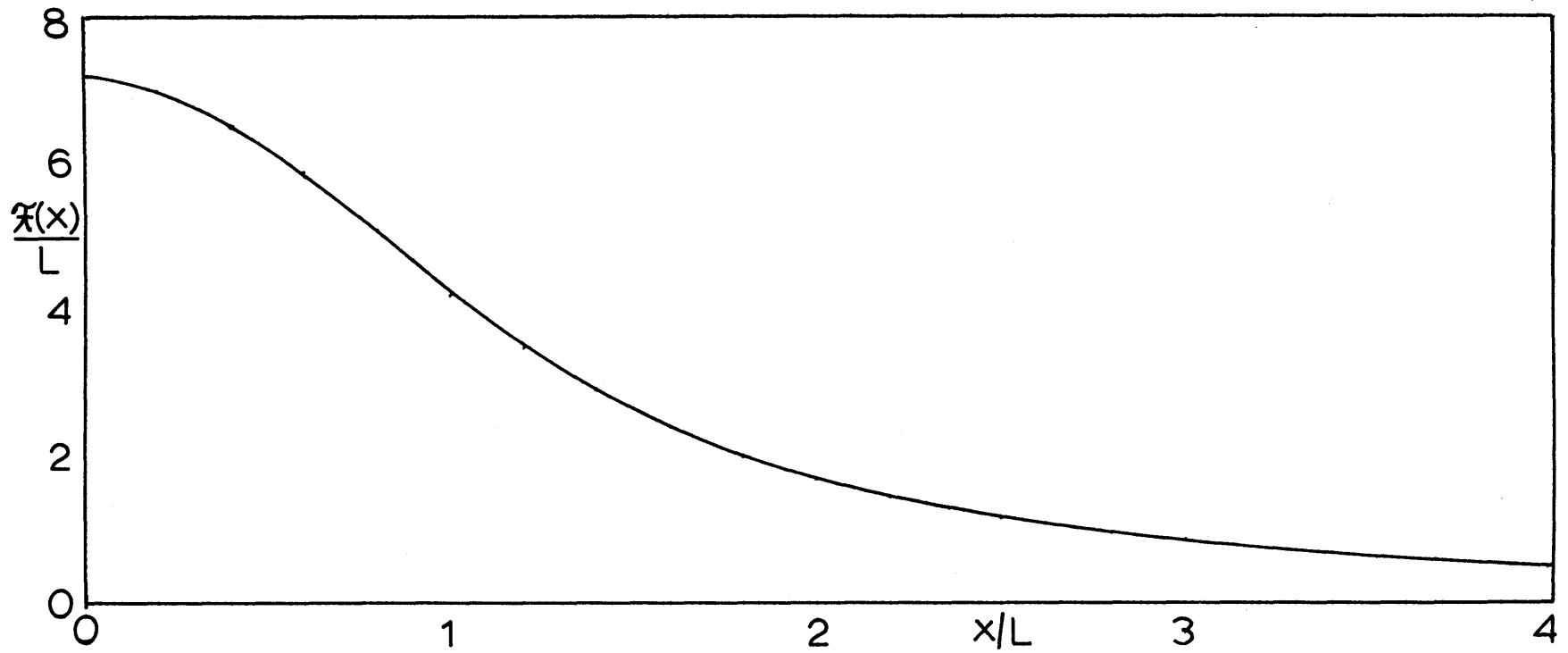


Figure B-3 Distribution of Radiation on a Surface 1.25" Below Eight Wires
(Center to Center Distance to Diameter Ratio Equal to 6.0)

wire as

$$\frac{dE}{dx} = \frac{Q_w}{L} \left[\frac{1}{2 \pi (1 + x/L)^2} \right] \quad \text{B-3}$$

The total integrated radiation flux between a distance $-x_1$ and infinity is given by

$$E = \frac{Q_w}{L} \int_{-x_1}^{\infty} \frac{dx}{2 \pi (1 + x/L)^2} \quad \text{B-5}$$

or

$$E = \frac{Q_w}{2 \pi} \left(\pi/2 + \tan^{-1} (x_1/L) \right) \quad \text{B-6}$$

The integrated radiation flux from any number of wires to a particular x_1/L is given by the proper summation of the values obtained from B-6. For the two systems in question

$$\begin{aligned} Q/L)_R &= 2.5744 Q_w && \text{eight wires} \\ Q/L)_R &= 1.0725 Q_w && \text{four wires} \end{aligned} \quad \text{B-7}$$

The strength of radiation from a single wire is obtained by measuring the radiation flux density at several distances around the wires with a thermopile. This flux density is divided by the exchange factor from either Figure B-2 or Figure B-3, depending on the wire arrangement. The average value is used in Equation B-7 to give the integrated radiation flux, $(Q/L)_R$.

C DERIVATION OF HEAT LOSS FROM FUEL SURFACE CONSIDERATING CONVECTION LOSSES

In Section 3-4 the integrated heat loss, $(Q/L)_L$, was found to be

$$(Q/L)_L = K \left[\frac{(Q/L)_R}{v^{1/2}} \right]^a \quad 3-13$$

when only incident radiation to a semi-infinite solid of constant thermal properties is considered. Since some heat is lost from the surface by back radiation and convection it is instructive to see how this could affect the relation 3-13. The surface temperature for a semi-infinite solid of constant thermal properties heated at the surface is given by equation 3-9 (6)

$$T - T_a = \frac{\sqrt{\alpha/\pi}}{k v^{1/2}} \int_{-\infty}^x \frac{Q(\bar{x}) d\bar{x}}{(x - \bar{x})^{1/2}} \quad 3-9$$

When heat loss at the surface is considered

$$Q(\bar{x}) = \frac{Q_w \mathcal{F}(\bar{x})}{L} - h(T - T_a)^a \quad 3-15$$

and equation 3-9 becomes

$$T - T_a = \frac{\sqrt{\alpha/\pi}}{k v^{1/2}} \left[\frac{Q_w}{L} \int_{-\infty}^x \frac{\mathcal{F}(\bar{x}) d\bar{x}}{(x - \bar{x})^{1/2}} - \int_{-\infty}^x \frac{h(T - T_a)^a d\bar{x}}{(x - \bar{x})^{1/2}} \right] \quad C-1$$

Equation C-1 is an integral equation with $T - T_a$ as the dependent variable and must be solved numerically. However, if it is assumed that $T - T_a$ under the integral can be given by the former solution which did not consider

convection losses

$$T - T_a = \frac{\sqrt{\alpha/\pi}}{\nu^{1/2}} \left[\frac{Q_w}{L} \int_{-\infty}^x \frac{\mathcal{F}(\bar{x}) d\bar{x}}{(x - \bar{x})^{1/2}} \right] \quad 3-11$$

Equation C-1 becomes

$$T - T_a = \frac{\sqrt{\alpha/\pi}}{k \nu^{1/2}} \left[\frac{Q_w}{L} \int_{-\infty}^x \frac{\mathcal{F}(\bar{x}) d\bar{x}}{(x - \bar{x})^{1/2}} \right] - h \int_{-\infty}^x \left[\frac{\sqrt{\alpha/\pi}}{k \nu^{1/2} (x - \bar{x})^{1/2}} \frac{Q_w}{L} \int_{-\infty}^{\bar{x}} \frac{\mathcal{F}(\bar{x}) d\bar{x}}{(\bar{x} - \bar{x})^{1/2}} \right]^a d\bar{x} \quad C-2$$

Therefore, $T - T_a$ takes the form

$$T - T_a = K_1(x) \frac{Q/L)_R}{\nu^{1/2}} - \frac{K_2(x)}{\nu^{1/2}} \left[\frac{Q/L)_R}{\nu^{1/2}} \right]^a \quad C-3$$

and

$$Q/L)_L = h \left[K_1 \frac{Q/L)_R}{\nu^{1/2}} - \frac{K_2}{\nu^{1/2}} \left[\frac{Q/L)_R}{\nu^{1/2}} \right]^a \right] \quad 3-18$$

D THE VIEW FACTOR BETWEEN A BLACK SURFACE INCLINED AT AN ANGLE α AND A
BLACK SPOT MIDWAY BETWEEN THE ENDS

The finite exchange factors discussed in Section 5-4 are required to find the radiation distribution around infinite flames from the data taken on finite flames. As was pointed out in Section 5-4, it is impossible to perform the integration except when the absorption coefficient k' goes to infinity and the wedge can be treated as a black surface. This derivation follows.

The YZ plane in Figure D-1 intersects the yx plane at an angle α forming the y axis. Consider the radiative exchange between an element of area located on the YZ plane at the coordinates y, z and an element of area Ldx located a distance x from the y axis and midway between the ends of the YZ plane. The line drawn between the two elements is of length r , and with the perpendiculars to the areas determines the angles ϕ_1 and ϕ_2 . The fraction of black body radiation leaving the element $dydz$ and intercepted by the element Ldx , is equal to the apparent area of the element, $\pi \cos \phi_2 dy dz$, times the solid angle subtended by Ldx , $\cos \phi_1 Ldx/r^2$, divided by π . Therefore,

$$d^3_{ss} = \frac{\cos \phi_1 \cos \phi_2 dy dz Ldx}{\pi r^2} \quad \text{D-1}$$

where

$$\cos \phi_1 = \frac{z}{r} \sin \alpha \quad \cos \phi_2 = \frac{x}{r} \sin \alpha$$

$$r^2 = y^2 + z^2 \sin^2 \alpha + (x - z \cos \alpha)^2 \quad \text{D-2}$$

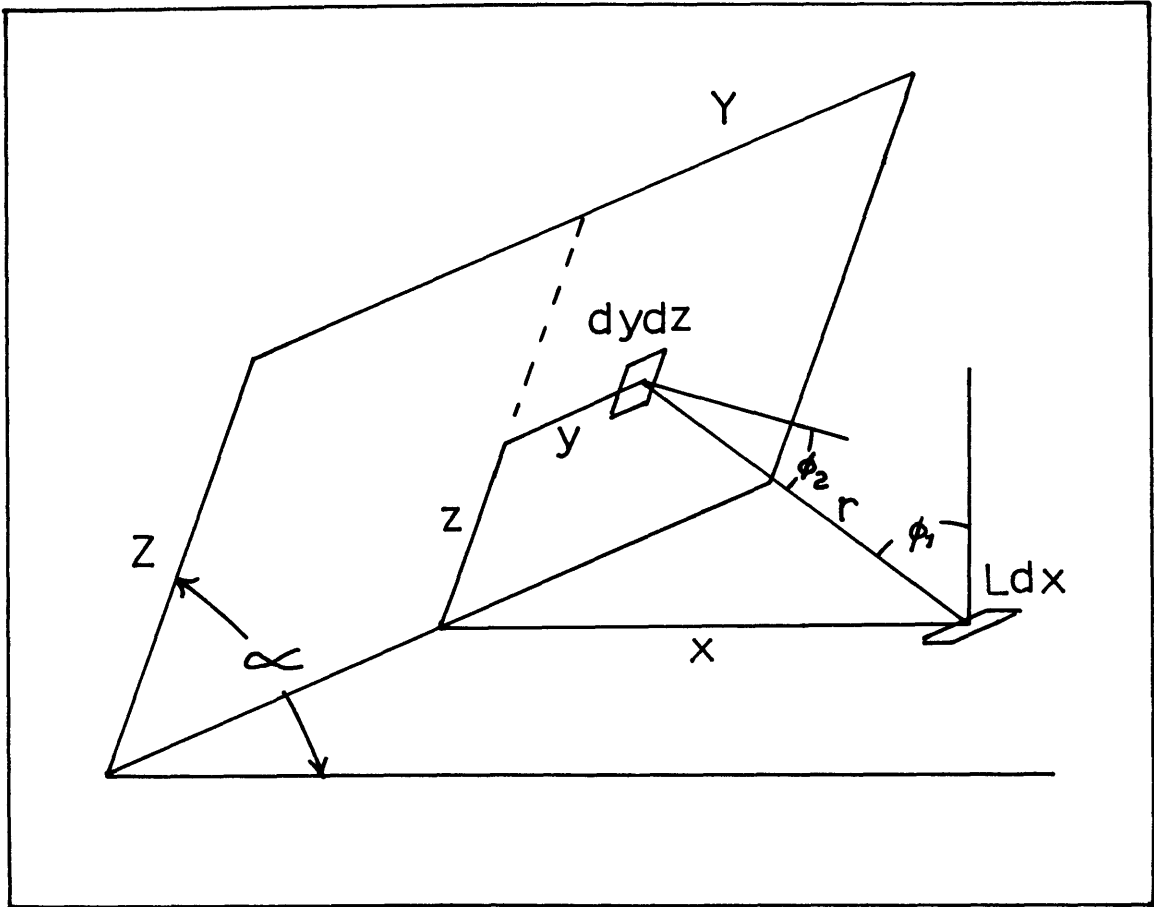


Figure D-1 Interchange Between a Finite Black Plane and a Black Spot

Substituting D-2 into D-1 and integrating from $-Y$ to Y and 0 to Z noting the symmetry over Y , gives

$$\frac{\overline{dss}}{Ldx} = \frac{2x \sin^2 \alpha}{\pi} \int_0^Z \int_0^Y \frac{dy dz}{(y^2 + z^2 + x^2 - 2xz \cos \alpha)^2} \quad D-3$$

The integration over Y yields

$$\begin{aligned} \frac{\overline{dss}}{Ldx} &= \frac{x \sin^2 \alpha}{\pi} \left[\int_0^Z \frac{Yz dz}{(z^2 - 2xz \cos \alpha + x^2)(z^2 + 2xz \cos \alpha + x^2 + Y^2)} \right. \\ &+ \left. \int_0^Z \frac{z}{(z^2 - 2xz \cos \alpha + x^2)^{3/2}} \tan^{-1} \left[\frac{Y}{(z^2 - 2xz \cos \alpha + x^2)^{1/2}} \right] dz \right] \quad D-4 \end{aligned}$$

In order to integrate the second integral by parts, let

$$\begin{aligned} dv &= \frac{z dz}{(z^2 - 2xz \cos \alpha + x^2)^{3/2}} \\ u &= \tan^{-1} \left[\frac{Y}{(z^2 - 2xz \cos \alpha + x^2)^{1/2}} \right] \quad D-5 \end{aligned}$$

then

$$\begin{aligned} v &= \frac{-(x - z \cos \alpha)}{x \sin^2 \alpha (z^2 - 2xz \cos \alpha + x^2)^{1/2}} \\ du &= \frac{-Y(z - x \cos \alpha) dz}{(z^2 - 2xz \cos \alpha + x^2 + Y^2)(z^2 - 2xz \cos \alpha + x^2)^{1/2}} \quad D-6 \end{aligned}$$

and equation D-4 becomes with rearrangement

$$\begin{aligned} \frac{dss}{Ldx} &= \frac{x \sin^2 \alpha}{\pi} \frac{-(x - z \cos \alpha)}{x \sin^2 \alpha (z^2 - 2xz \cos \alpha + x^2)^{1/2}} \\ &+ \tan^{-1} \left[\frac{Y}{(z^2 - 2xz \cos \alpha + x^2)} \right] \Bigg|_0^Z \\ &+ \int_0^Z \frac{Y \cos \alpha dz}{x \sin^2 \alpha (z^2 - 2xz \cos \alpha + x^2 + Y^2)} \end{aligned} \quad \text{D-7}$$

The solution of the above integral is standard and

$$\begin{aligned} \frac{dss}{Ldx} &= \frac{1}{\pi} \left\{ \frac{(Z \cos \alpha - x)}{(z^2 - 2xZ \cos \alpha + x^2)^{1/2}} \tan^{-1} \left[\frac{Y}{(z^2 - 2xZ \cos \alpha + x^2)^{1/2}} \right] \right. \\ &+ \tan^{-1} \frac{Y}{x} + \frac{Y \cos \alpha}{(x^2 \sin^2 \alpha + Y^2)^{1/2}} \left[\tan^{-1} \left[\frac{Z - x \cos \alpha}{(Y^2 + x^2 \sin^2 \alpha)^{1/2}} \right] \right. \\ &\left. \left. + \tan^{-1} \left[\frac{x \cos \alpha}{(Y^2 + x^2 \sin^2 \alpha)^{1/2}} \right] \right] \right\} \end{aligned} \quad \text{D-8}$$

E MOISTURE CONTENT OF THE FUEL

The moisture content of the fuel was obtained by weighing a sample of known volume at different humidities. The value for zero humidity was obtained by drying a sample in a desiccator for several days, and weighing it on successive days until the weight became constant. The results for the newspaper and computer fuels are shown in Figure E-1.

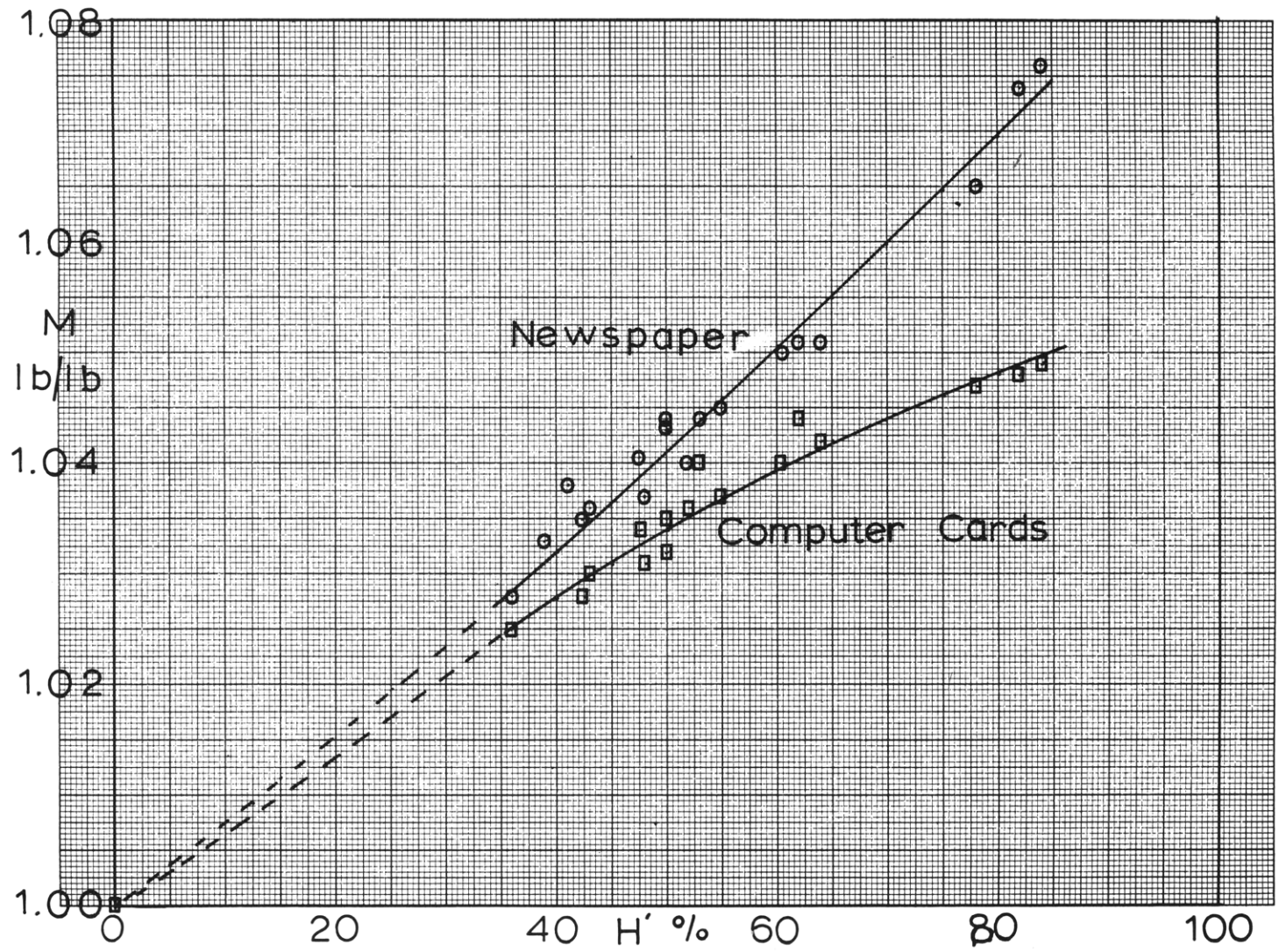


Figure E-1 Moisture Content as a Function of Humidity for Newspaper and Computer Cards

F ORIGINAL DATA

F-1 Data on Fire Spread Through Shredded Newspaper and Computer Cards

Table F-1

The Effect of Loading Density on the Rate of Fire Spread for Shredded
Newspaper (0.003" thick)

Run No.	Loading Density lb/ft ²	Temp. °F	Relative Humidity %	External* Radiation Btu/hr-ft	Velocity ft/hr	Residue lb/ft ²	% Burned
1	0.0720	75	40	296	79.8	-	-
2	0.1175	75	40	296	81.6	0.0284	76
3	0.0547	74	39.5	282	79.3	0.0066	88
4	0.0631	75	37	289	79.3	0.0093	85.2
5	0.0212	75	37	296	67.8	0.0014	93.4
6	0.0127	75	37	296	0	-	-
7	0.0375	75	46	296	63.6	0.0107	71.5

*Radiation from four wires

Table F-2

The Effect of Radiation on the Rate of Fire Spread for Shredded Newspaper

Run No.	Loading Density lb/ft ²	Temp. °F	Relative Humidity %	External* Radiation Btu/hr-ft	Velocity ft/hr	Residue lb/ft ²	& Burned
50	0.0625	75	49	554	94.8	0.0052	91.7
51	0.0625	73	48	450	89.5	0.0026	95.8
52	0.0625	73	48	348	75.0	0.0024	96.2
53	0.0625	73	48	250	70.2	0.0046	92.6
54	0.0625	75	49	140	57.6	0.0047	92.5
55	0.0625	73	48	0	33.6	0.0044	93.0
56	0.0625	73	48	206**	60.0	0.0047	92.5
57	0.0625	73	48	0	34.2	-	-
58	0.0625	73	48	554	95.5	-	-
59	0.0625	72	47	554	95.5	-	-

* Radiation from eight wires

** Radiation from four wires

Table F-3

The Effect of Humidity on the Rate of Fire Spread for Shredded Newspaper

Run No.	Loading Density lb/ft ²	Temp. °F	Relative Humidity %	External* Radiation Btu/hr-ft	Velocity ft/hr	Residue lb/ft ²	% Burned
4	0.0631	75	37	289**	79.3	0.0093	85.2
10	0.0627	75	37	173**	66.0	0.0062	90.1
11	0.0630	77	39	554	104.5	0.0145	77.0
12	0.0620	75	37	0	38.0	0.0134	78.5
13	0.0624	75	37	554	109.2	0.0137	78.1
14	0.0625	77	39	450	96.0	0.0155	75.2
15	0.0625	75	43	399	85.9	0.0150	76.0
16	0.0624	75	31	0	37.5	0.0145	76.8
17	0.0630	77	33	554	112.0	0.0139	78.0
60	0.0625	74	27	0	45.5	0.0012	98.1
61	0.0625	74	27	605	116.5	0.0013	97.9
62	0.0625	74	27	398	100.1	0.0013	97.9
63	0.0635	74	27	207	76.8	0.0013	97.9

* Radiation from eight wires

** radiation from four wires

Table F-4

The Effect of Radiation on the Rate of Fire Spread for Computer Punch

Outs (1/8"x1/16"x0.007")

Run No.	Loading Density lb/ft ²	Temp. °F	Relative Humidity %	External Radiation* Btu/hr-ft	Velocity ft/hr	Residue lb/ft ²	% Burned
21	0.0625	77	39	0	0	-	-
22	0.0625	77	39	566	14.90	0.0065	86.0
23	0.1275	77	44	554	14.47	0.0084	93.5
24	0.1275	75	43	348	9.96	0.0071	94.4
25	0.1275	77	44	207	7.56	0.0075	94.3
26	0.1275	77	44	0	0	-	-
27	0.1275	77	44	106	4.68	-	-
28	0.1275	77	44	554	13.80	0.0071	94.5

* Radiation from eight wires

Table F-5

The Effect of Radiation on the Rate of Fire Spread for Computer Cards

(1/2"x1/2"x0.007")

Run No.	Loading Density lb/ft ²	Temp. °F	Relative Humidity %	External* Radiation Btu/hr-ft	Velocity ft/hr	Residue lb/ft ²	% Burned
30	0.1275	77	47	554	20.50	0.0056	95.5
31	0.1275	77	47	0	0	-	-
32	0.1275	77	47	348	13.70	0.0145	88.6
33	0.1275	77	44	168	8.70	0.0059	95.3

* Radiation from eight wires

Table F-6

The Effect of Wind Velocity on the Rate of Fire Spread for Shredded
Newspaper Fuel

Run No.	Loading Density lb/ft ²	Temp. °F	Relative Humidity %	External Radiation Btu/hr-ft	Wind Velocity ft/sec	Velocity ft/hr
71	0.0625	84	72	0	0	29.3
72	0.0625	86	73	0	3.48	107.5
73	0.0625	86	73	0	2.42	59.0
74	0.0625	86	73	0	2.89	82.8
75	0.0625	75	77	0	1.30	31.5
76	0.0625	75	77	0	0	28.3

F-2 Data of Radiation Flux Densities Around Methane Flames (by de
Rochechouart (24))

Table F-7

Reproducibility of Data (Methane)

Q/L = 176,300 Btu/hr-ft

Run No. 6-4-3

Distance from the Center of the Slot ft	Reading mv	Flux Density Btu/hr-ft ²
0.217	0.71	5,580
0.296	0.64	5,000
0.361	0.59	4,600
0.427	0.58	4,520
0.493	0.53	4,020
0.624	0.47	3,620
0.755	0.42	3,280
0.886	0.35	2,700
1.018	0.30	2,320

Run No. 6-4-4

0.217	0.74	5,820
0.263	0.665	5,210
0.329	0.64	5,000
0.394	0.60	4,680
0.525	0.52	4,000
0.657	0.46	3,540
0.788	0.40	3,080
0.919	0.35	2,700
1.050	0.30	2,320

Run No. 6-4-5

0.217	0.73	5,740
0.247	0.675	5,300
0.312	0.68	5,320
0.378	0.60	4,670
0.443	0.57	4,440
0.575	0.48	3,680
0.706	0.42	3,240
0.837	0.35	2,700
0.968	0.31	2,400

Table F-7 (continued)

Distance from the Center of the Slot ft	Reading mv	Flux Density Btu/hr-ft ²
0.217	0.73	5,740
0.279	0.66	5,160
0.345	0.61	4,760
0.411	0.56	4,360
0.476	0.52	4,020
0.607	0.47	3,620
0.739	0.41	3,160
0.870	0.34	2,620
1.001	0.29	2,240

Table F-8

Radiation Flux Densities for Different Heat Liberation Rates (Methane)

Run No. 6-00

Q/L = 63,700 Btu/hr-ft

Distance from the Center of the Slot* ft	Reading mv	Flux Density Btu/hr-ft ²
0.217	0.51	3,920
0.296	0.39	3,000
0.361	0.36	2,780
0.427	0.31	2,400
0.493	0.29	2,240
0.624	0.25	1,940

Run No. 6-0

Q/L = 78,600 Btu/hr-ft

Distance from the Center of the Slot* ft	Reading mv	Flux Density Btu/hr-ft ²
0.217	0.54	4,190
0.296	0.435	3,300
0.361	0.39	3,000
0.427	0.35	2,700
0.493	0.32	2,480
0.624	0.28	2,100

Run No. 6-1

Q/L = 90,000 Btu/hr-ft

Distance from the Center of the Slot* ft	Reading mv	Flux Density Btu/hr-ft ²
0.217	0.56	4,360
0.296	0.44	3,400
0.361	0.41	3,160
0.427	0.37	2,860
0.493	0.34	2,620
0.624	0.28	2,160
0.755	0.22	1,700

Table F-8 (Continued)

Run No. 6-2

 $Q/L = 120,000 \text{ Btu/hr-ft}$

Distance from the Center of the Slot* ft	Reading mv	Flux Density Btu/hr-ft ²
0.217	0.59	4,600
0.296	0.48	3,700
0.361	0.45	3,470
0.427	0.43	3,320
0.493	0.41	3,160
0.624	0.34	2,620
0.755	0.28	2,160

Run No. 6-8

 $Q/L = 130,600 \text{ Btu/hr-ft}$

Distance from the Center of the Slot* ft	Reading mv	Flux Density Btu/hr-ft ²
0.217	0.65	5,090
0.296	0.54	4,190
0.361	0.50	3,850
0.427	0.51	3,920
0.493	0.46	3,540
0.624	0.37	2,860
0.755	0.32	2,470
0.886	0.26	2,010
1.018	0.20	1,550

Run No. 6-3

 $Q/L = 143,800 \text{ Btu/hr-ft}$

Distance from the Center of the Slot* ft	Reading mv	Flux Density Btu/hr-ft ²
0.217	0.69	5,420
0.296	0.60	4,680
0.361	0.56	4,360
0.427	0.54	4,190
0.493	0.48	3,770
0.624	0.43	3,280
0.755	0.35	2,700
0.886	0.30	2,320
1.018	0.25	1,920

Table F-8 (Continued)

Run No. 6-9

 $Q/L = 165,000 \text{ Btu/hr-ft}$

Distance from the Center of the Slot* ft	Reading mv	Flux Density Btu/hr-ft ²
0.217	0.70	5,500
0.296	0.61	4,760
0.361	0.57	4,440
0.427	0.55	4,270
0.493	0.52	4,020
0.624	0.44	3,420
0.755	0.37	2,860
0.886	0.31	2,400
1.018	0.27	2,090

Run No. 6-4

 $Q/L = 176,300 \text{ Btu/hr-ft}$

Distance from the Center of the Slot* ft	Reading mv	Flux Density Btu/hr-ft ²
0.217	0.71	5,580
0.296	0.64	5,000
0.361	0.59	4,600
0.427	0.58	4,520
0.493	0.53	4,020
0.624	0.47	3,620
0.755	0.42	3,280
0.886	0.35	2,700
1.018	0.30	2,320

Table F-8 (Continued)

Run No. 6-5

 $Q/L = 197,200 \text{ Btu/hr-ft}$

Distance from the Center of the Slot* ft	Reading mv	Flux Density Btu/hr-ft ²
0.217	0.73	5,740
0.296	0.66	5,170
0.361	0.61	4,760
0.427	0.59	4,600
0.493	0.57	4,440
0.624	0.48	3,680
0.755	0.43	3,320
0.886	0.36	2,780
1.018	0.31	2,400

Run No. 6-7

 $Q/L = 235,600 \text{ Btu/hr-ft}$

Distance from the Center of the Slot* ft	Reading mv	Flux Density Btu/hr-ft ²
0.217	0.75	5,900
0.296	0.67	5,270
0.361	0.64	5,000
0.427	0.60	4,680
0.493	0.58	4,510
0.624	0.49	3,770
0.755	0.46	3,540
0.886	0.40	3,090
1.018	0.34	2,620

*Slot Width = 2.0 inches

Table F-9

Radiation Flux Density for a Different Slot Width and Two Different
Heat Liberation Rates (Methane)

Run No. 9-2

$Q/L = 176,300$ Btu/hr-ft

Distance from the Center of the Slot* ft	Reading mv	Flux Density Btu/hr-ft ²
0.176	0.75	5,900
0.255	0.66	5,160
0.320	0.63	4,920
0.386	0.585	4,560
0.452	0.50	3,840
0.583	0.47	3,620
0.714	0.395	3,040
0.845	0.36	2,780
0.977	0.31	2,400

Run No. 9-3

$Q/L = 120,000$ Btu/hr-ft

Distance from the Center of the Slot* ft	Reading mv	Flux Density Btu/hr-ft ²
0.176	0.63	4,920
0.255	0.53	4,100
0.320	0.50	3,840
0.386	0.46	3,540
0.452	0.41	3,160
0.583	0.37	2,860
0.714	0.29	2,240
0.845	0.25	1,940

*Slot Width = 1.0 inch

F-3 Data of Radiation Flux Densities Around Propane Flames

Table F-10

Radiation Flux Densities for Different Heat Liberation Rates (Propane)

Run No. 7-1

Q/L = 153,000 Btu/hr-ft

Distance from the Center of the Slot* ft	Reading mv	Flux Density Btu/hr-ft ²
0.220	0.75	5,840
0.296	0.69	5,380
0.361	0.62	4,830
0.427	0.58	4,500
0.558	0.48	3,740
0.689	0.39	3,040
0.821	0.33	2,570
0.952	0.30	2,340

Run No. 7-2

Q/L = 193,000 Btu/hr-ft

Distance from the Center of the Slot* ft	Reading mv	Flux Density Btu/hr-ft ²
0.296	0.73	5,690
0.361	0.67	5,220
0.427	0.60	4,670
0.493	0.59	4,600
0.558	0.545	4,250
0.689	0.48	3,740
0.821	0.415	3,230
0.952	0.39	3,040

Table F-10 (Continued)

Run No. 7-3

 $Q/L = 108,000 \text{ Btu/hr-ft}$

Distance from the Center of the Slot* ft	Reading mv	Flux Density Btu/hr-ft ²
0.230	0.695	5,410
0.296	0.63	4,910
0.361	0.57	4,440
0.427	0.51	3,970
0.493	0.46	3,580
0.624	0.385	3,000
0.755	0.325	2,530
0.886	0.27	2,100
1.018	0.215	1,670

Run No. 7-4

 $Q/L = 83,600 \text{ Btu/hr-ft}$

Distance from the Center of the Slot* ft	Reading mv	Flux Density Btu/hr-ft ²
0.230	0.68	5,300
0.296	0.59	4,600
0.361	0.54	4,210
0.427	0.46	3,580
0.493	0.41	3,190
0.558	0.41	3,190
0.689	0.325	2,530
0.821	0.26	2,030
0.952	0.195	1,520

*Slot Width = 2.0 inches

F-4: Data on Flame Heights of Methane and Propane

Table F-11

Methane Flame Heights (by de Rochechouart (<u>24</u>))		Propane Flame Heights	
Heat Liberation Rate Btu/hr-ft	Flame Height ft	Heat Liberation Rate Btu/hr-ft	Flame Height ft
77,100	1.16	96,500	1.15
139,000	1.645	128,500	1.38
189,000	2.025	166,800	1.71
213,000	2.33	187,000	1.93
230,000	2.58	212,000	2.12
239,000	2.63	229,000	2.38
121,500	1.44	146,000	1.56
154,000	1.81		
214,500	2.17		

Slot Width = 2.0 inches

G. NOMENCLATURE

- a slope of a gray gas wedge, dimensionless
- a' reciprocal mean free path for radiation in the fuel bed, ft^{-1}
- A_s surface area of a fuel particle, ft^2
- b half width of a gray gas wedge, ft
- b' dimensionless half width of the base of a gray gas wedge, $k'b$
- B mean beam length, dimensionless
- B' coefficient of expansion, $(^\circ\text{F})^{-1}$
- c heat capacity of a gas, $\text{Btu/lb-}^\circ\text{F}$
- c_p heat capacity of dry fuel, $\text{Btu/lb-}^\circ\text{F}$
- \bar{c}_p heat capacity of moist fuel, $\text{Btu/lb-}^\circ\text{F}$
- d distance below fuel surface, ft
- D diameter of a circular source, ft
- σ_e eddy diffusivity at the flame front, ft^2/hr
- F $u_o^2/y_o g$ modified Froude Number, dimensionless
- F_v volumetric flow rate at a circular source, ft^3/hr
- F_v/L volumetric flow rate at a line source, $\text{ft}^3/\text{hr-ft}$
- $F(x)$ interchange factor between a gray wall and an element of fuel, dimensionless
- $\mathcal{F}(x)/L$ interchange factor between the wires and an element of fuel dx , dimensionless
- g acceleration due to gravity, ft/hr^2
- h convection heat transfer coefficient, $\text{Btu/hr-ft}^2\text{-}^\circ\text{F}$
- h_c convection heat transfer coefficient, $\text{Btu/hr-ft}^2\text{-}^\circ\text{F}$

h_r	radiation heat transfer coefficient based on a first power temperature difference, Btu/hr-ft ² -°F
H	flame height, ft
ΔH	total enthalpy of moisture (sensible plus latent heat), Btu/lb
I	flux density of radiation, Btu/ft ² -hr
k	thermal conductivity of the fuel, Btu/hr-ft ² -°F/ft
k'	absorption coefficient of a gray gas, ft ⁻¹
k''	entrainment coefficient of a jet, dimensionless
K	constant determining importance of heat lost from fuel surface, ft/(Btu-hr) ^{1/3}
K'	$k'Q_c/r_f cT_a$, dimensionless
l	thickness of the fuel, ft
l'	distance over which convection heat transfer at the flame front occurs, ft
L	distance from the wires to the fuel, ft
\bar{L}	distance between fuel particles, ft
m	number of equivalent layers of fuel if evenly distributed, dimensionless
M	moisture content of the fuel, lbs water/lb dry fuel
M_a	molecular weight of air, lbs/mole
n_x	molal flow rate of products at height x, lb-moles/hr
n_o	molal flow rate of fuel at source, lb-moles/hr
n_a	molal flow rate of entrained air up to height x, lb-moles/hr
P	pressure of gas, lbs/ft ²
q	total rate of heat transfer to an element of fuel, Btu/hr-ft ²

- $q_1(x)$ rate of heat transfer by radiation from embers under the fire to an element of unburned fuel per unit of horizontal area, Btu/hr-ft²
- $q_2(x)$ rate of heat transfer by convection at the flame front to an element of unburned fuel per unit of horizontal area, Btu/hr-ft²
- $q_3(x)$ rate of heat transfer by radiation from the overhead flame to an element of fuel per unit of horizontal area, Btu/hr-ft²
- $q_4(x)$ rate of heat transfer from an element of unburned fuel by convection and radiation per unit of horizontal area, Btu/hr-ft²
- $q_5(x)$ rate of heat liberation by combustion within an element of fuel per unit of horizontal area, Btu/hr-ft²
- q_G rate of chemical energy liberation from an element of fuel during decomposition, Btu/hr-ft²
- q_c rate of heat transfer to unburned fuel by convection, Btu/hr
- q_r rate of heat transfer to unburned fuel by radiation, Btu/hr
- Q_c heat of combustion of the fuel, Btu/lb
- Q_i energy required to produce piloted ignition per unit of horizontal area, Btu/ft²
- Q_o energy required to produce piloted ignition per unit of horizontal area at a standard velocity of fire spread, Btu/ft²
- Q_w heat liberation rate from a single wire per unit length, Btu/hr-ft
- $Q(\lambda)$ heat input rate per unit surface area as a function of time, Btu/hr-ft²
- Q/L rate of heat liberation by the flame per foot length, Btu/hr-ft

- $Q/L)_B$ integrated heat transfer rate by radiation from embers under the gas flame, Btu/hr-ft
- $Q/L)_C$ integrated heat transfer rate by convection at the flame front to unburned fuel, Btu/hr-ft
- $Q/L)_L$ integrated rate of heat loss from the unburned fuel, Btu/hr-ft
- $Q/L)_R$ integrated rate of heat transfer by radiation from the overhead flame to unburned fuel, Btu/hr-ft
- $Q/L)_I'$ integrated rate of heat generation within the burning fuel by combustion, Btu/hr-ft
- $Q/L)_R'$ integrated rate of heat transfer by radiation from the overhead flame to the burning fuel, Btu/hr-ft
- r distance between elements exchanging radiation, ft
- r' dimensionless distance, $k'r$
- r_f air required for stoichiometric combustion, lbs air/lb fuel
- R universal constant for an ideal gas, lbs/lb mole °F
- s distance of paths through gray gas between elements exchanging radiation, ft
- s' dimensionless distance, $k's$
- S surface area of a jet, ft²
- t time, hr
- T temperature, °F
- T_a ambient temperature, °F
- T_f flame temperature, °F
- T_i ignition temperature of the fuel, °F
- T_o temperature of a jet at its source, °F

T_1	temperature of the fuel particle when the particle next to it ignites, °F
u	vertical velocity of a jet at height x , ft/hr
u_e	eddy velocity at the flame front, ft/hr
u_o	velocity of a jet at the source, ft/hr
u'	dimensionless jet velocity, u/u_o
U	overall convection heat transfer coefficient, Btu/hr-ft ² -°F
V	rate of fire spread, ft/hr
v_e	entrainment velocity, ft/hr
V_w	wind velocity, ft/hr
v'	shortest dimensionless distance between an infinite element and a spot exchanging radiation
V_x	volumetric flow at height x per unit length, ft ³ /hr-ft
V_a	volumetric rate of entrainment up to height x per unit length, ft ³ /hr-ft
V_o	volumetric flow at source, per unit length, ft ³ /hr-ft
v'_x	dimensionless volumetric flow rate at height x
\bar{V}	volume of a fuel particle, ft ³
w	distance variable, ft
w'	$k'w$, dimensionless
W	width of a parallelepiped of gray gas, ft
W'	dimensionless width of a parallelepiped of gray gas, $k'W$
\mathcal{W}	width of the base of the line fire, ft
x	distance variable, ft
x'	$k'x$, dimensionless

x'	dimensionless distance from the source of a jet, x/y_0
y	distance variable, ft
y'	$k'y$, dimensionless
y_x	half width of a jet at height x , ft
y_0	half width of a jet at the source, ft
y'_x	dimensionless half width of a jet at height x , y_x/y_0
Y	half the length of a gray gas parallelepiped, ft
Y'	kY , dimensionless
z	distance variable, ft
z'	$k'z$, dimensionless
Z	height of a rectangular parallelepiped or wedge of gray gas, ft
Z'	kZ , dimensionless

Greek Letters

α	thermal diffusivity, ft^2/hr
β	constant of proportionality between chemical energy of gases liberated during fuel decomposition and the heat absorbed by the fuel, dimensionless
$\bar{\gamma}$	density of moist fuel, lbs/ft^3
ϵ	emissivity of the fuel, dimensionless
ϵ_f	emissivity of the flame, dimensionless
ξ	fuel loading density, lbs/ft^2
η	fraction of the fuel burned by the passing fire, dimensionless
λ	dummy variable in time, hr
σ	Stefan-Boltzmann constant, $\text{Btu}/\text{hr-ft}^2-\text{R}^4$

$\bar{\sigma}$	surface of volume ratio, ft^2/ft^3
ρ	density of a gas, lbs/ft^3
ρ_a	density of air, lbs/ft^3
ρ_o	density of fuel at source, lbs/ft^3
ρ'	dimensionless density of gas, ρ/ρ_a
ρ'_o	dimensionless density of fuel at source, ρ_o/ρ_a
θ	time of heating from ignition of the previous ignited fuel particle, hr
θ_i	time of ignition from the ignition of the previous fuel particle, hr
μ	viscosity of a gas, $\text{lbs}/\text{ft}\text{-hr}$
ω	inverse volumetric expansion of gas due to combustion, dimensionless

IX REFERENCES

1. Atallah, S. I., "Model Studies on the Propagation of Fire", Eng. Thesis, Chem. Eng. Dept., M.I.T., Jan. 1960
2. Blinev, V. I., and Khudiakov, G.N., Reviewed by Hottel, H.C., "Certain Laws Governing Diffusive Burning of Liquids", Fire Research Abstracts and Reviews, Vol. 1, No. 2, Jan. 1959
3. Broido, A., and Martin, S. B., "Effects of Potassium Bicarbonate on the Ignition of Cellulose by Thermal Radiation", U. S. Naval Radiological Defence Laboratory, USNRDL-TR-536, DASA-1255, Oct. 1961
4. Bruce, H. D., and Downs, L. E., "Ignition of Newspaper by Radiation with Variation in Moisture Content and Pulse Time", U. S. Dept. of Agriculture, Forest Service, Technical Report AFSWP-1099
5. Burington, R. S., "Handbook of Mathematical Tables and Formulas", page 61
6. Carslaw, H. S., and Jaeger, J. C., "Conduction of Heat in Solids", Second Edition, Oxford at Clarendon Press, page 76
7. Fons, W. L., "Analysis of Fire Spread in Light Forest Fuels", Journal of Agricultural Research, 72, 93, 1946
8. Fons, W. L., Bruce, H. D., Pong, W. Y., and Richards, S. S., "Project Fire Model", Summary Progress Report, U. S. Dept. Agriculture, Forest Service, May 1960
9. Homsy, C. A., "Similitude in Turbulent Free-Jet Diffusion Flames", ScD Thesis, Chem. Eng. Dept., M.I.T., 1959
10. Hottel, H. C., "Heat Transmission", Third Edition, Chapter 4, (Mc Adams), Mc Graw-Hill Book Co., New York, 1959, pages 55-139
11. Hottel, H. C., "Fire Modeling", "The Use of Models in Fire Research", National Academy of Science, Publication 786, 1961
12. Hottel, H. C., Personal Communication, 1961
13. Hottel, H. C., and Williams, C. C., "Transient Heat Flow in Organic Materials Exposed to High Intensity Radiation", Industrial and Engineering Chemistry, 47, 1136-1143, (1955)
14. Lawson, D. I., and Simms, D. L., "The Ignition of Wood by Radiation", British Journal of Applied Physics, 3, 288-292, (1952)
15. Lee and Emmons, H. W., 1961, to be published
16. Martin, S., Lincoln, K. A., and Ramstad, R. W., "Thermal Radiation Damage to Cellulose Materials", Part IV, U. S. Radiological Defence Laboratory, USNRDL-TR-295, Dec. 1958

17. Martin, W. T., and Reissner, E., "Elementary Differential Equations", Addison-Wesley Publishing Co., Cambridge, Mass., pages 42, 94-95
18. Mc Adams, W. H., "Heat Transmission", Third Edition, Mc Graw-Hill Book Co., New York, 1954, page 177
19. Morton, B. R., Journal of Fluid Mechanics, 2, 127, (1957)
20. Morton, B. R., Journal of Fluid Mechanics, 5, 156, (1959)
21. Morton, B. R., Journal of Fluid Mechanics, 10, 101, (1961)
22. Morton, B. R., Taylor, G. I., and Turner, J. S., "Proceedings of the Royal Society A, 236, 1, (1956)
23. Murgai, M. P., and Emmons, H. W., Journal of Fluid Mechanics, 8, 611, (1960)
24. de Rochechouart, C. L., "Radiation from a Line Fire", M. S. Thesis, Chem. Eng. Dept., M.I.T., May 1961
25. Rouse, H., Yih, C. S., and Humpreys, H. W., Tellus, 4, 201, (1952)
26. Schaefer, V. J., "The Relationship of Jet Dstreams to Forest Wildfires", Journal of Forestry, 55, 419, (1957)
27. Schmidt, F. H., "On the Diffusion of Heated Jets", Tellus, 9, 378, (1959)
28. Schmidt, W., angew Math. Mech., 21, 265,351, (1941)
29. Simms, D. L., "The Influence of External Air Movements on the Ignition of Materials by Radiation", Dept. of Scientific and Industrial Research and Fire Offices, Committee Jount Fire Research Organization, F. R. Note 305
30. Stout, H. P., "Ignition of Wood by Radiation", British Journal of Applied Physics, 3, 394, (1952)
31. Thomas, P. H., Webster, C. T., and Raftery, M. M., "Some Experiments on Buoyant Diffusion Flames", Combustion and Flame, 5, No. 4, (1961)
32. "A Study of Fire Problems", National Academy of Sciences, National Research Council, Publication 949
33. Priestly and Ball, "Continuous Convection from an Isolated Source of Heat", Quarterly Journal of the Royal Meteorological Society, 81, (1955)

AUTOBIOGRAPHICAL NOTE

The author was born on May 16, 1937 in Woodbury, New Jersey, the third son of Owen F. Steward and his wife, the former Mary Waddington. He attended the local elementary and high school from which he was graduated in June, 1955 and entered M.I.T. the following September. He received his Bachelor of Science in Chemical Engineering in June, 1959 and his Master of Science in Chemical Engineering in February of 1960 after spending the fall term at the Bayway-Bound Brook Practice School in New Jersey. At this time he commenced the present project. The author married the former Jacqueline Bourcier of Alexandria, Ontario on June 24, 1961. They now have a son, Richard Michel, born April 18, 1962.

The author was a Teaching Assistant from February to June, 1960 and a Research Assistant for the remainder of this work. He has accepted a position as Assistant Lecturer at the University of Edinburgh.